



DETERMINATION OF ABCC11-GLYCOPROTEIN (MRP8) TRANSPORTER  
FUNCTION ON TENOFOVIR DISOPROXIL FUMARATE (TDF) TRANSPORT.



By  
MR. Wisith TUN-YHONG

A Thesis Submitted in partial Fulfillment of Requirements  
for Doctor of Philosophy BIOPHARMACEUTICAL SCIENCES  
Pharmacy Silpakorn University  
Academic Year 2016  
Copyright of Graduate School, Silpakorn University

การศึกษาหน้าที่ของกลัยโคโปรตีนขนส่งชนิด ABCC11 (MRP8) ในการขนส่งยา  
tenofovir disoproxil fumarate (TDF)



วิทยานิพนธ์นี้เป็นส่วนหนึ่งของการศึกษาตามหลักสูตรเภสัชศาสตรดุษฎีบัณฑิต  
สาขาวิชาเภสัชศาสตร์ชีวภาพ แบบ 2.2 เภสัชศาสตรดุษฎีบัณฑิต  
เภสัชศาสตร์ มหาวิทยาลัยศิลปากร  
ปีการศึกษา 2559  
ลิขสิทธิ์ของบัณฑิตวิทยาลัย มหาวิทยาลัยศิลปากร

DETERMINATION OF ABCC11-GLYCOPROTEIN (MRP8)  
TRANSPORTER FUNCTION ON TENOFOVIR  
DISOPROXIL FUMARATE (TDF) TRANSPORT.



By  
MR. Wisith TUN-YHONG

A Thesis Submitted in partial Fulfillment of Requirements  
for Doctor of Philosophy BIOPHARMACEUTICAL SCIENCES  
Pharmacy Silpakorn University  
Academic Year 2016  
Copyright of Graduate School, Silpakorn University



55355802 : Major BIOPHARMACEUTICAL SCIENCES

Keyword : Tenofovir, Tenofovir disoproxil fumarate, TDF, TFV, ATP-binding cassette subfamily C11, MRP8, ABCC11, Nephrotoxicity

MR. Wisith TUN-YHONG : Determination of ABCC11-glycoprotein (MRP8) transporter function on tenofovir disoproxil fumarate (TDF) transport. Thesis advisor : Associate Professor Chatchai Chinpaisal, Ph.D.

Tenofovir disoproxil fumarate (TDF), a nucleotide reverse transcriptase inhibitor, after conversion to TFV, is mainly eliminated by glomerular filtration and active tubular secretion. The major adverse effect of tenofovir is nephrotoxicity, however, the exact mechanism remains poorly understood. In this study, ABCC11 (MRP8) transporter, a member of ATP-binding cassette subfamily C11, which is abundant in proximal tubular cells, was demonstrated to efflux tenofovir. Real-time polymerase chain reaction (rt-PCR) and indirect immunofluorescence assays were used to determine MRP8 overexpression in a continuous cell line. Tenofovir accumulations were assessed by cytotoxicity, cellular transport, and vesicular uptake assays. Substrate specificity was confirmed using MK-571, an MRP-specific inhibitor, and methotrexate which served as a known substrate. Intracellular and intravesicular concentrations of tenofovir were determined by liquid chromatography-tandem mass spectrometry (LC-MS/MS). The 50% cytotoxic concentrations ( $CC_{50}$ ) of TDF in MRP8-overexpressed cells was 4.78 times higher when compared to that of parental cells. Transport assays also showed that the intracellular accumulation of tenofovir in MRP8-overexpressed cells was 55 times lower than that of the parental cells, and was partly reversed by MK-571. Similarly, the inside-out vesicular uptake assay demonstrated higher intravesicular concentration of tenofovir in MRP8-overexpressed vesicles than that of the Sf9 insect vesicles. These effects were effectively reversed by increasing concentrations of specific inhibitor, MK-571. In conclusion, tenofovir is a new substrate of MRP8 transporter. An alteration in the activity of this efflux pump may increase the intracellular accumulation of tenofovir in proximal renal tubular cells.

## ACKNOWLEDGEMENTS

I would like to gratefully and sincerely thank my thesis advisor, Associate Professor Dr. Chatchai Chinpaisal and Assistant Professor Dr. Perayot Pamonsinlapatham whose encouragement, guidance and support from the initial to the final level enabled me to develop an understanding of the dissertation.

I would be thankful for Assoc. Prof. Dr. Sindhchai kaewkittichai, Assoc. Prof. Dr. Titinun Auamnoy and Assoc. Prof. Dr. Manat Pongchaidecha for expert help in the discussion.

I also special thank for all professor staff in Faculty of Pharmacy, Silpakorn University, and Burapha University, for giving me the place, equipment, knowledge, and friendship.

Wisith TUN-YHONG

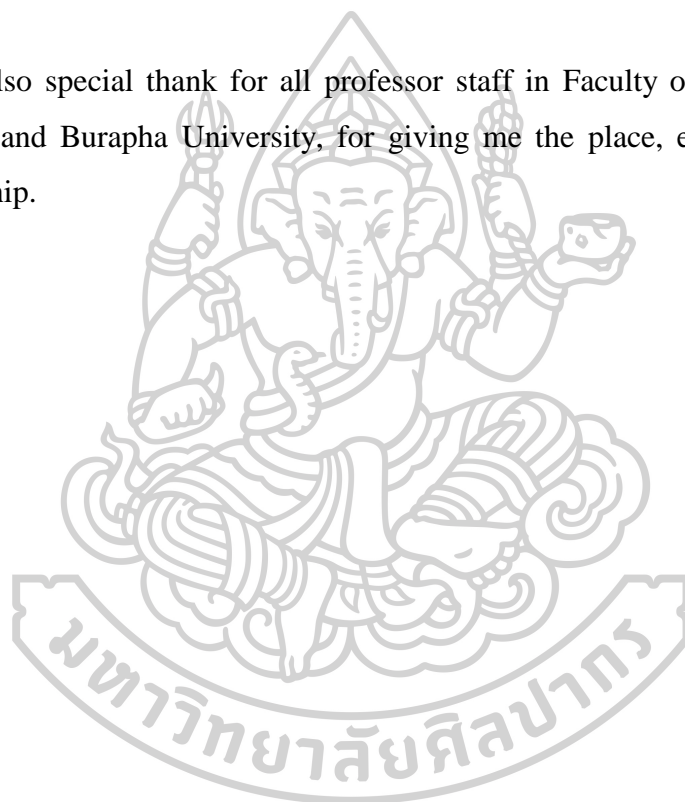


## TABLE OF CONTENTS

	<b>Page</b>
ABSTRACT.....	D
ACKNOWLEDGEMENTS.....	E
TABLE OF CONTENTS.....	F
LIST OF FIGURES.....	9
LIST OF TABLES.....	12
CHAPTER 1.....	17
INTRODUCTION.....	17
1.1 Statement and significance of the research problem.....	17
1.2 Objective of this research.....	20
1.3 The research hypothesis.....	20
CHAPTER 2.....	21
LITERATURE REVIEWS.....	21
2.1 Background information.....	22
2.2 Tenofovir-induced nephrotoxicity.....	25
2.3 Role of renal transporters in tenofovir metabolism and toxicity.....	29
CHAPTER 3.....	35
MATERIALS AND METHODS.....	35
3.1 Materials.....	36
3.1.1 Chemicals and reagents.....	36
3.2 Equipment.....	38
3.3 Methods.....	40
3.3.1 Cells and vesicles preparation.....	42
3.3.2 mRNA isolation and Real Time-PCR (rt-PCR).....	43

3.3.3 Immunofluorescent staining and imaging .....	47
3.3.4 Cytotoxic assays .....	49
3.3.5 Drug transport assays .....	51
3.3.6 ATP-dependent vesicular uptake assays.....	53
3.3.7 Statistical analysis .....	56
CHAPTER 4 .....	1
RESULTS AND DISCUSSION.....	1
4.1 Characterization of cells lines .....	2
4.2 Cells viability and cytotoxicity assays .....	4
4.3 Tenofovir transport assays.....	6
4.4 Vesicular uptake assays.....	8
4.5 Discussion.....	10
CHAPTER 5 .....	12
CONCLUSIONS .....	12
REFERENCES .....	13
APPENDIX.....	22
APPENDIX A.....	22
1. Protein determination by using Bradford assayed.....	23
1. Cytotoxicity evaluation using MTT assay.....	26
2. Calculation of 50% cytotoxic concentration value (CC <sub>50S</sub> , μM) of tenofovir and methotrexate by using GraphPad™ 6.0 with nonlinear regression model.....	34
3. Determination of intracellular tenofovir accumulation in transport assay .....	46



4.	Determination of intracellular methotrexate accumulation in transport assay .....	47
5.	Determination of intravesicular tenofovir accumulation in uptake assay	48
6.	Determination of intravesicular methotrexate accumulation in uptake assay .....	50
7.	Calculation of relative gene expression.....	52
8.	Chromatogram of tenofovir and methotrexate in transport assay and uptake assay.....	53
VITA.....		59

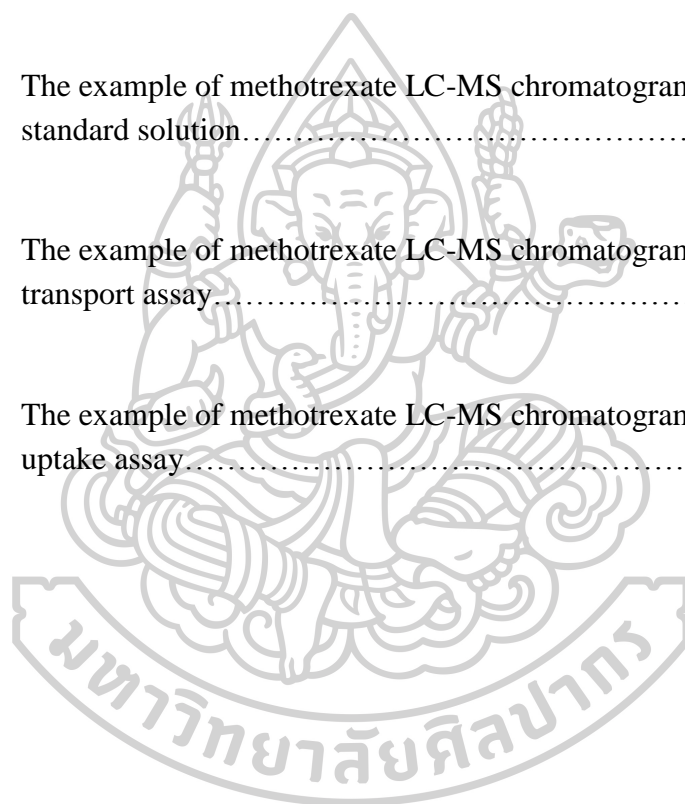


## LIST OF FIGURES

	Page
Figure 1.1.1 Tenofovir disoproxil fumarate (TDF) is an oral prodrug and acyclic nucleotide analog of adenosine monophosphate that inhibits HIV-1 ..	19
Figure 2.1.1 Multiple mechanisms and targets of action of highly active antiretroviral drugs (HAART) which inhibits HIV replication.....	23
Figure 2.1.2 Chemical structures of acyclic nucleotides and prodrug ester form of tenofovir.....	24
Figure 2.1.3 Plasma and intracellular metabolism of tenofovir and their metabolites. ....	25
Figure 2.2.1 Toxic mechanism of tenofovir-induced nephrotoxicity at proximal tubular epithelium via inhibition of mitochondrial DNA (mtDNA) replication.....	27
Figure 2.2.2 The light microscopic findings in TDF nephrotoxicity broadly resemble changes seen in other forms of toxic acute tubular necrosis (ATN).....	28
Figure 2.2.3 The electron microscopic findings in TDF-induced mitochondria toxicity.....	29
Figure 2.3.1 Protein transporters involved in tenofovir elimination at basolateral and luminal surface of the proximal renal tubule. ....	32
Figure 2.3.2 Immunohistochemistry staining of human kidney shows strong granular cytoplasmic positivity in proximal tubular epitheliums in tubules but not in glomerulus.....	34

Figure 3.3.1	Conceptual framework of this experimental research.....	41
Figure 3.3.1.1	ABCC11 or MRP8-overexpressed cells and parental cells handling procedure.....	43
Figure 3.3.2.1	Diagram of human ABCC11 or MRP8 mRNA isolation and storage..	46
Figure 3.3.2.2	Diagram of the determination of human ABCC11 or MRP8 mRNA expression levels by real-time polymerase chain reaction. ....	47
Figure 3.3.3.1	Diagram of the determination of human ABCC11 or MRP8 transporter protein expression level by indirect immunofluorescence assay. ....	49
Figure 3.3.4.1	Diagram of cytotoxic assay.....	50
Figure 3.3.5.1	Diagram of drug transport assay.....	52
Figure 3.3.6.1	Diagram of ATP-dependent vesicular uptake assay.....	55
Figure 3.3.6.2	Diagram of colorimetric protein assay (Bradford reagent assay) for standard curve. ....	56
Figure A.2	Standard curve of tenofovir (areas under the curve (m/z ratio = 208)) in cellular transport assay.....	46
Figure A.3	Standard curve of methotrexate (areas under the curve (m/z ratio = 455)) in cellular transport assay.....	47
Figure A.4	Standard curve of tenofovir (areas under the curve (m/z ratio = 208)) in vesicular uptake assay.....	48
Figure A.5	Standard curve of methotrexate (areas under the curve (m/z ratio = 455)) in vesicular uptake assay.....	50

Figure A.6	The example of tenofovir LC-MS chromatogram ( $m/z = 208$ ) in standard solution.....	53
Figure A.7	The example of tenofovir LC-MS chromatogram ( $m/z = 208$ ) in transport assay.....	54
Figure A.8	The example of tenofovir LC-MS chromatogram ( $m/z = 208$ ) in uptake assay.....	55
Figure A.9	The example of methotrexate LC-MS chromatogram ( $m/z = 455$ ) in standard solution.....	56
Figure A.10	The example of methotrexate LC-MS chromatogram ( $m/z = 455$ ) in transport assay.....	57
Figure A.11	The example of methotrexate LC-MS chromatogram ( $m/z = 455$ ) in uptake assay.....	58



## LIST OF TABLES

	Page
Table 2.3.1	Expression of ABCC transporters in normal tissues.....33
Table 4.2.1	Effect of MRP8-overexpression on cytotoxicity of tenofovir in LLC-PK1 cells. ....4
Table A.1	Protein content detection in vesicular transport assay of tenofovir at different time point by using spectrophotometer at 595 nm. ....23
Table A.2	Protein content detection in vesicular transport assay of methotrexate at different time point by using spectrophotometer at 595 nm. ....23
Table A.3	Quantification of protein content ( $\mu\text{g}$ ) in vesicular transport assay of tenofovir at different time point by using spectrophotometer at 595 nm. ....25
Table A.4	Quantification of protein content ( $\mu\text{g}$ ) in vesicular transport assay of methotrexate at different time point by using spectrophotometer at 595 nm. ....25
Table A.5	The percentage of cells viability of MK-571 on MRP8-overexpressed cells after incubation for 96 h. ....26
Table A.6	The percentage of cells viability of MK-571 on LLC-PK1 cells after incubation for 96 h. ....26
Table A.7	The percentage of cells viability of tenofovir without MK-571 on MRP8-overexpressed cells after incubation for 96 h. ....27
Table A.8	The percentage of cells viability of tenofovir with 50 $\mu\text{M}$ MK-571 on MRP8-overexpressed cells after incubation for 96 h. ....27

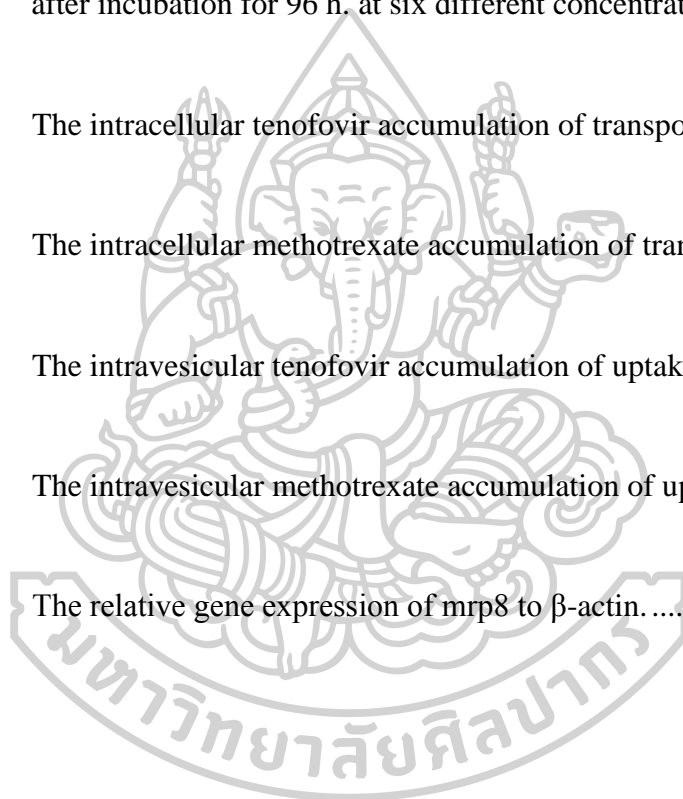
Table A.9	The percentage of cells viability of tenofovir with 100 $\mu$ M MK-571 on MRP8-overexpressed cells after incubation for 96 h. ....	27
Table A.10	The percentage of cells viability of tenofovir without MK-571 on LLC-PK1 cells after incubation for 96 h. ....	28
Table A.11	The percentage of cells viability of tenofovir with 50 $\mu$ M MK-571 on LLC-PK1 cells after incubation for 96 h. ....	29
Table A.12	The percentage of cells viability of tenofovir with 100 $\mu$ M MK-571 on LLC-PK1 cells after incubation for 96 h. ....	29
Table A.13	The percentage of cells viability of methotrexate without MK-571 on MRP8-overexpressed cells after incubation for 96 h. ....	30
Table A.14	The percentage of cells viability of methotrexate with 50 $\mu$ M MK-571 on MRP8-overexpressed cells after incubation for 96 h. ....	30
Table A.15	The percentage of cells viability of methotrexate with 100 $\mu$ M MK-571 on MRP8-overexpressed cells after incubation for 96 h. ....	31
Table A.16	The percentage of cells viability of methotrexate with 150 $\mu$ M MK-571 on MRP8-overexpressed cells after incubation for 96 h. ....	31
Table A.17	The percentage of cells viability of methotrexate without MK-571 on LLCPK1 cells after incubation for 96 h. ....	32
Table A.18	The percentage of cells viability of methotrexate with 50 $\mu$ M MK-571 on LLCPK1 cells after incubation for 96 h. ....	32
Table A.19	The percentage of cells viability of methotrexate with 100 $\mu$ M MK-571 on LLCPK1 cells after incubation for 96 h. ....	33

Table A.20	The percentage of cells viability of methotrexate with 150 $\mu$ M MK-571 on LLC-PK1 cells after incubation for 96 h. ....	33
Table A.21	The $CC_{50S}$ ( $\mu$ M) value of methotrexate without MK-571 on LLC-PK1 cells after incubation for 96 h. (Calculation by GraphPad™ 6.0 with nonlinear regression model) .....	34
Table A.22	The $CC_{50S}$ ( $\mu$ M) value of methotrexate with 50 $\mu$ M of MK-571 on LLC-PK1 cells after incubation for 96 h. (Calculation by GraphPad™ 6.0 with nonlinear regression model) .....	34
Table A.23	The $CC_{50S}$ ( $\mu$ M) value of methotrexate with 100 $\mu$ M of MK-571 on LLC-PK1 cells after incubation for 96 h. (Calculation by GraphPad™ 6.0 with nonlinear regression model) .....	35
Table A.24	The $CC_{50S}$ ( $\mu$ M) value of methotrexate with 150 $\mu$ M of MK-571 on LLC-PK1 cells after incubation for 96 h. (Calculation by GraphPad™ 6.0 with nonlinear regression model) .....	35
Table A.25	The $CC_{50S}$ ( $\mu$ M) value of methotrexate without MK-571 on MRP8-overexpressed cells after incubation for 96 h. (Calculation by GraphPad™ 6.0 with nonlinear regression model) .....	36
Table A.26	The $CC_{50S}$ ( $\mu$ M) value of methotrexate with 50 $\mu$ M MK-571 on MRP8-overexpressed cells after incubation for 96 h. (Calculation by GraphPad™ 6.0 with nonlinear regression model) .....	36
Table A.27	The $CC_{50S}$ ( $\mu$ M) value of methotrexate with 100 $\mu$ M MK-571 on MRP8-overexpressed cells after incubation for 96 h. (Calculation by GraphPad™ 6.0 with nonlinear regression model) .....	37
Table A.28	The $CC_{50S}$ ( $\mu$ M) value of methotrexate with 150 $\mu$ M MK-571 on MRP8-overexpressed cells after incubation for 96 h. (Calculation by GraphPad™ 6.0 with nonlinear regression model) .....	37

Table A.29	The CC <sub>50S</sub> (μM) value of tenofovir without MK-571 on LLC-PK1 cells after incubation for 96 h. (Calculation by GraphPad™ 6.0 with nonlinear regression model) .....	38
Table A.30	The CC <sub>50S</sub> (μM) value of tenofovir with 50 μM MK-571 on LLC-PK1 cells after incubation for 96 h. (Calculation by GraphPad™ 6.0 with nonlinear regression model) .....	38
Table A.31	The CC <sub>50S</sub> (μM) value of tenofovir with 100 μM MK-571 on LLC-PK1 cells after incubation for 96 h. (Calculation by GraphPad™ 6.0 with nonlinear regression model) .....	39
Table A.32	The CC <sub>50S</sub> (μM) value of tenofovir without MK-571 on MRP8-overexpressed cells after incubation for 96 h. (Calculation by GraphPad™ 6.0 with nonlinear regression model) .....	39
Table A.33	The CC <sub>50S</sub> (μM) value of tenofovir with 50 μM MK-571 on MRP8-overexpressed cells after incubation for 96 h. (Calculation by GraphPad™ 6.0 with nonlinear regression model) .....	40
Table A.34	The CC <sub>50S</sub> (μM) value of tenofovir with 100 μM MK-571 on MRP8-overexpressed cells after incubation for 96 h. (Calculation by GraphPad™ 6.0 with nonlinear regression model) .....	40
Table A.35	The CC <sub>50S</sub> (μM) value of tenofovir on MRP8-overexpressed cells and LLC-PK1 cells after incubation for 96 h. (Calculation by GraphPad™ 6.0 with nonlinear regression model) .....	41
Table A.36	The CC <sub>50S</sub> (μM) value of methotrexate on MRP8-overexpressed cells and LLC-PK1 cells after incubation for 96. (Calculation by GraphPad™ 6.0 with nonlinear regression model) .....	41
Table A. 37	The percentage of cells viability of tenofovir on MRP8-overexpressed cells after incubation for 96 h. at six different concentrations. ....	42



Table A.38	The percentage of cells viability of tenofovir on LLC-PK1 cells after incubation for 96 h. at six different concentrations.....	43
Table A.39	The percentage of cells viability of methotrexate on MRP8-overexpressed cells after incubation for 96 h. at six different concentrations.....	44
Table A.40	The percentage of cells viability of methotrexate on LLC-PK1 cells after incubation for 96 h. at six different concentrations. ....	45
Table A.41	The intracellular tenofovir accumulation of transport assay.....	46
Table A.42	The intracellular methotrexate accumulation of transport assay.....	47
Table A.43	The intravesicular tenofovir accumulation of uptake assay. ....	49
Table A.44	The intravesicular methotrexate accumulation of uptake assay.....	51
Table A.45	The relative gene expression of mrp8 to $\beta$ -actin.....	52



## CHAPTER 1

### INTRODUCTION

#### 1.1 Statement and significance of the research problem

Tenofovir disoproxil fumarate is an orally bioavailable pro-drug of tenofovir, an acyclic nucleotide analog reverse transcriptase inhibitor [1, 2]. Tenofovir (TFV) is widely used as an anti-viral agent for effective treatment of HIV and hepatitis B infection [1, 2]. Concerns regarding nephrotoxicity were initially raised because of the similarity of chemical structure of tenofovir and other cyclic nucleotide analogs such as adefovir and cidofovir (Figure 1.1.1 A and B). Use of adefovir and cidofovir was associated with proximal tubulopathy due to decreased mitochondrial DNA replication through inhibition of mitochondria DNA polymerase- $\gamma$  [3]. Furthermore, numerous clinical studies have indicated significant association between tenofovir use and decline in estimated glomerular filtration rate (eGFR). The nephrotoxicity of tenofovir varied widely, ranging from less than minimal to severe cases of renal Fanconi syndrome or acute kidney injury [4]. The incidences of tubular dysfunction were demonstrated in 17 - 22% of the tenofovir-treated patients [1, 4]. The risk factors for nephrotoxicity included long-term use, pre-existing kidney diseases, increased age, lower CD4<sup>+</sup> cells count, baseline elevation of serum creatinine, dose, concomitant nephrotoxic medications and low body mass [1, 2, 4, 5]. Mitochondria of the proximal tubular cells are the major target of tenofovir toxicity due to its complement of cells membrane transporters that favor tenofovir accumulation, but the exact mechanism of toxicity remains unclear [1, 4, 5]. Tenofovir undergoes elimination unchanged in urine via the combination of glomerular filtration and active proximal tubular secretion [1, 2]. Approximately, 20 - 30% of tenofovir is actively transported into renal proximal tubular cells by organic anion transporters at the basolateral membrane, hOAT1 and to lesser extent by OAT3 [1, 4]. Subsequently, the drug is secreted into the tubular lumen via apical membrane efflux transporters ABCC2 (MRP-2), ABCC4 (MRP-4) and ABCC10 (MRP-7) [1, 4, 5]. Therefore, multidrug resistant transporter protein MRP-2, MRP-4 and MRP-7 malfunctions could contribute to renal tubular cells damage.

Recently, genetic variants in a number of transporter proteins involved in tenofovir excretion have not been clearly associated with renal damage. It remains controversial by which genetic variants may predispose renal cells to TDF toxicity. Kiser *et al.* [6] characterized associations between intracellular tenofovir diphosphate concentrations and polymorphisms in the drug transporter genes SLC22A6, ABCC2, and ABCC4 in HIV-infected patients. The author found that ABCC4 3463G variants had higher intracellular tenofovir diphosphate concentrations (35% higher than wild type). Izzedine *et al.* [7] also investigated the correlations between genetic variations of genes encoding the ABCC2 and ABCC4 transporters and renal proximal tubulopathy. No association was observed between ABCC4 polymorphism and tenofovir-induced renal proximal tubulopathy in their study. However, ABCC2 haplotypes were associated with renal proximal tubulopathy induced by TDF in HIV-1-infected patients. Pushpakom *et al.* [8] explored whether MRP-7 was able to transport tenofovir and whether ABCC10 single-nucleotide polymorphisms [SNPs] were associated with kidney tubular damage. Two ABCC10 SNPs [rs9349256 and rs2125739] and their haplotype were significantly associated with kidney tubular damage. Therefore, genetic variability within the ABCC10 gene may influence TFV renal tubular transport and contribute to the development of kidney tubular damage. Nishijima *et al.* [9] had determined the association between polymorphisms in genes encoding drug transporters and kidney tubular damage in Japanese patients treated with tenofovir. Univariate and multivariate analyses showed significant association between kidney tubular damage and genotype CC at position -24 CC and genotype AA at position 1249 of ABCC2. ABCC2 haplotype -24T and 1249G was a protective haplotype for kidney tubular damage. This was the first study, to our knowledge, to identify the association between SNPs in ABCC2 and tenofovir-induced kidney tubular damage in an Asian population. As mentioned earlier, since multiple players of efflux transporters existed, it might be difficult to find significant proteins whose polymorphisms could be of significance in tenofovir nephrotoxicity. It was also possible that other compensated efflux mechanisms via other MRPs located on the renal proximal tubular region may play a role. Furthermore, there existed over 48 distinct members of multidrug resistance proteins encoded by *abcc* genes that belong

to the ATP-Binding Cassette (ABC) transporter superfamily at the renal proximal tubular region [10-16].

Among the members of ABC-transporter subfamily C, ABCC11 or MRP8 encoded by *abcc11* gene belongs to a new class of MRP members [17]. MRP8 expression is low in all normal human tissues except lung, fetal tissue, kidney, spleen, colon and brain [18-23]. At the kidney, MRP8 is highly expressed on proximal region but is not found on glomeruli. MRP8 is able to transport a diverse range of lipophilic anions, including cyclic nucleotides, estradiol-17beta-glucuronide, steroid sulfates such as dehydroepiandrosterone (DHEAS) and estrone sulfate (E(1)S), glutathione conjugates such as leukotriene C4 and dinitrophenyl-S-glutathione, and monoanionic bile acids [22, 24]. MRP8 transmembrane protein configuration structure resembles MRP4 and MRP5 with respect to possessing only two membrane spanning domains [24]. Amino acid comparison indicates that MRP8 more closely resembles MRP5, and the substrate selectivity of MRP8 is more similar to that of MRP4 [25-27]. Moreover, cyclic nucleotides are the only physiological transport substrates that MRP4, MRP5, and MRP8 are known to have in common [24, 28, 29] and tenofovir has chemical structure related to cyclic nucleotide analog [1, 2].

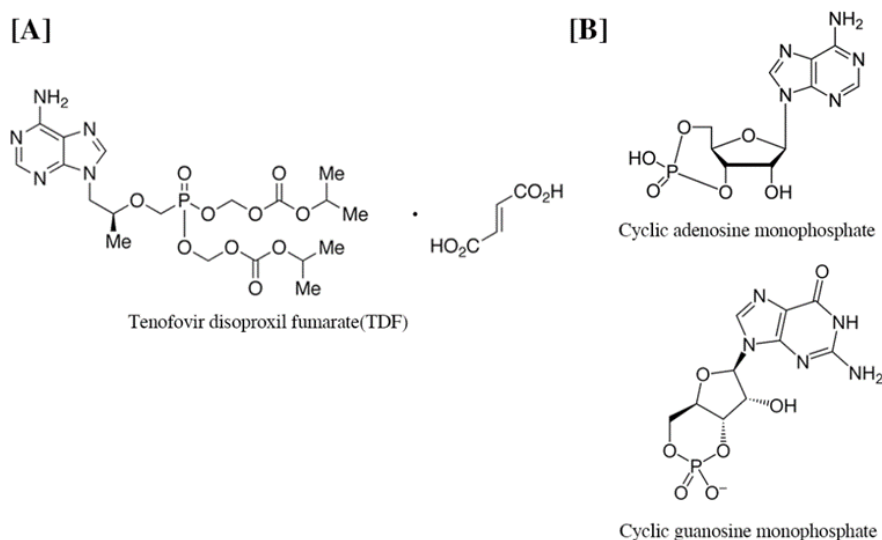


Figure 1.1.1 A) Tenofovir disoproxil fumarate (TDF) is an oral prodrug and acyclic nucleotide analog of adenosine monophosphate that inhibits HIV-1. B) Chemical structure of cyclic nucleotide analog, cAMP and cGMP.

With the abundance of ABCC11 in the kidney, in this study we hypothesized that ABCC11 plays a role in TDF transport in renal proximal tubular cells. Pig Kidney Epithelial (LLC-PK1) MRP8-overexpressed and parental cells were selected as a suitable epithelium model to demonstrate the efflux transport of TDF of proximal renal tubular region [30, 31].

## **1.2 Objective of this research**

- 1.2.1 To demonstrate the functions of MRP8 glycoprotein on tenofovir transport using MRP8-overexpressed cells lines and MRP8-overexpressed vesicles.
- 1.2.2 To examine the effects of intracellular tenofovir accumulation on cells viability in MRP8-overexpressed cells.

## **1.3 The research hypothesis**

- 1.3.1 Tenofovir is transported by MRP8 glycoprotein.
- 1.3.2 Overexpression of MRP8 increases viability of culture cells treated with tenofovir through efflux mechanism.
- 1.3.3 Intracellular accumulation of tenofovir is associated with decrease in cells viability.

## CHAPTER 2

### LITERATURE REVIEWS

2.1 Background information.

2.2 Tenofovir-induced nephrotoxicity.

2.3 Role of renal transporters in tenofovir metabolism and toxicity.



## 2.1 Background information

Tenofovir disoproxil fumarate (TDF) is an orally bioavailable prodrug of tenofovir, an acyclic nucleotide analogue reverse transcriptase inhibitor (NtRTI) (Figure 2.1.1) structurally similar to adefovir and cidofovir [32-38]. Their acyclic phosphonate group side chains also differ (Figure 2.1.2): namely, hydroxylphosphonomethoxypropyl (HPMP) for cidofovir, phosphonmethoxyethyl (PME) for adefovir, and phosphonomethoxypropyl (PMP) for tenofovir [34, 35, 37]. TDF was approved in 2001 by the US Food and Drug Administration (FDA) for the treatment of HIV infection [34, 35, 39]. TDF was also approved for treatment of chronic hepatitis B in adults in 2008 [24, 39-43].

TDF has many beneficial characteristics, including once-daily dosing, high efficacy both as single agent and in combination with other antiretroviral drugs, and lack of interaction with cytochrome P450 [24, 44]. TDF is water-soluble, and has an oral bioavailability of 27% [39, 45-47] when taken in the fasted state, distribution volume = 0.813 L/kg, plasma half-life = 12 - 14.4 h. and protein binding = 7.2 % [39, 45-47]. After ingestion, TDF is hydrolyzed to free tenofovir by plasma esterase enzymes. Free tenofovir contains a phosphate group with negative charge on the chemical structure at physiological pH, and this gives the drug an affinity for anion-specific influx transporters. Tenofovir uptake from plasma into the intracellular compartment is mediated by organic anion transporters [1, 45, 48] to form tenofovir diphosphate by double intracellular phosphorylation (Figure 2.1.3). Tenofovir diphosphate is a structural analog of deoxyadenosine -5'- triphosphate [24, 49, 50], the usual substrate for viral RNA-directed DNA polymerase, and is a weak inhibitor of mammalian DNA polymerase- $\alpha$ , DNA polymerase- $\beta$ , and mitochondrial DNA (mtDNA) polymerase- $\gamma$  [1, 45, 51].

TDF mainly undergoes excretion via a combination of glomerular filtration and active tubular secretion such that 70 - 80% of an intravenous dose is recovered unchanged in the urine within 72 h [48]. About 20 - 30% of the drug is actively transported into renal proximal tubule cells by hOATs (mainly hOAT1 and, to a lesser

extent, hOAT3) in the basolateral membrane [1, 24, 45, 52]. Subsequently, the drug is secreted into the tubular lumen by the apical membrane transporters MRP-4 [1, 24, 45, 52] and MRP-7 [8, 12, 53]. TDF has less adverse effects on blood lipids, fat accumulation, gastrointestinal symptoms and mitochondrial toxicity than other nucleoside phosphonate reverse transcriptase inhibitors [29, 54-58]. Currently, the most common precaution of this drug in the clinical setting is nephrotoxicity. The prevalence of tenofovir-induced nephropathy reported in Europe and Thailand were 10 - 22% [1, 8, 24, 35, 59, 60] and 5 - 18%, respectively [61, 62]. With widespread use clinically, however, the prevalence of tenofovir-associated nephropathy have been steadily increased to more than 5 times the prevalence presented in early report during clinical trials [1, 43, 45, 55, 60, 63, 64].

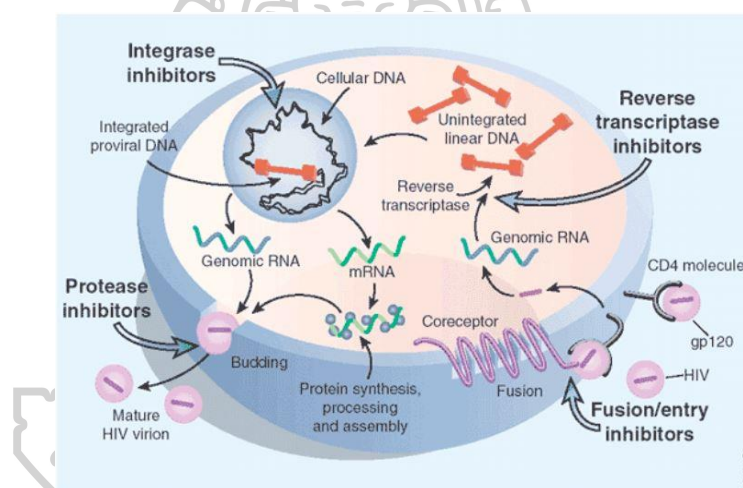


Figure 2.1.1 Multiple mechanisms and targets of action of highly active antiretroviral drugs (HAART) which inhibits HIV replication.

Source: Fauci AS. (2003). "HIV and AIDS: 20 years of science." **Nature medicine** 9, 839-43 (reprinted with permission).



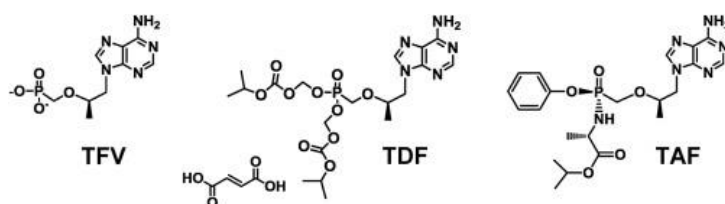
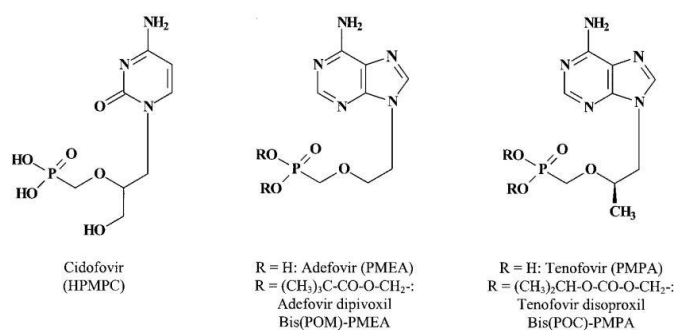
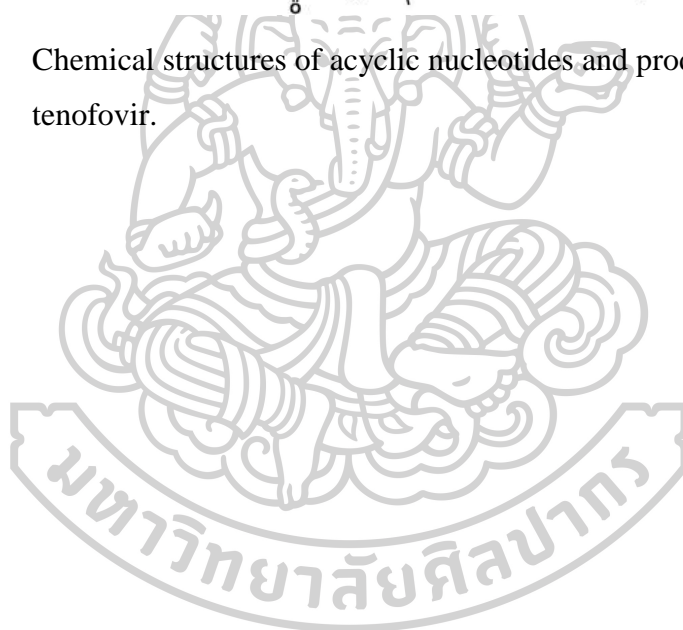


Figure 2.1.2 Chemical structures of acyclic nucleotides and prodrug ester form of tenofovir.



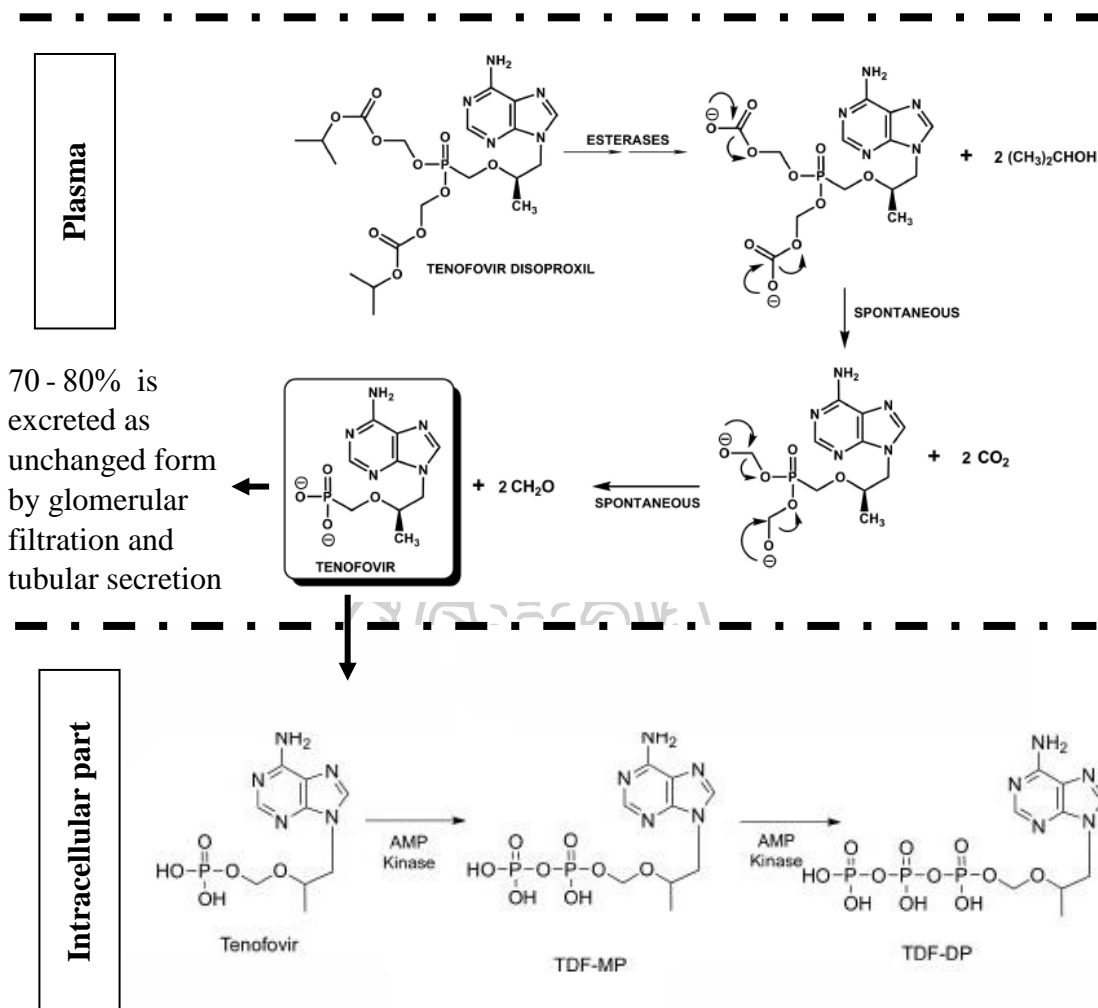


Figure 2.1.3 Plasma and intracellular metabolism of tenofovir and their metabolites.

## 2.2 Tenofovir-induced nephrotoxicity.

The risk factors of tenofovir-induced nephrotoxicity include long-term use, pre-existing kidney diseases, increased age, lower CD4+cells count, elevated Scr baseline, dose, concomitant nephrotoxic medications and low body mass [4, 5, 7, 61, 62]. The proximal tubular cells are the main target of tenofovir-induced nephrotoxicity due to its complement of cells membrane transporters that favor tenofovir accumulation. Current evidence suggests that mitochondria at the proximal tubular epithelium cells are the target organelles of tenofovir-induced nephrotoxicity [1, 45, 51]. The presentations of tenofovir induced-nephropathy are proximal tubular

dysfunction with preserved renal function and proximal tubular dysfunction associated with decreased renal function [12, 53]. Concerns regarding nephropathy were initially raised by the structural similarity between tenofovir and other nephrotoxic acyclic nucleotide analogues, such as adefovir and cidofovir. These two drugs cause proximal tubulopathy, possibly due to decreasing mitochondrial DNA replication through inhibition of mitochondria DNA polymerase- $\gamma$  [39, 45, 48, 55].

The inhibition of mtDNA polymerase- $\gamma$  encoded by *POLG* gene has been proposed to play a central role in tenofovir-induced mitochondrial toxicity which contributed to nephropathy [1, 53, 65]. Inherited *POLG* abnormalities lead to decrease mtDNA content and accumulation of mtDNA defects (Figure 2.2.1) [66]. Depletion of mtDNA may lead to fatty acid and dicarboxylic acid accumulation, lactic acidosis and reactive oxygen species (ROS) damage, and sensitivity to apoptosis. Although tenofovir has not been studied, NRTI with similar structure such as cidofovir was known to induce proximal tubular apoptosis by caspase activation throughout the mitochondrial pathway [66]. That may also be a potential mechanism of tenofovir-induced tubular cells injury worthy of further investigation.

The histological findings of tenofovir-induced nephropathy exhibit diffuse and severe acute degenerative changes including luminal ectasia, cytoplasmic simplification, irregular luminal contours, loss of brush border, interstitial fibrosis and focal apoptosis with epithelial desquamation and adjacent interstitial edema (Figure 2.2.2) [67]. These findings are typical of toxic tubular necrosis. The electron microscopy shows mitochondrial enlargement, depletion and dysmorphic changes (Figure 2.2.3). A characteristic feature of TDF nephropathy is eosinophilic intracytoplasmic inclusion within proximal tubular epithelial cells, corresponding to the giant mitochondria [67, 68]. In addition, cidofovir and adefovir have been well-described in association with nephrotoxicity, including acute renal failure and Fanconi syndrome. Fanconi syndrome is a term used to describe a global dysfunction of the proximal tubule that is responsible for the reabsorption of solutes, including bicarbonate, glucose, amino acids and phosphate. This solute loss leads to acidosis, bone disease and serum electrolyte abnormalities [4, 45, 57, 69].

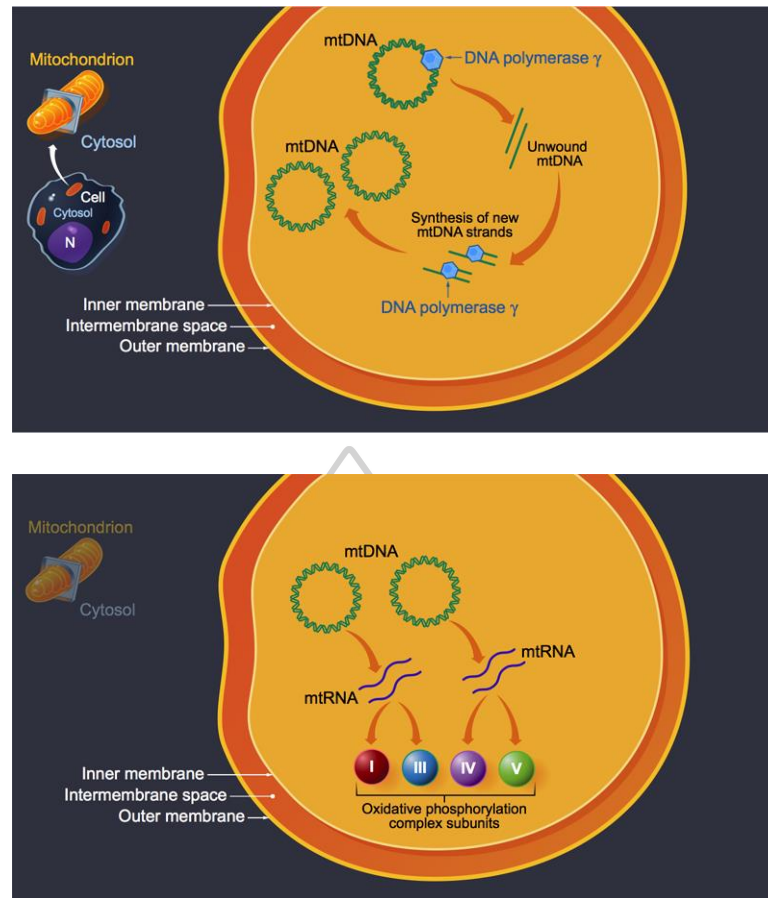
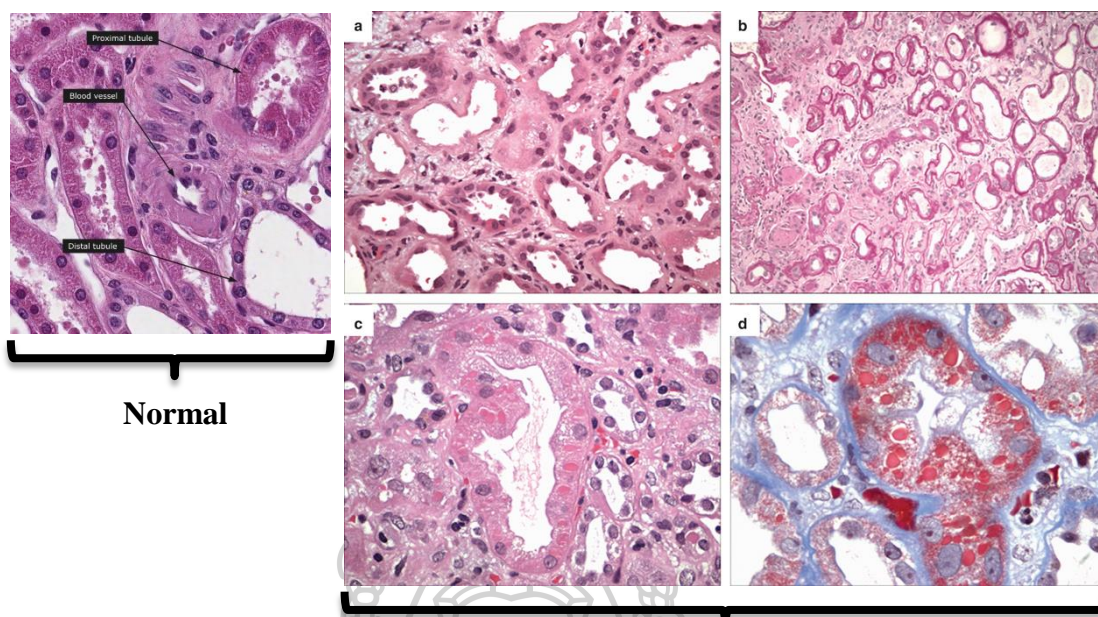


Figure 2.2.1 Toxic mechanism of tenofovir-induced nephrotoxicity at proximal tubular epithelium via inhibition of mitochondrial DNA (mtDNA) replication.

Source: Brinkman K, Kakuda TN. (2000). "Mitochondrial toxicity of nucleoside analogue reverse transcriptase inhibitors: a looming obstacle for long-term antiretroviral therapy?". **Current opinion in infectious diseases** 13, 5-11 (reprinted with permission).



### Histopathology of tenofovir-induced renal toxicity

Figure 2.2.2 The light microscopic findings in TDF nephrotoxicity broadly resemble changes seen in other forms of toxic acute tubular necrosis (ATN). **[A]** Proximal tubules exhibit diffuse and severe acute degenerative changes including luminal ectasia, cytoplasmic simplification, irregular luminal contours, loss of brush border, and focal apoptosis with epithelial desquamation, with adjacent interstitial edema. These findings are typical of toxic ATN (hematoxylin and eosin,  $\times 400$ ). **[B]** A low-power view demonstrates tubular simplification, as well as more chronic tubular atrophy and interstitial fibrosis. These light microscopic findings are consistent with an acute and chronic tubulointerstitial nephropathy (periodic acid-Schiff,  $\times 200$ ). **[C]** A characteristic feature of TDF nephrotoxicity is eosinophilic intracytoplasmic inclusions within proximal tubular epithelial cells, corresponding to the giant mitochondria seen ultrastructurally (hematoxylin and eosin,  $\times 600$ ). **[D]** The proximal tubular inclusions stain red (or fuchsinophilic) with trichrome stain ( $\times 1000$ ).

Source: Herlitz LC, et al. (2010). "Tenofovir nephrotoxicity: acute tubular necrosis with distinctive clinical, pathological, and mitochondrial abnormalities." **Kidney international** 78, 1171-7 (reprinted with permission).

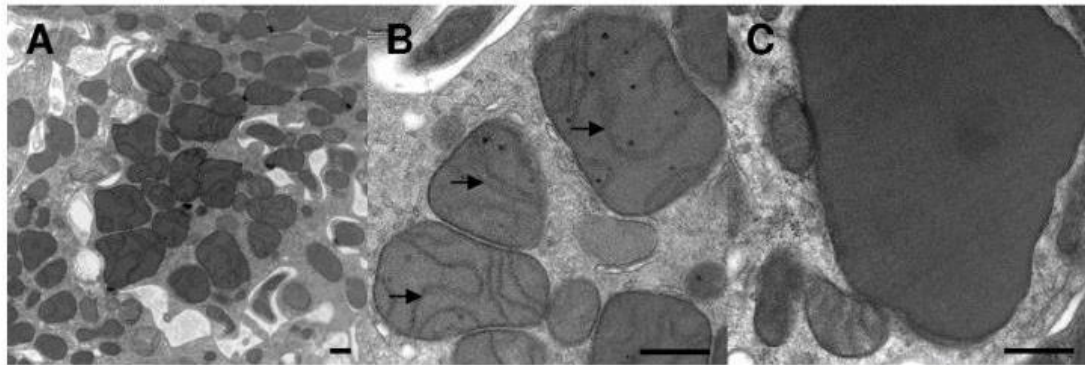


Figure 2.2.3 The electron microscopic findings in TDF-induced mitochondria toxicity. [A] A low-magnification field demonstrates the wide range in size and shape of mitochondria within proximal tubular epithelial cells ( $\times 5000$ ). [B] and [C] Markedly enlarged mitochondria are interspersed with normal-sized mitochondria in proximal tubular cells ( $\times 20000$ ).

Source: Herlitz LC, et al. (2010). “ Tenofvir nephrotoxicity: acute tubular necrosis with distinctive clinical, pathological, and mitochondrial abnormalities.”

**Kidney international** 78, 1171-7 (reprinted with permission).

### 2.3 Role of renal transporters in tenofvir metabolism and toxicity.

The exact mechanism of tenofvir-induced nephrotoxicity is not certain; however, it appears to result from drug accumulation in the proximal tubular cells. There are two theories that may explain how the accumulation leads to nephrotoxicity [45, 53]. The first is that tenofvir accumulation may be directly cytotoxic to the tubular cells. The second theory is supported by the observation that Fanconi syndrome is the most common renal manifestation of mitochondria cytopathies, a diverse group of diseases that are caused by abnormalities in mtDNA that result in mitochondrial dysfunction in various tissues [53]. The most effective treatment of tenofvir-induced nephropathy is to discontinue tenofvir [53]. Features of nephrotoxicity frequently improve following discontinuation of the drug [1, 53]. However, nephroprotection has been demonstrated by preventing tenofvir entry into proximal tubular cells or facilitating its exit or administering drugs that protect tubular cells from injury. Probenecid, an inhibitor of hOAT1 is also demonstrated to prevent

cidofovir toxicity and may also protect renal function from tenofovir due to structural similarity [53]. For that reason, numerous researches were focused to demonstrate the handling pathway of tenofovir at proximal renal tubular cells [1, 4, 8, 24, 45, 55, 68]. The result showed that about 20 - 30% of tenofovir is actively transported into renal proximal tubule cells by hOATs (mainly hOAT1 and, to lesser extent, hOAT3) in the basolateral membrane [1, 4, 8, 24, 53]. Subsequently, tenofovir is secreted into the tubular lumen via apical membrane efflux transporters ABCC4 (MRP-4) [24, 53] and ABCC10 (MRP-7) (Figure 2.3.1) [8, 53, 70, 71].

Therefore, multidrug resistant transporter protein MRP-4 and MRP-7 malfunctions could contribute to renal tubular cells damage. Recently, the information of genetic variants in transporter protein involved in tenofovir excretion, however, has not been clearly associated with renal damage. Currently, it is still controversial whether *ABCC2* and *ABCC4* polymorphisms alter the risk of tenofovir-induced nephrotoxicity [6, 7, 9, 53, 71]. *ABCC2* is not a tenofovir transporter at proximal tubular cells [24], nonetheless, the association study was demonstrated that *ABCC2* polymorphisms at positions -24 (rs717620) was associated with increased risk of tenofovir-induced nephrotoxicity [7, 15, 71].

A study in HIV-infected patients found that a 669C>T (rs899494) polymorphisms in the *ABCC4* gene was associated with tenofovir-induced nephrotoxicity, but this was not found in a subsequent study [7, 71]. Several additional single nucleotide polymorphism of *ABCC4* were investigated in HIV-infected patients [559G>T (rs11568658), 912G>T (rs2274407), 519G>T (rs2274406), 969G>A (rs2274405), 1497C>T (rs1557070), 3310T>C (rs11568655), 3348A>G (rs1751034)], but no association with tenofovir-induced nephrotoxicity was found [6]. In HIV-infected patients with *ABCC4* 3463A>G genotype receiving tenofovir diphosphate, patients with *ABCC4* 3463G variants had 35% higher tenofovir diphosphate concentrations than wild type [6].

The *ABCC10* efflux transporter is capable to transport tenofovir *in vitro*. Genetic polymorphisms at position 526G>A (rs9349256) and 2843T>C (rs212739) were associated with nephrotoxicity [8] but no replicated studies have been conducted. This may be partly explained that these SNPs were not significant

polymorphisms, or that there exist other compensated efflux mechanisms via other MRPs located on the renal proximal tubular region [1, 33, 45, 53].

At the renal proximal tubular region, there exist different multidrug resistance proteins encoded by a superfamily of 48 distinct members of the ATP-Binding Cassette (ABC) transporters [70, 72-77]. Among the members of ABC-transporter subfamily C, ABCC11 or MRP8 encoded by *abcc11* gene belongs to a new class of MRP members [10]. MRP8 expression is low in all normal human tissues except in lung, fetal tissue, kidney, spleen, colon and brain [11-16, 78] (Table 2.3.1). At the kidney, MRP8 is highly expressed on proximal region but not on glomeruli [79-81] (Figure 2.3.2). MRP8 is able to transport a diverse range of lipophilic anions, including cyclic nucleotides, estradiol-17 beta-d-glucuronide (E(2)17betaG), steroid sulfates such as dehydroepiandrosterone (DHEAS) and estrone sulfate (E(1)S), glutathione conjugates such as leukotriene C4 and dinitrophenyl-S-glutathione, and monoanionic bile acids [15, 17]. MRP8 transmembrane protein configuration structure resembles MRP4 and MRP5 with respect to possessing only two membrane spanning domains [17]. Amino acid comparisons indicate that MRP8 more closely resembles MRP4 and MRP5, and the substrate selectivity of MRP8 is more similar to that of MRP4 [18-20]. Moreover, cyclic nucleotides are the only physiological transport substrates that MRP4, MRP5, and MRP8 are known to have in common [17, 21-23] and chemical structure of tenofovir is similar to cyclic nucleotide analog [1, 2].

Therefore, we are interested to demonstrate the physiologic functions of MRP8 transporter protein in tenofovir efflux. Pig Kidney Epithelial (LLC-PK1) MRP8-overexpression and parental cells have been selected for this experiment to demonstrate this hypothesis due to its representation of the suitable monolayer of renal tubular epithelium at proximal region [17, 82, 83].



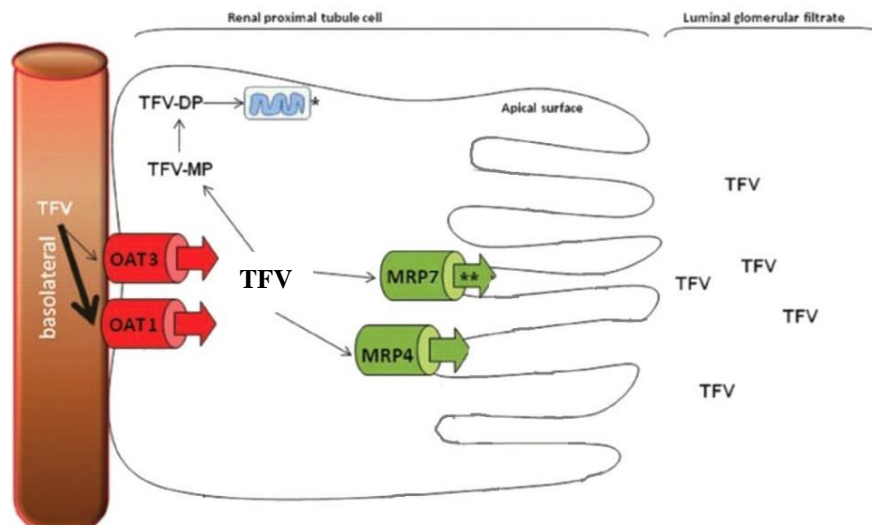


Figure 2.3.1 Protein transporters involved in tenofovir elimination at basolateral and luminal surface of the proximal renal tubule. OAT1, organic anion transporter 1; OAT3, organic anion transporter 3; MRP4, multidrug resistant protein 4; MRP7, multidrug resistant protein 7.

Source: Rodriguez-Novoa S, et al. (2009). "Predictors of kidney tubular dysfunction in HIV-infected patients treated with tenofovir: a pharmacogenetic study." **Clinical infectious diseases: an official publication of the Infectious Diseases Society of America** 48, e108-16 (reprinted with permission).

Table 2.3.1 Expression of ABCC transporters in normal tissues.

<b>Members: Symbol/alias</b>	<b>Human tissue expression</b>
ABCC1/MRP1	Lung, testes, peripheral blood mononuclear cells, lateral membrane
ABCC2/MRP2/CMOAT	Liver, intestine, kidney, apical membrane
ABCC3/MRP3/CMOAT2	Lung, intestine, liver, kidney, lateral membrane
ABCC4/MRP4/MOATB	Many tissue
ABCC5/MRP5/MOATC	Many tissue
ABCC6/MRP6/MOATE/PXE	Kidney, liver, lateral membrane
ABCC7/CFTR	Exocrine tissues, apical membrane
ABCC8/SUR1	Pancreas
ABCC9/SUR2	Skeleton muscle, heart
ABCC10/MRP7	Low in all tissues except pancreas
ABCC11/MRP8	Lung, kidney, colon, spleen, brain, breast and fetal tissue
ABCC12/MRP9	Breast, testes, brain, skeleton and ovary
ABCC13/PRED6	-

Source: Chen ZS, et al. (2005). "Transport of bile acids, sulfated steroids, estradiol 17-beta-D-glucuronide, and leukotriene C4 by human multidrug resistance protein 8 (ABCC11)." **Molecular pharmacology** 67, 545-57 (reprinted with permission).

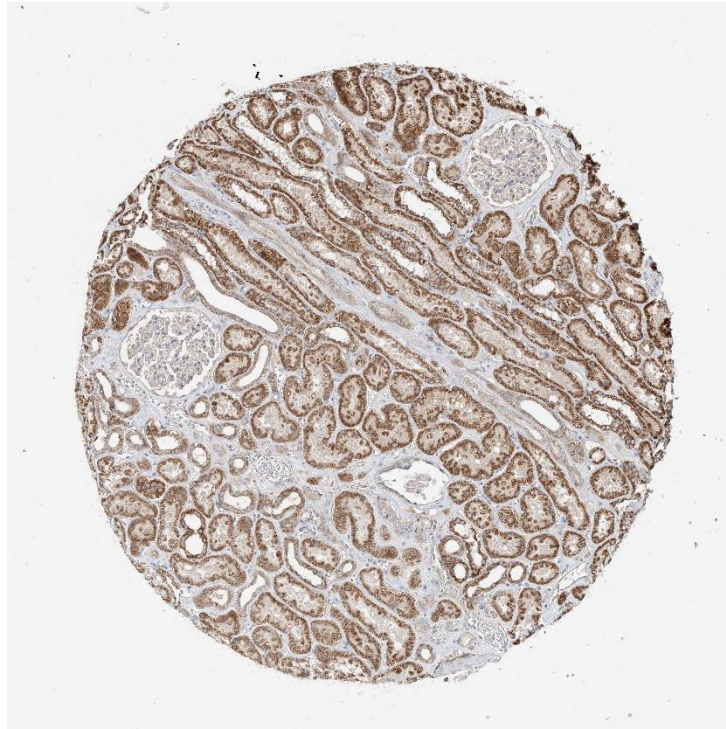


Figure 2.3.2 Immunohistochemistry staining of human kidney shows strong granular cytoplasmic positivity in proximal tubular epitheliums in tubules but not in glomerulus.

Source: Uhlen M, et al. (2005). "A human protein atlas for normal and cancer tissues based on antibody proteomics." **Molecular & cellular proteomics: MCP** 4, 1920-32 (reprinted with permission).

## CHAPTER 3

### MATERIALS AND METHODS

3.1 Materials

3.2 Equipment

3.3 Methods

3.3.1 Cells and vesicles preparation

3.3.2 mRNA isolation and real time-PCR (rt-PCR)

3.3.3 Indirect immunofluorescent staining

3.3.4 Cytotoxic assays

3.3.5 Drug transport assays

3.3.6 Uptake assays.

3.4 Statistical analysis



### 3.1 Materials

#### 3.1.1 Chemicals and reagents

0.25% trypsin-EDTA (GIBCO™, Grand Island, NY, U.S.A)

ABCC11 antibody (Invitrogen™ by Life Technologies Corporation, Grand Island, NY)

ABCC11-Primer (Invitrogen™ by Life Technologies Corporation, Grand Island, NY)

β-actin Primer (Invitrogen™ by Life Technologies Corporation, Grand Island, NY)

Alexa flour® 488 Phallo, 4', 6-Diamidino-2-Phenylin (Invitrogen™ by Life Technologies Corporation, Grand Island, NY)

Alexa flour® 488 goat anti-mouse serum IgM (Invitrogen™ by Life Technologies Corporation, Grand Island, NY)

Bio-Rad Protein Assay kit (Bio-Rad Laboratories, U.S.A)

Bovine serum albumin (BSA) (Bio-Rad Laboratories, U.S.A)

Bradford reagent (Bio-Rad Laboratories, U.S.A)

Chloroform (VWR International Ltd. England analytical reagent grade)

DAPI (Invitrogen™ by Life Technologies Corporation, Grand Island, NY)

DEPC-treated water 500ml (Thermo Fisher Scientific, Waltham, MA)

Dimethyl sulphoxide (DMSO) (Fisher Scientific; analytical reagent grade)

DPBS with magnesium and phosphate (GIBCO™, Grand Island, NY, U.S.A)

DPBS without magnesium and phosphate (GIBCO™, Grand Island, NY, U.S.A)

Fetal Bovine Serum (FBS) (GIBCO™, Grand Island, NY, U.S.A)

GM3010 MRPs-BCRP vesicular transport assay reagent set (Life Technologies Corporation, Grand Island, NY)

Goat serum (GIBCO™, Grand Island, NY, U.S.A)

L-glutamine (200 mM) (GIBCO™, Grand Island, NY, U.S.A)

LLC-PK1 cells (Genscript® Inc., UAS)

LLC-PK1-MRP8-overexpression cells (Genscript® Inc., U.A.S)

M199® medium (GIBCO™, Grand Island, NY, U.S.A)

Methanol (Merck, Germany; purity ≥ 99.9%)

Methotrexate (Sigma Aldrich®, St. Louis, MO, U.S.A)

MK-571 (Merck Millipore Inc., Darmstadt, Germany).

Paraformaldehyde (Sigma Aldrich®, St. Louis, MO, U.S.A)

Penicillin (GIBCO™, Grand Island, NY, U.S.A)

Penicillin-Streptomycin (GIBCO™, Grand Island, NY, U.S.A)

PrestoBlue® (GIBCO™, Grand Island, NY, U.S.A)

Purelink™ RNA mini purification kit (Invitrogen™ by Life Technologies Corporation, Grand Island, NY)

Puromycin dihydrochloride (GIBCO™, Grand Island, NY, U.S.A)

Pyruvate (GIBCO™, Grand Island, NY, U.S.A)

SF9-insect vesicles (Invitrogen™ by Life Technologies Corporation, Grand Island, NY)

SF9-MPR8-overexpression vesicles (Invitrogen™ by Life Technologies Corporation, Grand Island, NY)

Sodium pyruvate (GIBCO™, Grand Island, NY, U.S.A)

SS-III platinum SYBR green one step QRT-PCR (Invitrogen™ by Life Technologies Corporation, Grand Island, NY, U.S.A)

Sterile water for irrigation (General Hospital Products Public Co., Ltd.)

Streptomycin (GIBCO™, Grand Island, NY, U.S.A)

Synthetic ABCC11-primary antibody (Invitrogen™ by Life Technologies Corporation, Grand Island, NY, U.S.A)

Tenofovir disoproxil fumarate (Santa Cruz Biotechnology Inc, Dallas, TA)

Tenofovir (Santa Cruz Biotechnology Inc, Dallas, TA)

Triton®-X100 (Sigma Aldrich®, St. Louis, MO, U.S.A)

Trypan blue stain 0.4% (GIBCO™, Grand Island, NY, U.S.A)

Trypsin-EDTA 0.25% (GIBCO™, Grand Island, NY, U.S.A)

Vinblastine (Sigma Aldrich®, St. Louis, MO, U.S.A)

1 µm 96-well glass filters plate (Pall Corporation, Port Washington, NY)

### **3.2 Equipment**

- 20 degree Ultra Freezer (Haier, Chaina)

- 40 degree Ultra Freezer (Haier, Chaina)

- 80 degree Ultra Freezer (Haier, Chaina)

Automatic Autoclave (Model: LS-2D, Scientific Promotion Co., Ltd., Bangkok, Thailand)

Cells viability counters (Intivroten™ (Attune), U.S.A)

Centrifuge (Hermle Z300K; Labnet®; Lab Focus CO., Ltd.)

CO<sub>2</sub> incubator (HERA Cells 240 Heraeus)

EVOS-II™ imaging station (Intivroten™ - EVOS, U.S.A)

Incubation shaker (SHEL Lab, U.S.A)

Inverted Microscope (Model: ECLIPSE TE 2000-U, Nikon, Japan)

Laminar air flow (BIO-II-A)

Liquid nitrogen tank (Cryo Diffusion SA, France)

Microcentrifuge tube (Eppendorf<sup>®</sup>, Corning Incorporated, NY, U.S.A)

Microcentrifuge (Microfuge 16<sup>®</sup>, Model: A46473, Beckman Coulter Inc., Germany)

Micropipette 0.1 - 2.5  $\mu$ L, 2 - 20  $\mu$ L, 20 - 200  $\mu$ L, 100 - 1000  $\mu$ L and micropipette tip

Microplate reader (M965+ model, Metertech, Taiwan)

rt-PCR Analytika<sup>™</sup> (qTower 2.2, Analytika JENA AG Inc., Germany)

Spectrofluorometer (RF-1501, Shimadzu, Tokyo, Japan)

Tissue culture plate (96-, 24-, 12-, 6-Well plate) (Corning Incorporated, NY, U.S.A)

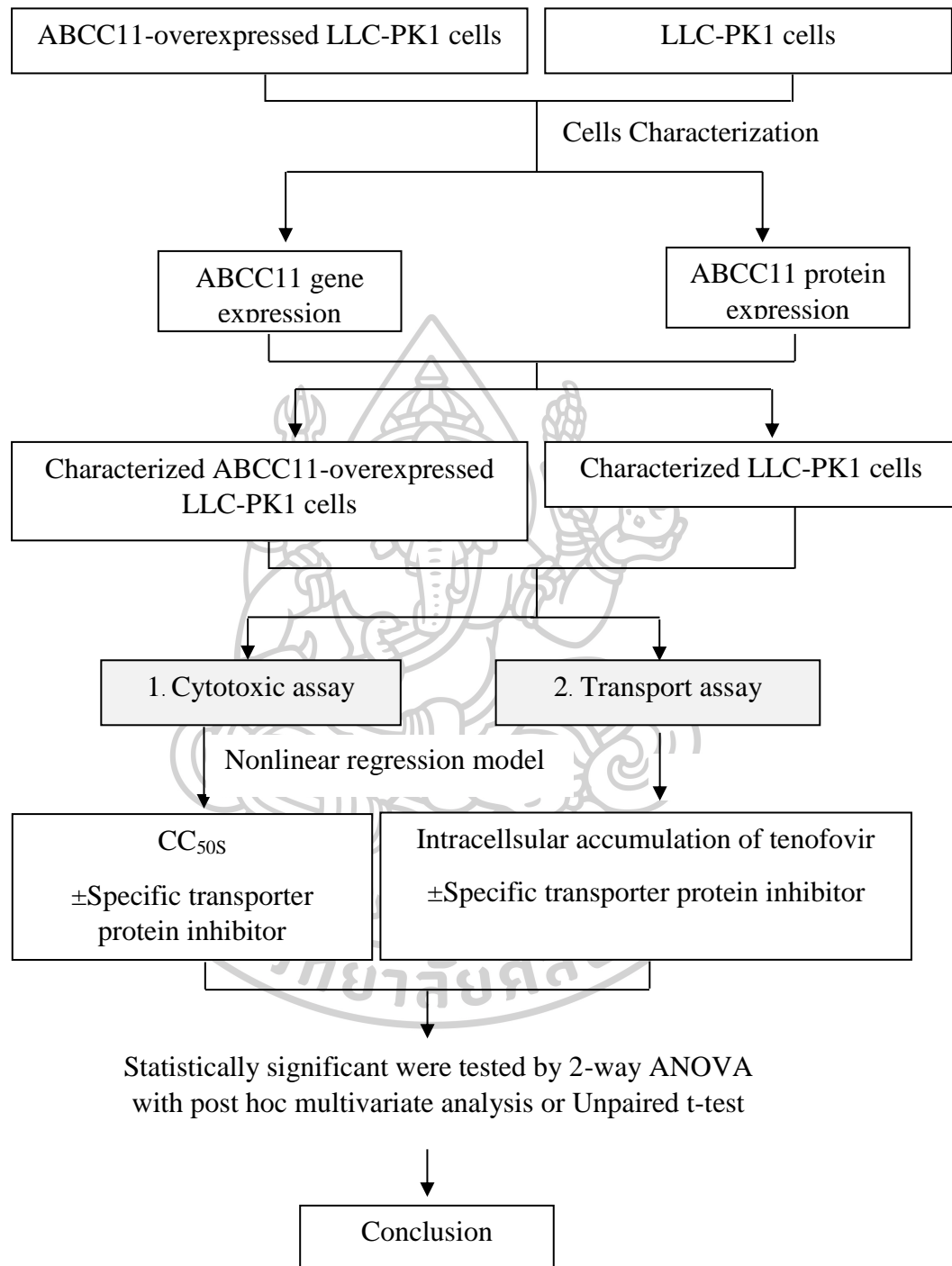
Vacuum filter (Pall Corporation, Port Washington, NY)

Vortex mixer (Model: Labnet, U.S.A)





### 3.3 Methods



(Continue on next page)

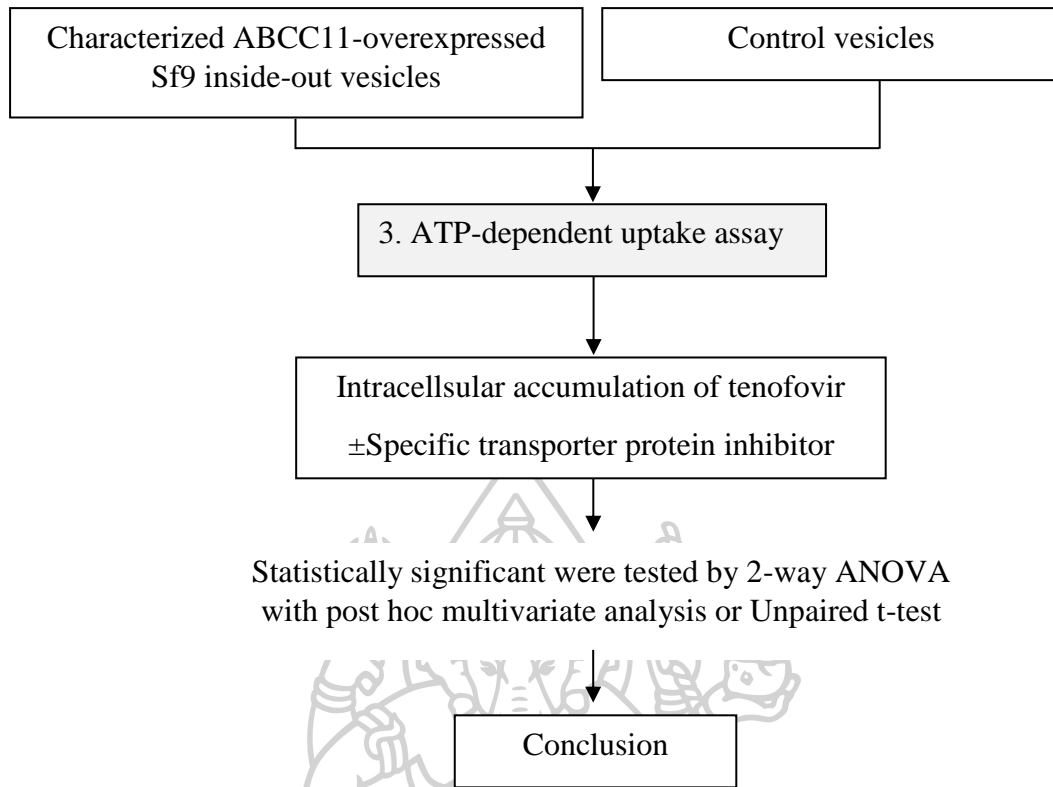
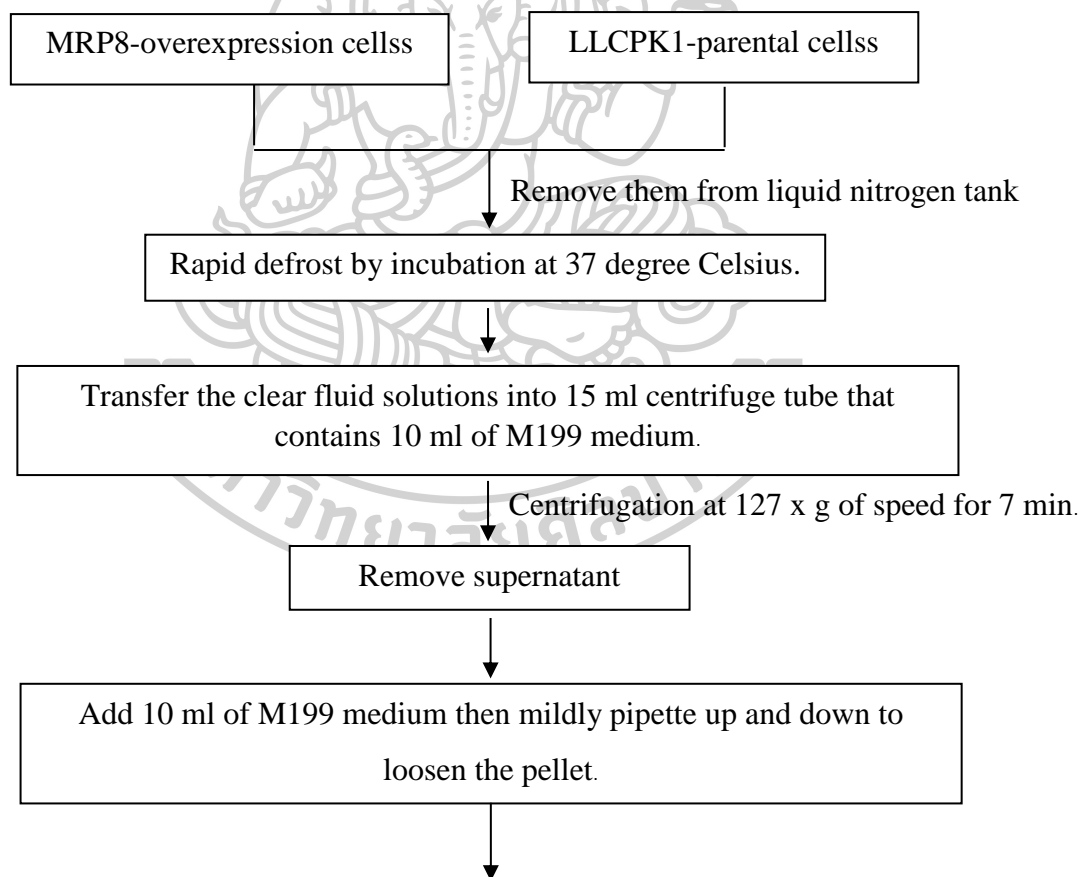


Figure 3.3.1 Conceptual framework of this experimental research

### 3.3.1 Cells and vesicles preparation.

LLC-PK1-ABCC11-overexpressed cells and LLC-PK1-parental cells (ATCC No.123546) were purchased from GenScript Inc. (Piscataway, NJ). Human ABCC11-overexpressed inside-out vesicle, control ABC transporter vesicle, and primers were purchased from Life Technologies Corporation (Grand Island, NY). LLC-PK1-ABCC11 and parental cells were grown under recommended conditions in M199 medium with 3% heat-inactivated fetal bovine serum, 100 µg/ml penicillin-streptomycin and 2 µg/ml puromycin dihydrochloride. Cells were passaged twice a week. Gene expression and protein expression were characterized by real-time PCR and indirect immunofluorescence assay, respectively.



(Continue on next page)

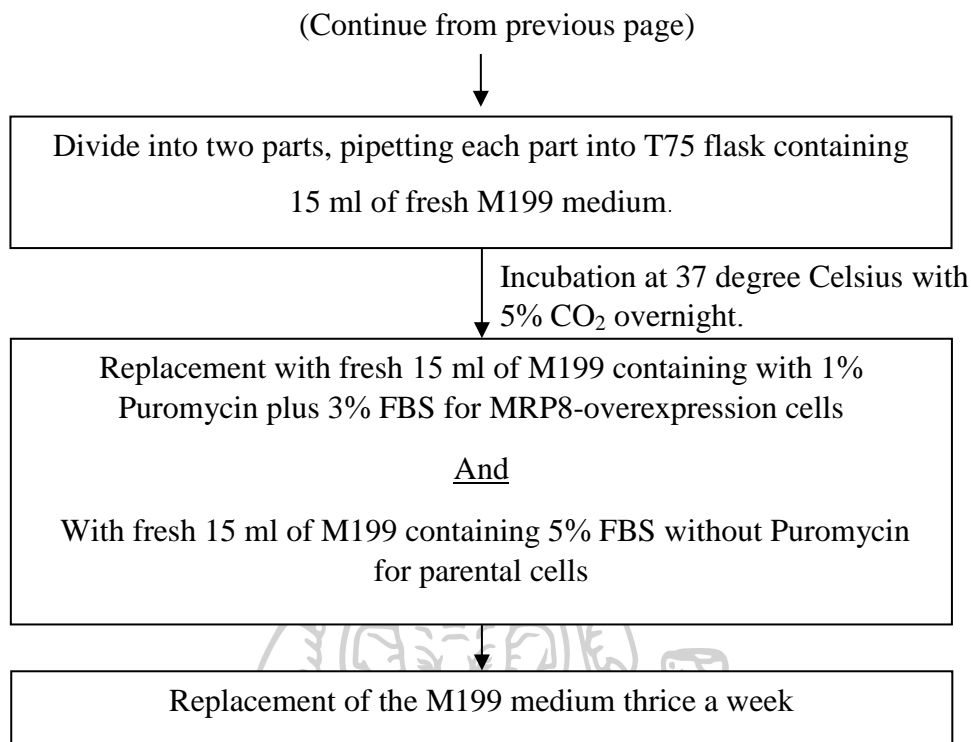
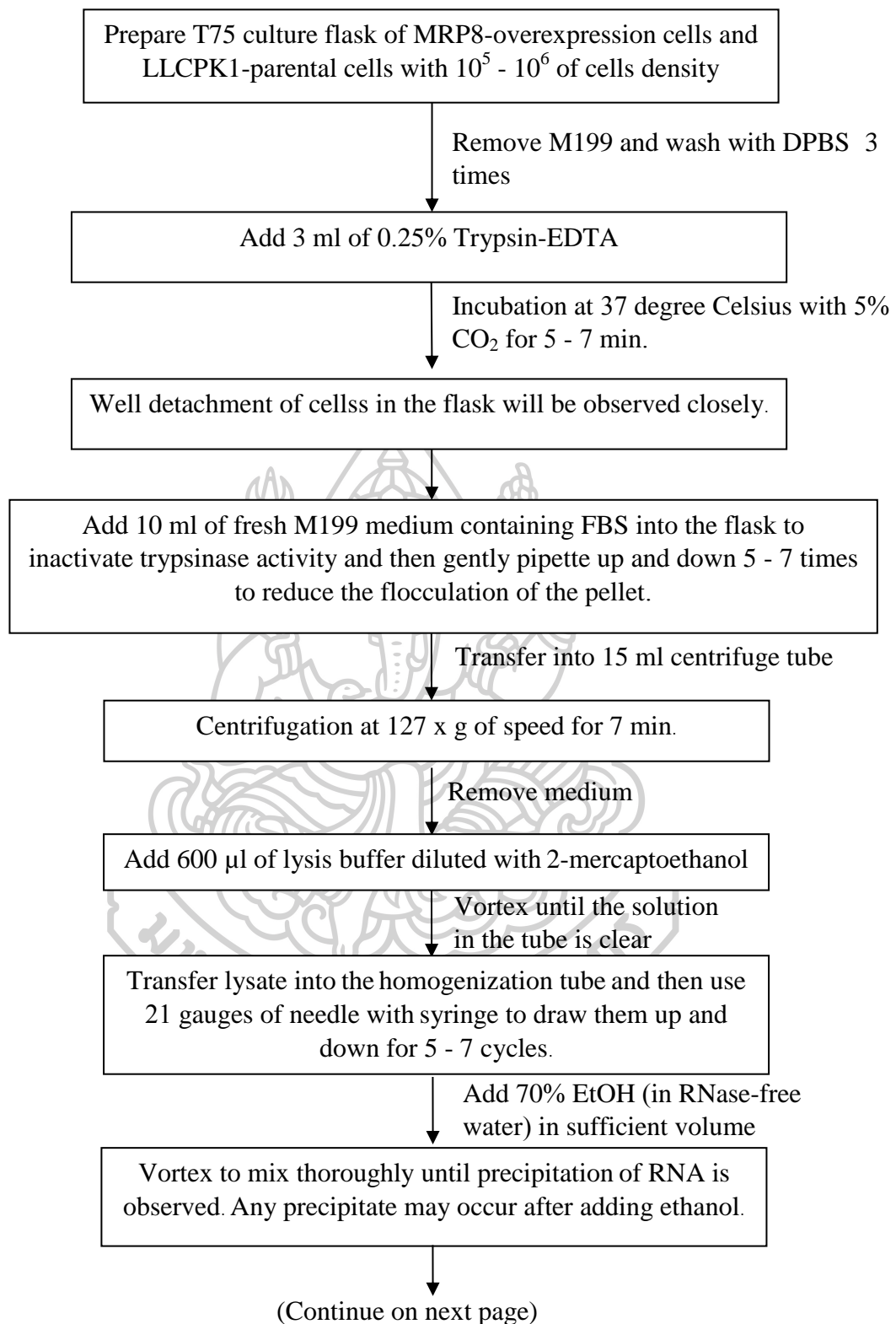
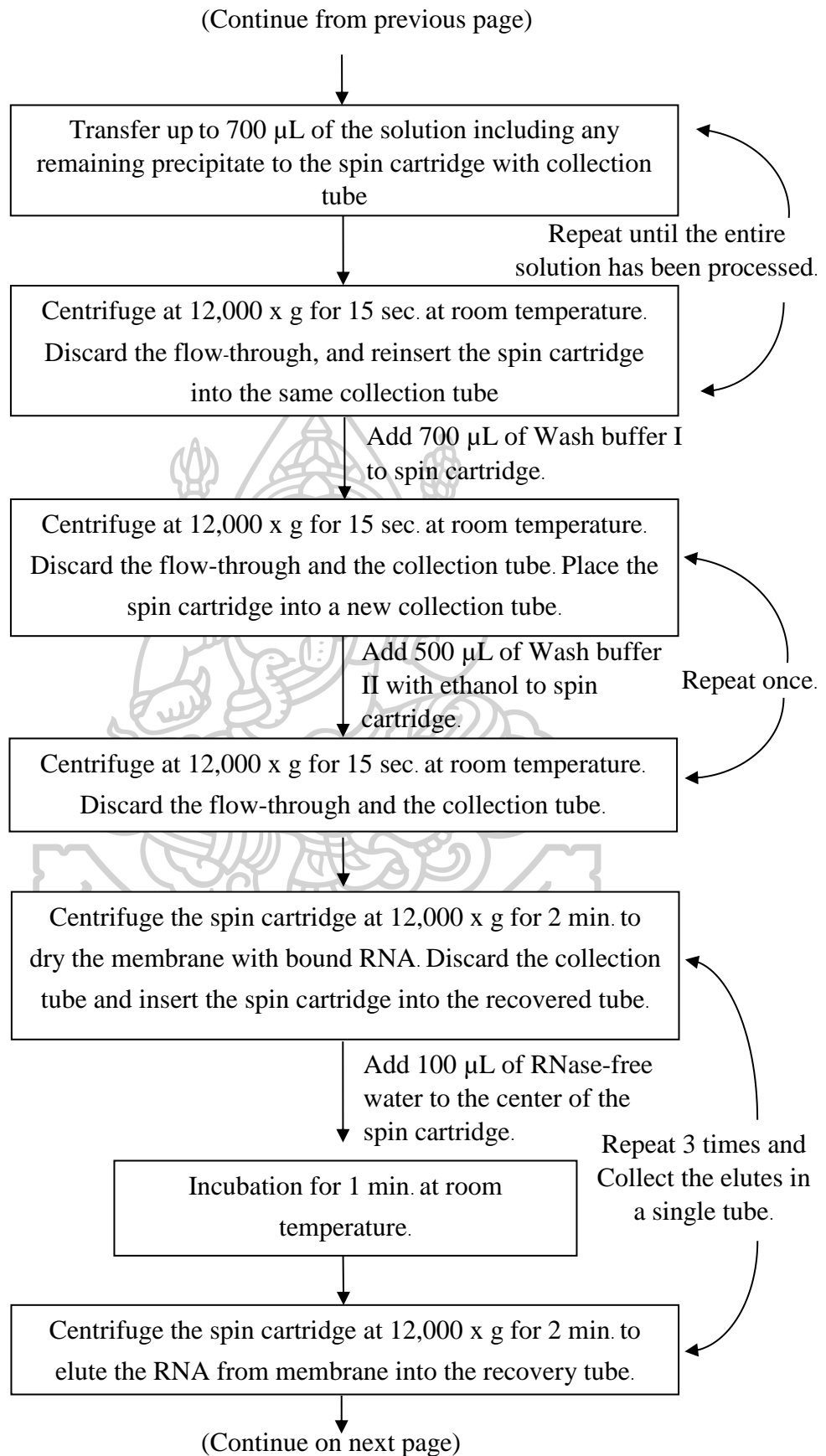


Figure 3.3.1.1 ABCC11 or MRP8-overexpressed cells and parental cells handling procedure.

### 3.3.2 mRNA isolation and Real Time-PCR (rt-PCR).

To evaluate human *abcc11* mRNA levels in MRP8-overexpressed LLC-PK1 cells compared with parental cells, a relative quantification was determined by real-time PCR. Briefly, cells were seeded in T75 cells culture flask until 80-95% confluence. For RNA extraction, Purelink™ reagent was added into cells and mRNA was isolated according to the manufacturer's protocol. The ABCC11-primer base (Forward primer = AGTATGATGCTGCCTTGA, Reverse primer = GGTGAGGTAGGAGAACAG),  $\beta$ -actin primer base (Forward primer = AACTACCTTCAACTCCATCA, Reverse primer = ATCTCCTTCTGCATCCTG) were purchased from Life Technologies Corporation (Grand Island, NY). A one-step quantitative RT-PCR SuperScript® III Platinum® SYBR® Green qRT-PCR kit was used for quantification mRNA expression as following conditions; 48°C for 3 minutes hold (cDNA synthesis), then, 40 cycles of 95°C for 15 seconds, 60°C for 30 seconds, 40°C for 1 minute. Data were quantified in relative expression using  $\beta$ -actin as reference gene.





(Continue from previous page)

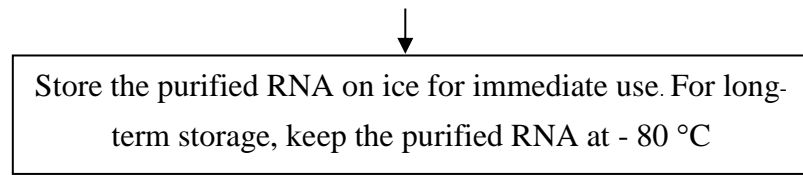
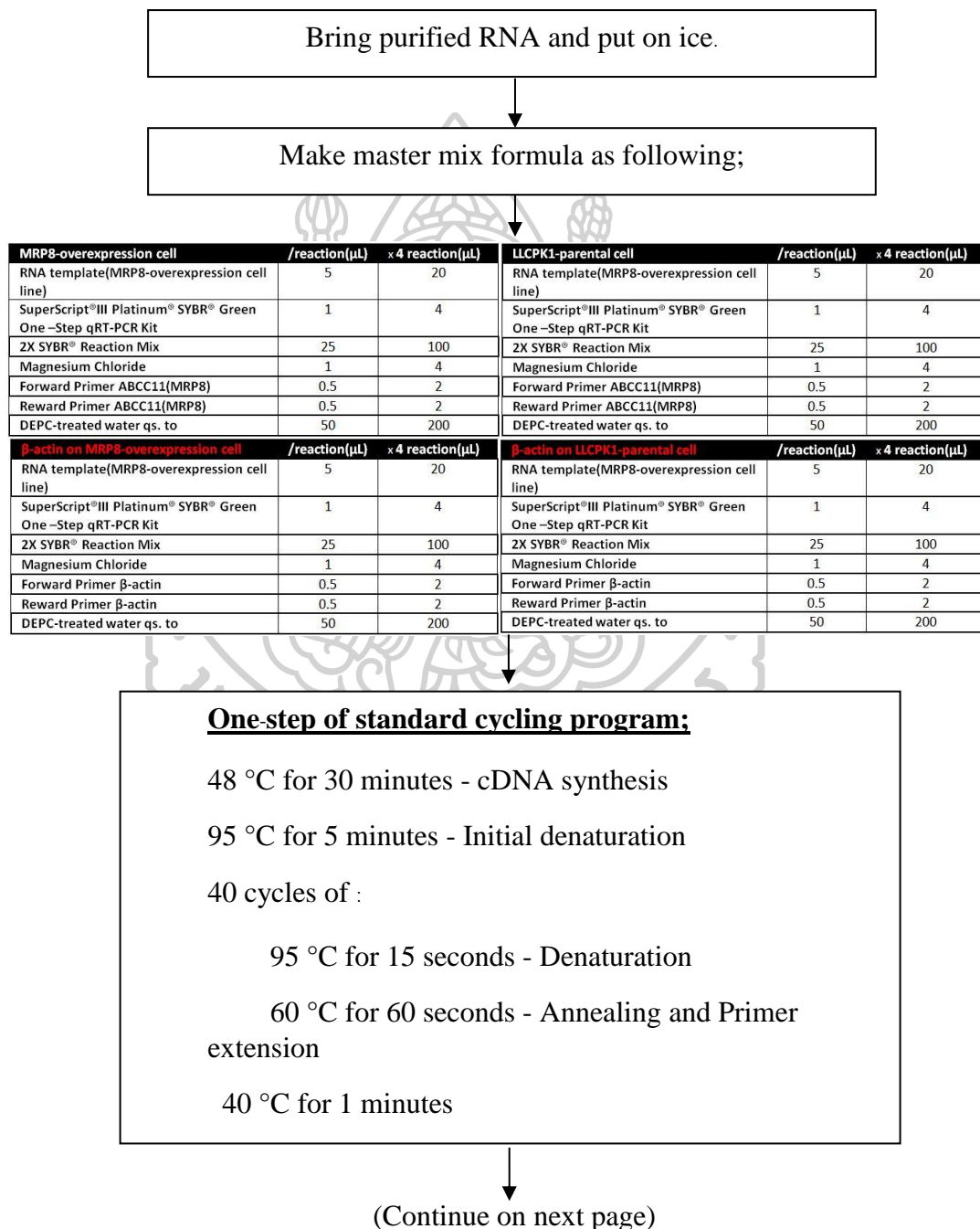


Figure 3.3.2.1 Diagram of human ABCC11 or MRP8 mRNA isolation and storage.



(Continue from previous page)

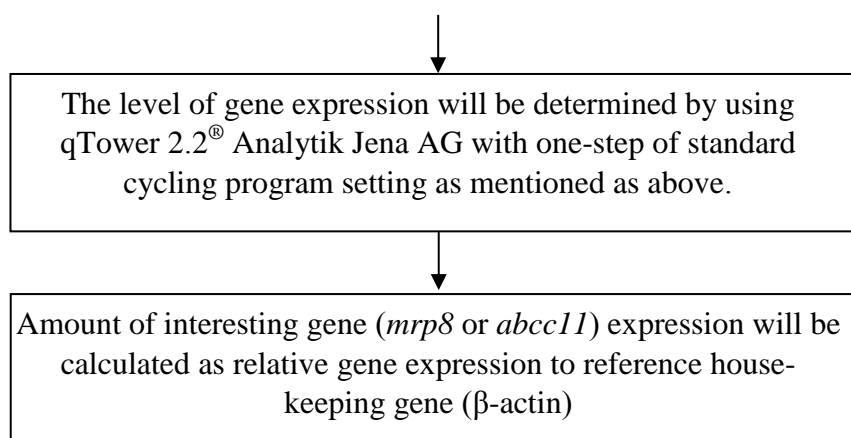
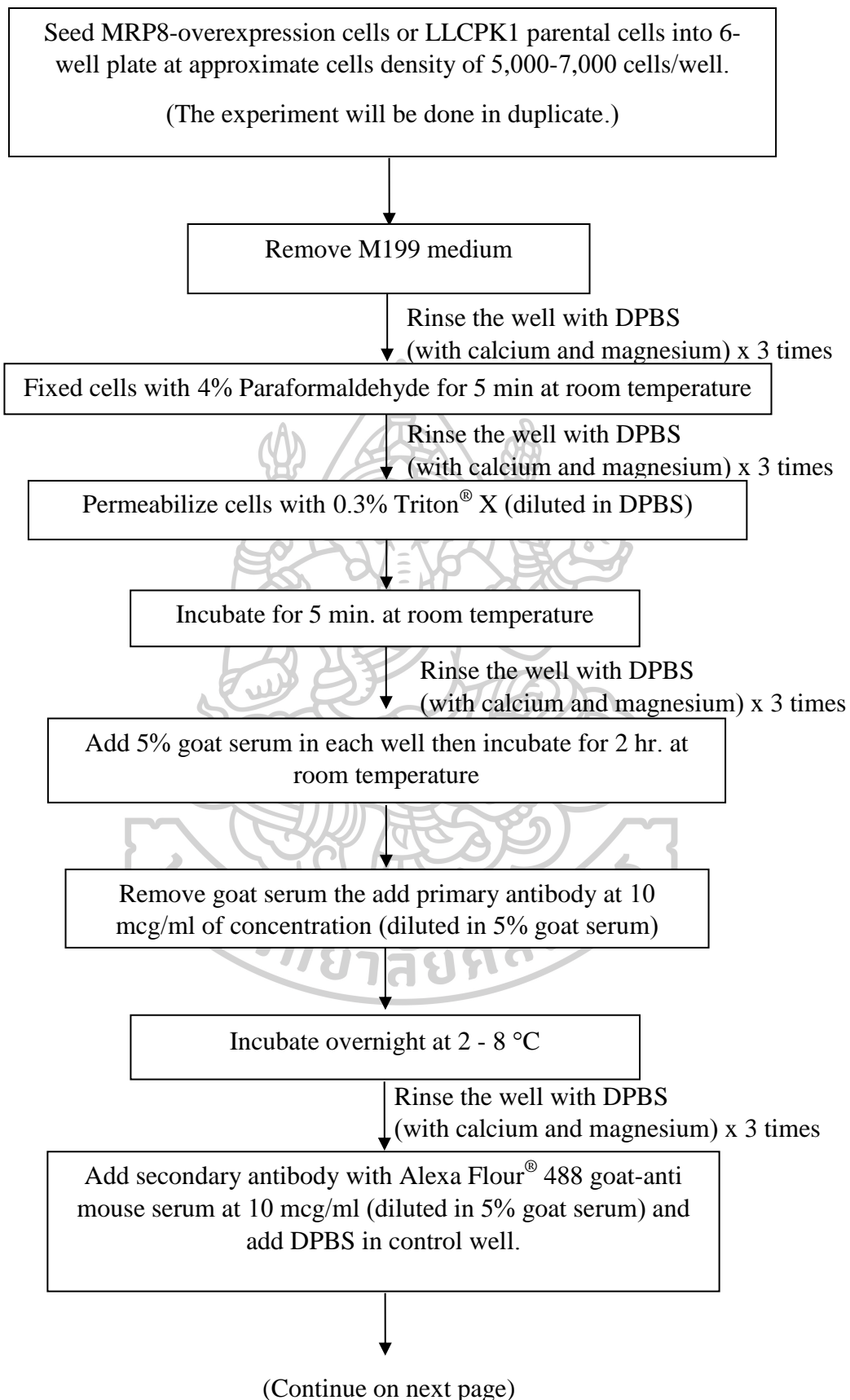


Figure 3.3.2.2 Diagram of the determination of human ABCC11 or MRP8 mRNA expression levels by real-time polymerase chain reaction.

### 3.3.3 Immunofluorescent staining and imaging.

To assess *in situ* MRP8 protein expression immunofluorescent technique using an anti-MRP8 antibody was performed in MRP8-overexpressed and parental LLC-PK1 cells. This method was adopted from Robillard KR et al [84]. Cells were seed in 24-well tissue culture plate at density of 5,000 cells/well. Cells were incubated at 37°C, 5% CO<sub>2</sub> overnight. The experiments were duplicated. Briefly, cells were fixed with 4% paraformaldehyde for 20 minutes. Permeabilized solution with 0.3%v/v Triton<sup>®</sup> X was added for 5 minutes at 37°C. Thereafter, 5% v/v goat serum diluted in DPBS solution was added into cells and incubated for 60 minutes at room temperature. Cells were incubated at 4°C overnight with primary mouse anti-MRP8 antibody (10 µg/ml). Then, cells were washed three times with PBS, incubated with an Alexa Fluor<sup>®</sup> 488 goat anti-mouse antibody (10 µg/ml) for 60 minutes at room temperature. For staining of actin and nucleus, Alexa Fluor<sup>®</sup> 488 Phalloidin (10 µg/ml) and DAPI solution (3 ng/ml), respectively, were used according to the manufacture's protocol. Photos of selected areas of cells were taken under the EVOS-II<sup>™</sup> imaging station at 1,000 X magnification.





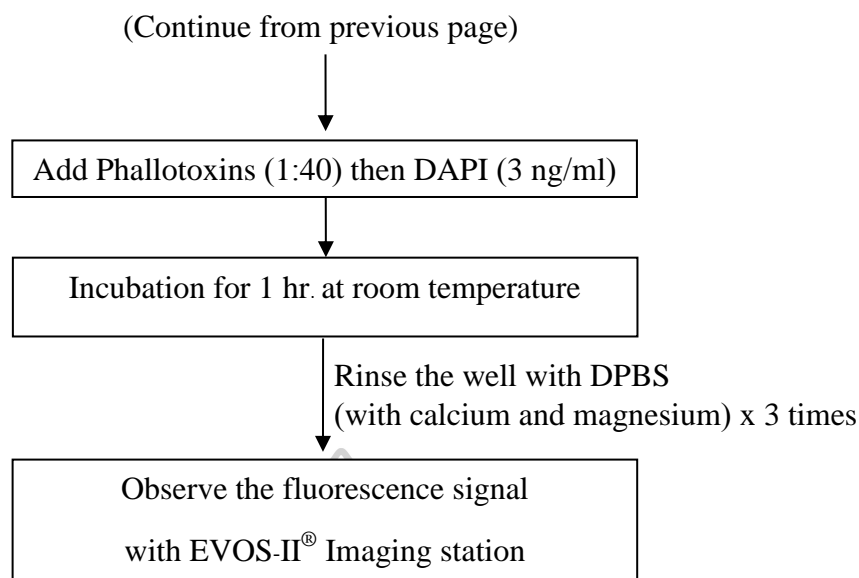


Figure 3.3.3.1 Diagram of the determination of human ABCC11 or MRP8 transporter protein expression level by indirect immunofluorescence assay.

### 3.3.4 Cytotoxic assays.

The modified MTT assay was performed to determine the cells viability and CC50s between MRP8-overexpressed and parental cells in the presence of various concentrations of TDF with or without MRP-specific inhibitor MK-571. Methotrexate was used as a positive control. This method was adopted from Ray et al. [24] Cells were seeded in 96-well tissue culture plates at approximate density of 5,000 cells/well in 100  $\mu$ l of M199 medium. Twenty-four hours later, both cells types were pre-incubated at 37 °C, 5% CO<sub>2</sub> with various concentrations of MRP-specific inhibitor (50, 100 or 150  $\mu$ M MK-571) for 1 hr. Serially diluted test drugs or methotrexate were then added in triplicate and mixed well. Following 4 days (96 hr.) of incubation, cells viability was determined using a PrestoBlue™ assay kit (purchased from Life Technologies Corporation, Grand Island, NY) according to the manufacturer's protocol. After 2 hours of continuous incubation, the luminescence signal was measured at excitation 550 nm of wavelength using a microplate reader (M-965+, Metertech, Taiwan), and percentage of cells viability was calculated.

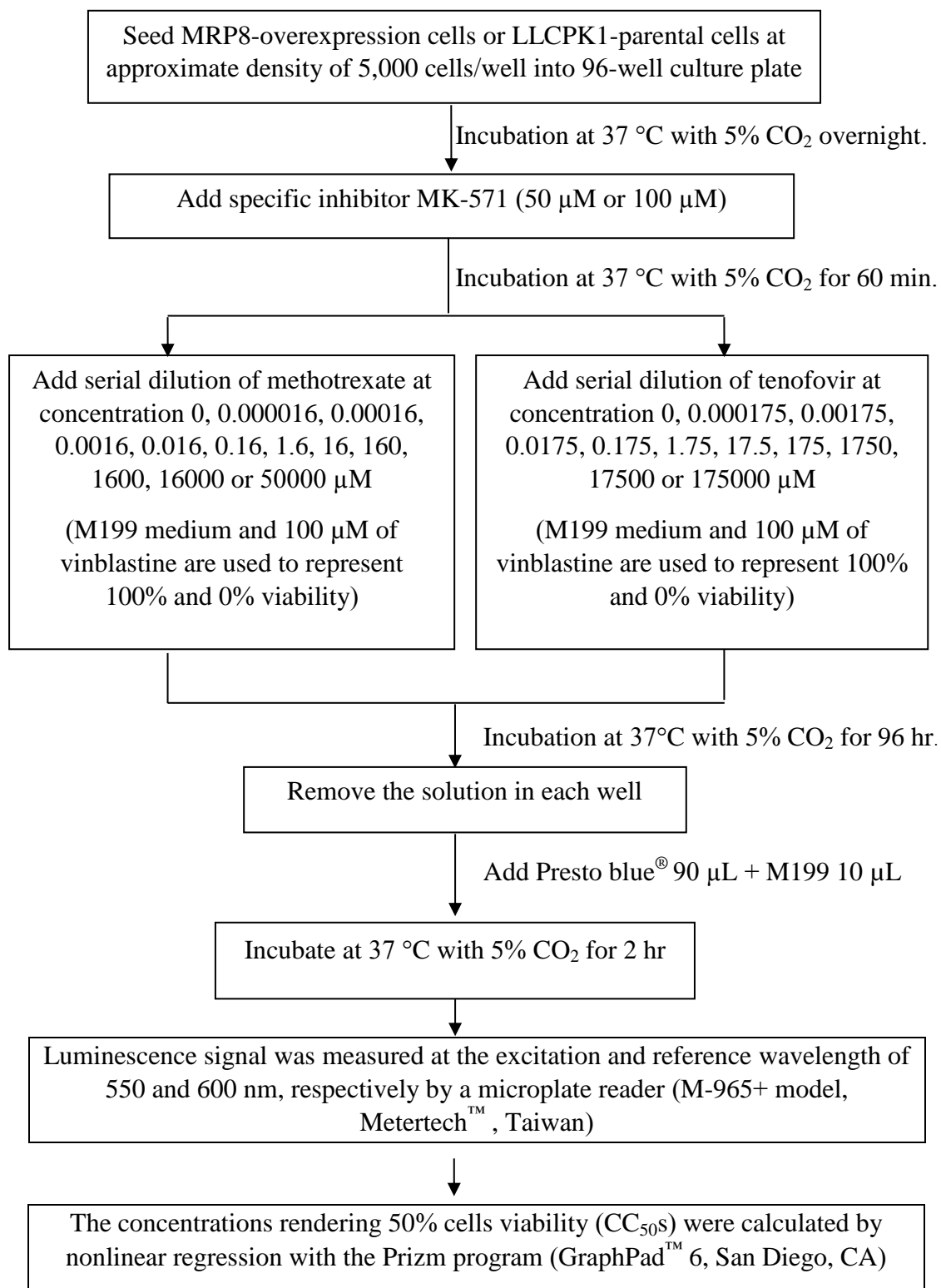


Figure 3.3.4.1 Diagram of cytotoxic assay.

### 3.3.5 Drug transport assays

To compare the intracellular accumulation of tenofovir and methotrexate between MRP8-overexpressed and parental cells, cellular transport assay with or without MK-571 was performed as previously described [8, 24, 85]. LLC-PK1-ABCC11 and parental cells were seeded at approximate density of 300,000 cells/well into 12-well tissue culture plate and then incubated at 37 °C, 5% CO<sub>2</sub> for overnight. Cells were pre-incubated with 50 μM or 100 μM MK-571 solution at 37 °C, 5% CO<sub>2</sub> for 1 h, followed by addition of 200 μM tenofovir disoproxil fumarate (TDF) or 160 μM methotrexate (MTX). After 1 h of shaking incubation at 37 °C, 5% CO<sub>2</sub>, reactions were stopped by washing 3 times with ice-cold phosphate-buffered saline to remove extracellular drug. Cells were harvested by adding 70% v/v ice-cold methanol, followed by overnight incubation at - 20 °C. Cellular debris was removed by centrifugation at 10,000 g for 15 minutes. Supernatants were collected, and intracellular concentrations of tenofovir and methotrexate were determined by a validated liquid chromatography coupled with tandem mass spectrometry, which is operated with electrospray ionization (ESI) technology, as described previously. [25-28, 86]. The reference method was validated [25, 28, 86, 87], exhibited the lower limits of quantification and the calibration curves demonstrated the linearity with average correlation coefficients greater than 0.99 for both tenofovir and methotrexate. Chromatographic separation of tenofovir and methotrexate was achieved by using a mobile phase of acetonitrile: 1 mM ammonium acetate buffer in water pH 6.5 ± 0.3 (50 : 50, v/v) and acetonitrile: 1mM ammonium formate containing 0.1% formic acid (18 : 82, v/v), respectively. Delivered flow rate was 0.4 ml/min through an analytical column (C18 Zorbax Eclipse XDB, Agilent™, U.S.A). The column temperatures were maintained at 10 °C for tenofovir and 35 °C for methotrexate.

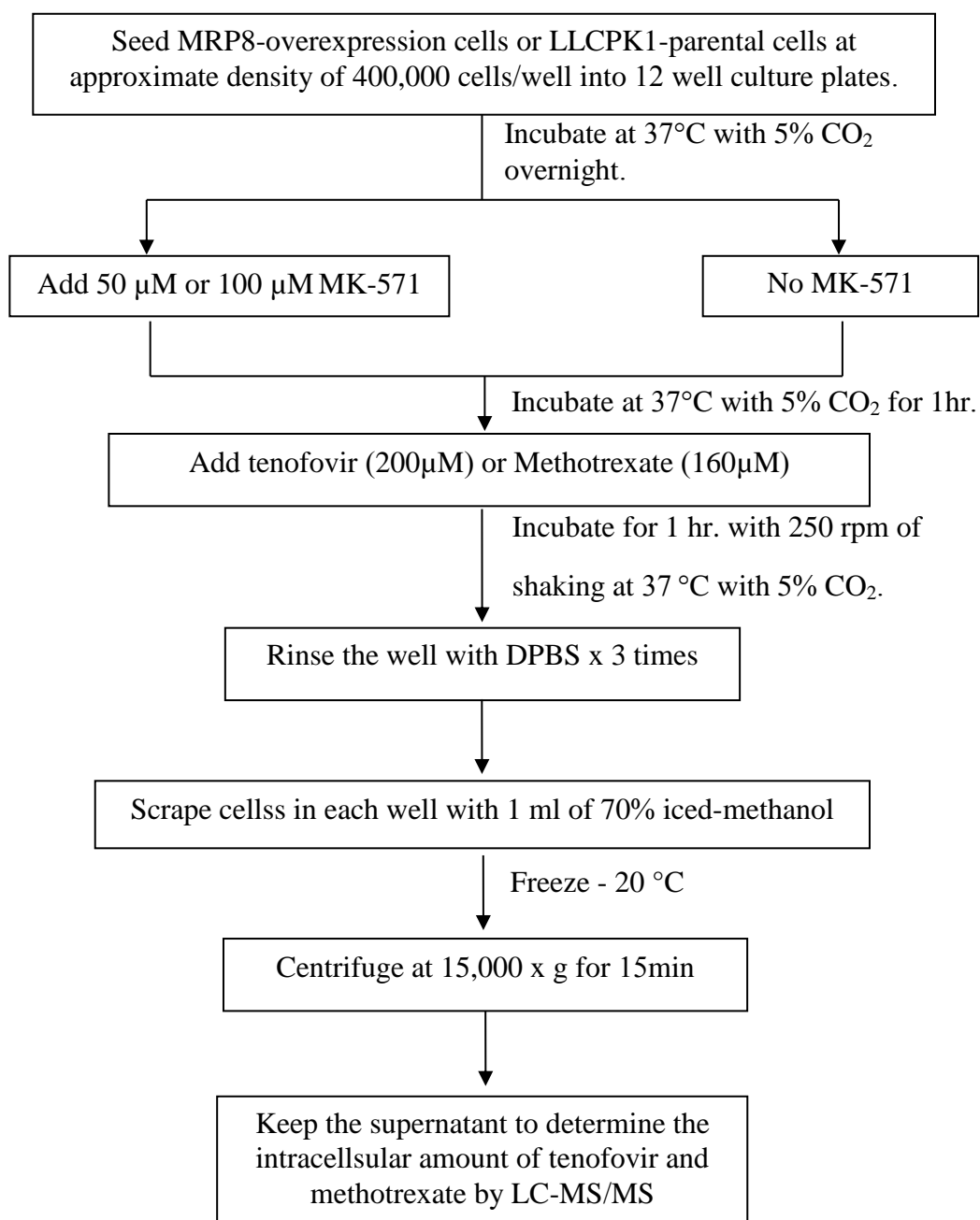
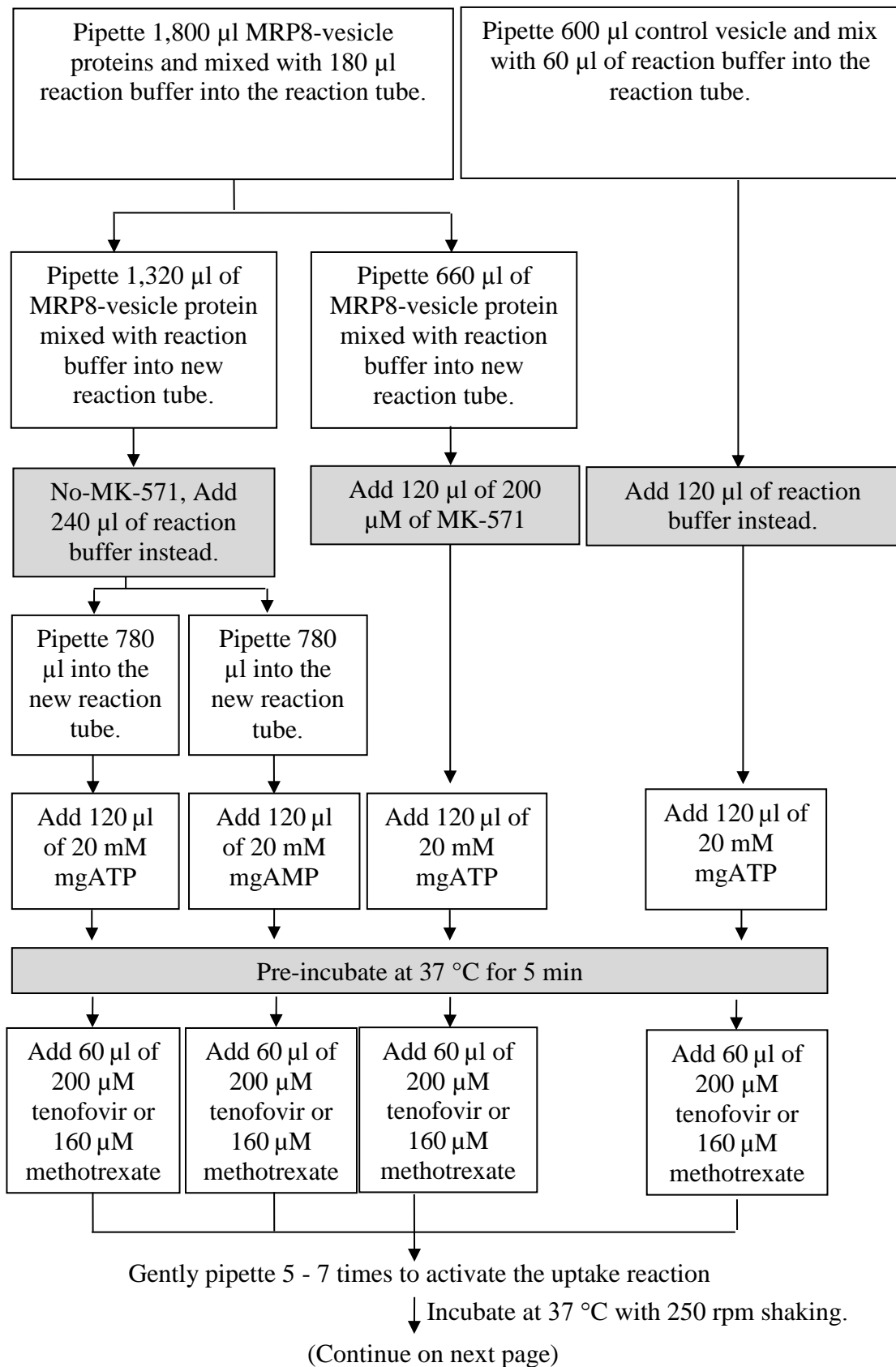


Figure 3.3.5.1 Diagram of drug transport assay.

### 3.3.6 ATP-dependent vesicular uptake assays

To demonstrate active transport of tenofovir and methotrexate through MRP8, time course uptake of tenofovir and methotrexate was performed by an inside-out Sf9 vesicle to compare the intravesicular accumulation of drugs between MRP8 (ABCC11)-overexpressed vesicles and Sf9 vesicles with or without MK-571. This assay was adopted from Ray AS, *et al* [24]. Briefly, membrane vesicles from Sf9 insect cells overexpressing MRP8 (ABCC11) protein and control vesicles were purchased (Life Technologies Corporation, NY). They were tested by the company to contain no other protein transporters. The vesicle transport assays were performed with a combination of 1) transport buffer obtained in GM3010 MRPs-BCRP vesicular transport assay reagent kit (Life Technologies Corporation, NY) ; 2) 100  $\mu$ M MK-571 (Merck Millipore Inc., Germany) ; 3) 200  $\mu$ M Tenofovir (Santa Cruz Biotechnology Inc., TA) or 160  $\mu$ M methotrexate (Sigma-Aldrich, MO) ; and 4) vesicles at a total protein concentration of 500  $\mu$ g/ml. The total reaction volume was 1,000  $\mu$ l. After 37 °C, 1 hour of incubation, 160  $\mu$ l reaction mixture aliquots were collected at time points (0, 0.5, 5, 10, 15, 30 minutes). They were diluted into 1 ml ice-cold Stop buffer, and pass to vacuum filtered through 1  $\mu$ m 96-well glass filters plate (Pall Corporation, Port Washington, NY). Filters were washed 5 times with 200  $\mu$ l ice-cold Wash buffer. Vesicles were harvested by adding 70 % iced-methanol, followed by incubation at - 20 °C overnight. Cellular debris was removed by centrifugation at 10,000 g for 15 minutes. Supernatants were collected and intracellular concentrations of tenofovir and methotrexate were determined as previously described [25-28]. To determine the transporter-specific uptake of the substrates, MRP8 overexpressed vesicles were assayed side by side with the control vesicles and MRP-specific inhibitor. Accumulation of substrates in vesicles was expressed in nanomoles per milligram of total protein (nM/mg-protein).



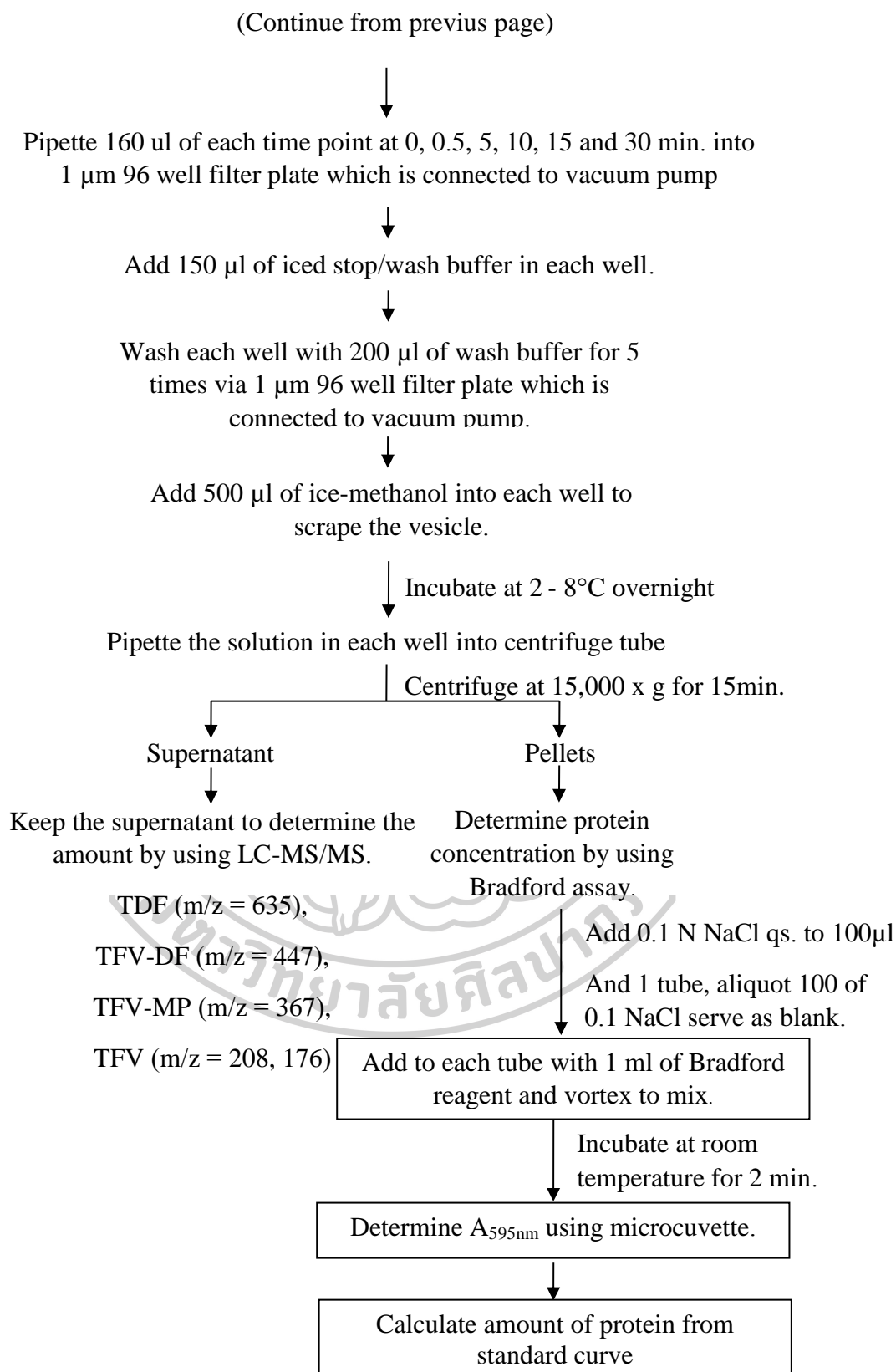


Figure 3.3.6.1 Diagram of ATP-dependent vesicular uptake assay.



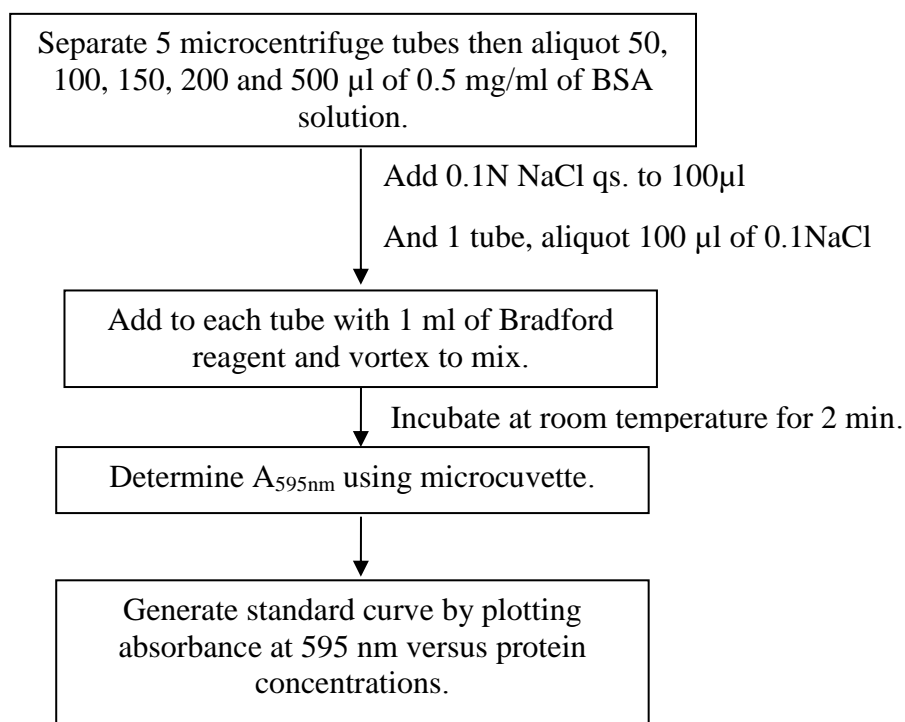


Figure 3.3.6.2 Diagram of colorimetric protein assay (Bradford reagent assay) for standard curve.

### 3.3.7 Statistical analysis

Significance of the results were determined by a 2-way ANOVA multiple comparison and unpaired t-test assuming equal variance with Prizm program (GraphPad™ 6, San Diego, CA). The concentrations rendering 50% cells viability (CC<sub>50S</sub>) were calculated and fitted to Richard's five-parameter logistical dose-response curve [88] (asymmetric sigmoidal, with robust fit,  $\text{LogXb} = \text{LogEC50} + (1/\text{HillSlope}) * \text{Log}((2^{1/S}) - 1)$ , Denominator =  $(1 + 10^{((\text{LogXb} - X) * \text{HillSlope}))^S}$ , an initial hill slope value = 1.0 and S = 0.5) by Prizm program (GraphPad™ 6, San Diego, CA). Untreated cells and treated cells with 100 µM vinblastine were used as reference cells viability for 100 % and 0 %, in respectively.

## CHAPTER 4

### RESULTS AND DISCUSSION

- 4.1 Characterization of cells lines
- 4.2 Cells viability and cytotoxicity assays
- 4.3 Tenofovir transport assays
- 4.4 ATP-dependent vesicular tenofovir uptake assays
- 4.5 Discussion



#### 4.1 Characterization of cells lines

Human *abcc11* mRNA levels in MRP8-overexpressed LLC-PK1 cells exhibited higher expression level than that of the parental cells (Figure 4.1.1A). Indirect immunofluorescence staining of MRP8 also showed that the transporter protein was highly expressed as seen from fluorescence signal in MRP8-overexpressed LLC-PK1 cells whereas no signal was observed in parental cells by EVOS-II™ imaging station (Figure 4.1.1B; upper panel). The findings confirmed the suitable characteristics of the MRP8-overexpressed LLC-PK1 for further experimental assays.



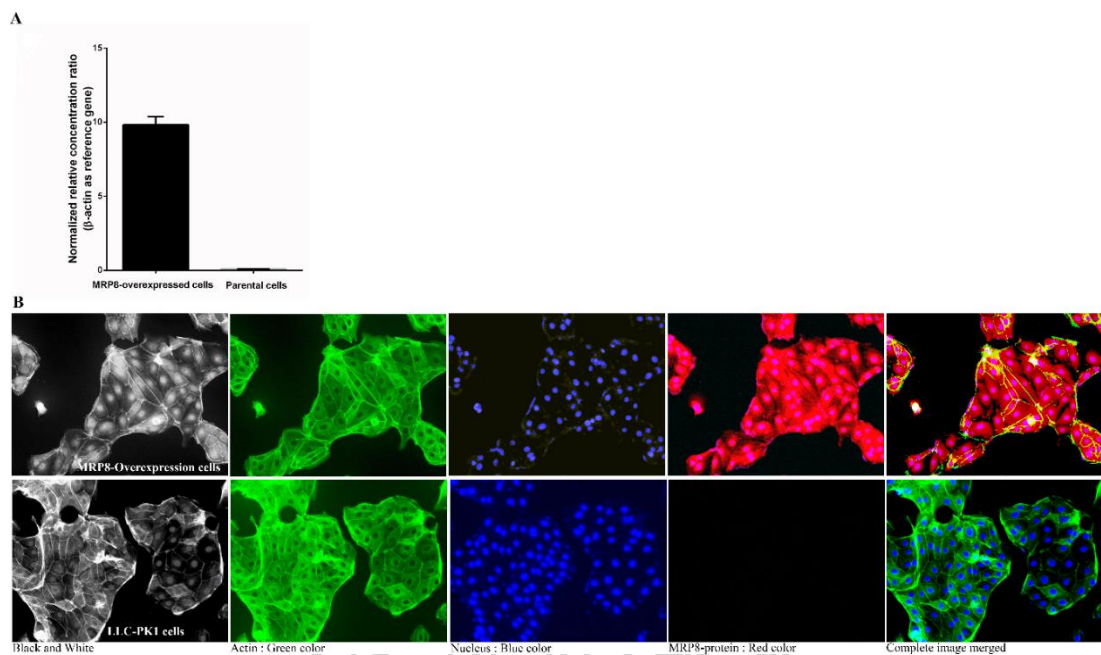


**Figure 4.1.1** Expression of recombinant MRP8 in LLC-PK1 cells. **A)** RNA expression of recombinant human ABCC11 gene in LLC-PK1 overexpressed cells (LLC-PK1-ABCC11) was significantly higher (left bar) than that of the parental cells (LLC-PK1). Data were shown in relative ratio of ABC11 gene expression normalized with beta-actin gene expression by real-time PCR as described in Materials and Methods. Values were the means  $\pm$  SD from at three independent experiments. Error bar represented standard errors from three independent experiments. Statistical significance was assessed by 2-way ANOVA multiple comparison assuming equal variance (\*\*\*, p-value < 0.0001). **B)** Human MRP8 overexpressed protein in LLC-PK1-ABCC11 (upper panel) and LLC-PK1 parental cells (lower panel). Immunofluorescent staining of MRP8 protein (red color),  $\beta$ -actin (green color), and DAPI (blue color) in both cells types were described in Materials and Methods. Photos were taken under the EVOS-II™ imaging station at 1000 x magnification.

## 4.2 Cells viability and cytotoxicity assays

MK-571 did not reduce MRP8-overexpressed and parental cells viability at the concentrations used (Figure 4.2.1A). At 17,500  $\mu\text{M}$ , TDF alone reduced a significant proportion of parental cells viability whereas no effect was seen on MRP8-overexpressed cells (Figure 4.2.1B). When MK-571 was added, TDF significantly reduced MRP8-overexpressed cells viability only (Figure 4.2.1C). Methotrexate was, however, more cytotoxic to both cells. Similarly, MTX toxicity was markedly increased when MK-571 was added in MRP8-overexpressed cells only (Figure 4.2.1D). When ten serial concentrations of TDF were used to determine 50% cytotoxic concentrations ( $\text{CC}_{50\text{s}}$ ) in both cells lines, TDF was found to be more toxic to parental cells. However,  $\text{CC}_{50\text{s}}$  of TDF was significantly reduced in the presence of MK-571 only in MRP8-overexpressed cells (Table 4.2.1, Figure 4.2.1E). Similarly,  $\text{CC}_{50\text{s}}$  of MTX was also dramatically reduced when MK-571 concentrations were increased only in MRP8-overexpressed cells (Figure 4.2.1F).

Table 4.2.1 Effect of MRP8-overexpression on cytotoxicity of tenofovir in LLC-PK1 cells.

Compound	$\text{CC}_{50\text{s}}(\mu\text{M})$		Fold change <sup>a</sup>
	Wild type	MRP8-overexpressed	
Tenofovir	33,694 $\pm$ 839	161,076 $\pm$ 5478	4.78 <sup>b</sup>
+ 50 $\mu\text{M}$ MK-571	34,938 $\pm$ 770	138,115 $\pm$ 976	3.95 <sup>c</sup>
+ 100 $\mu\text{M}$ MK-571	33,530 $\pm$ 466	10,713 $\pm$ 132	0.32 <sup>d</sup>

<sup>a</sup>Values represent the mean  $\pm$  standard deviation of five independent experiments. Calculation was fitted to Richard's five-parameter dose-response curve [88] (asymmetric sigmoidal, 5PL with robust fit.,  $\text{LogXb} = \text{LogEC}_{50} + (1/\text{HillSlope}) * \text{Log}((2^{(1/S)}) - 1)$ , Denominator =  $(1 + 10^{((\text{LogXb} - X) * \text{HillSlope}))^S}$ , initial hill slope value = 1.0 and  $S = 0.5$ )

<sup>b</sup>Fold change is the quotient of 50 % cytotoxic concentration ( $\text{CC}_{50\text{s}}$ ) of MRP8-overexpressed cells by parental cells ( $\text{CC}_{50\text{s MRP8}}/\text{CC}_{50\text{s WT}}$ ).

<sup>c, d, e</sup> Significant ( $P < 0.0001$ ) decrease in toxicity due to MRP8-overexpressed base on 2-way ANOVA multiple comparison assuming equal variance.

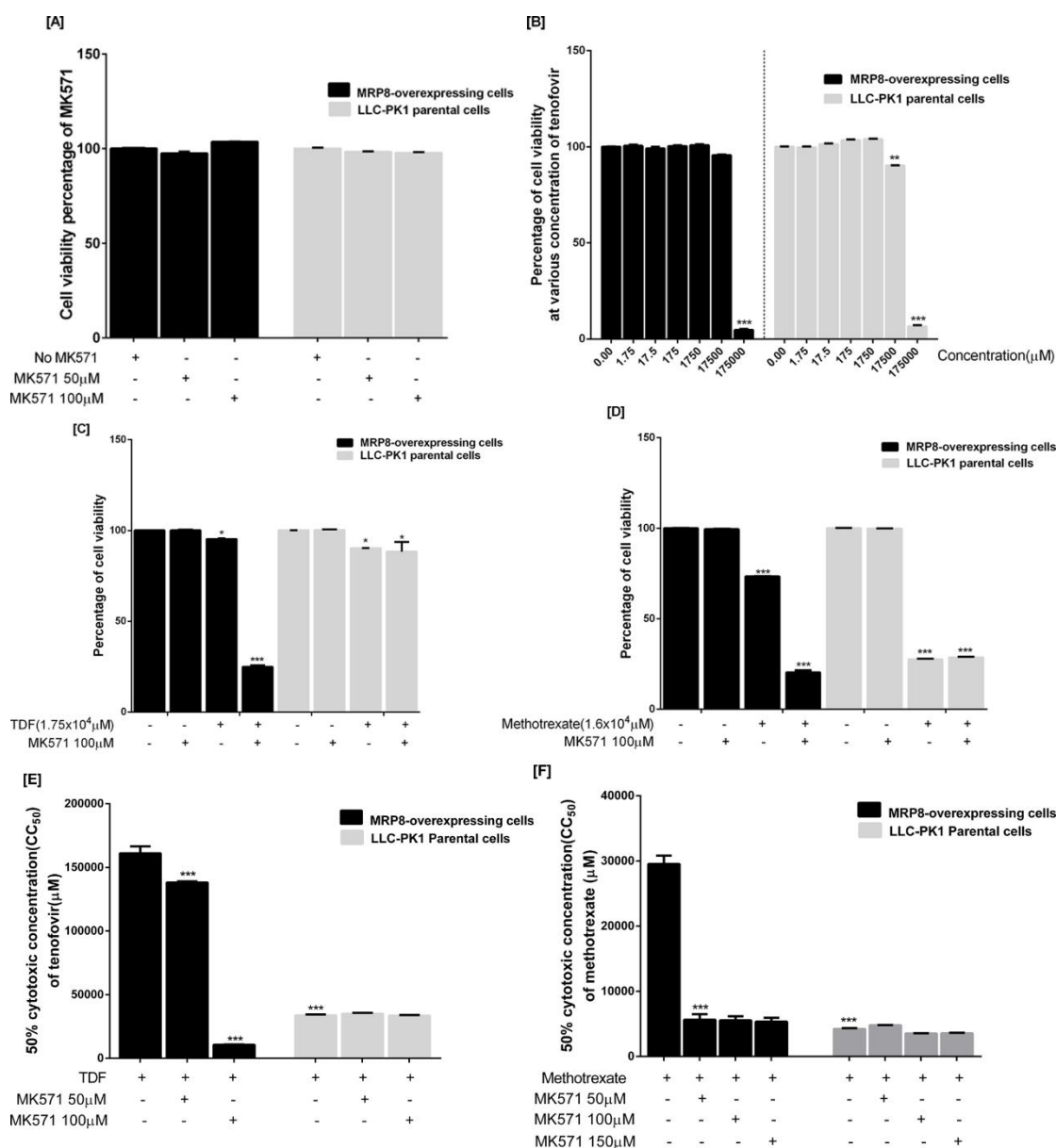
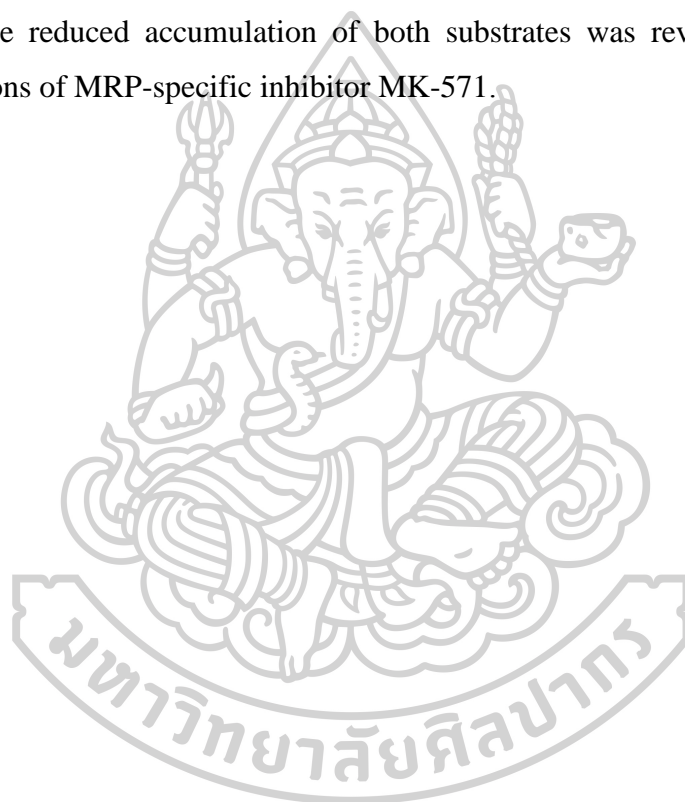


Figure 4.2.1 Cells viability assays of TDF and methotrexate in the presence and absence of MRP-specific inhibitor MK-571 (A) MRP-specific inhibitor MK-571 at various concentrations did not reduce MRP8-overexpressed and parental cells viability. (B) Cytotoxic effects of TDF on MRP8-overexpressed and parental cells (C) MK-571 further reduced viability of the MRP8-overexpressed, but not parental cells treated with TDF. (D) MK-571 also enhanced cytotoxicity of methotrexate only in MRP8-overexpressed cells. (E) And (F) Cytotoxic assays showing methotrexate and TDF concentrations that reduced cells viability by 50 % (CC<sub>50</sub>s) in MRP8-overexpressed LLC-PK1 or parental cells with or without MRP-specific inhibitor MK-571. Statistical significance was analyzed by 2-way ANOVA multiple comparison assuming equal variance (\*, p-value < 0.01; \*\*, p-value < 0.001 and \*\*\*, p-value < 0.0001). All values were the means  $\pm$  SD from five independent experiments.

### 4.3 Tenofovir transport assays.

Transport assay was performed by measuring intracellular accumulation of TDF and MTX after they entered the cells. The intracellular concentration was determined by the LC-MS/MS quantification. After conversion to TFV, the amount of TDF was found to be very little. Only area under the curves of tenofovir (m/z ratio = 208) and methotrexate (m/z ratio = 455) were used in the Figure 4.3.1. Compared to parental cells (shaded bars) MRP8-overexpression (dark bars) significantly reduced intracellular accumulation of tenofovir (Figure 4.3.1A) and methotrexate (Figure 4.3.1B). The reduced accumulation of both substrates was reversed by increasing concentrations of MRP-specific inhibitor MK-571.



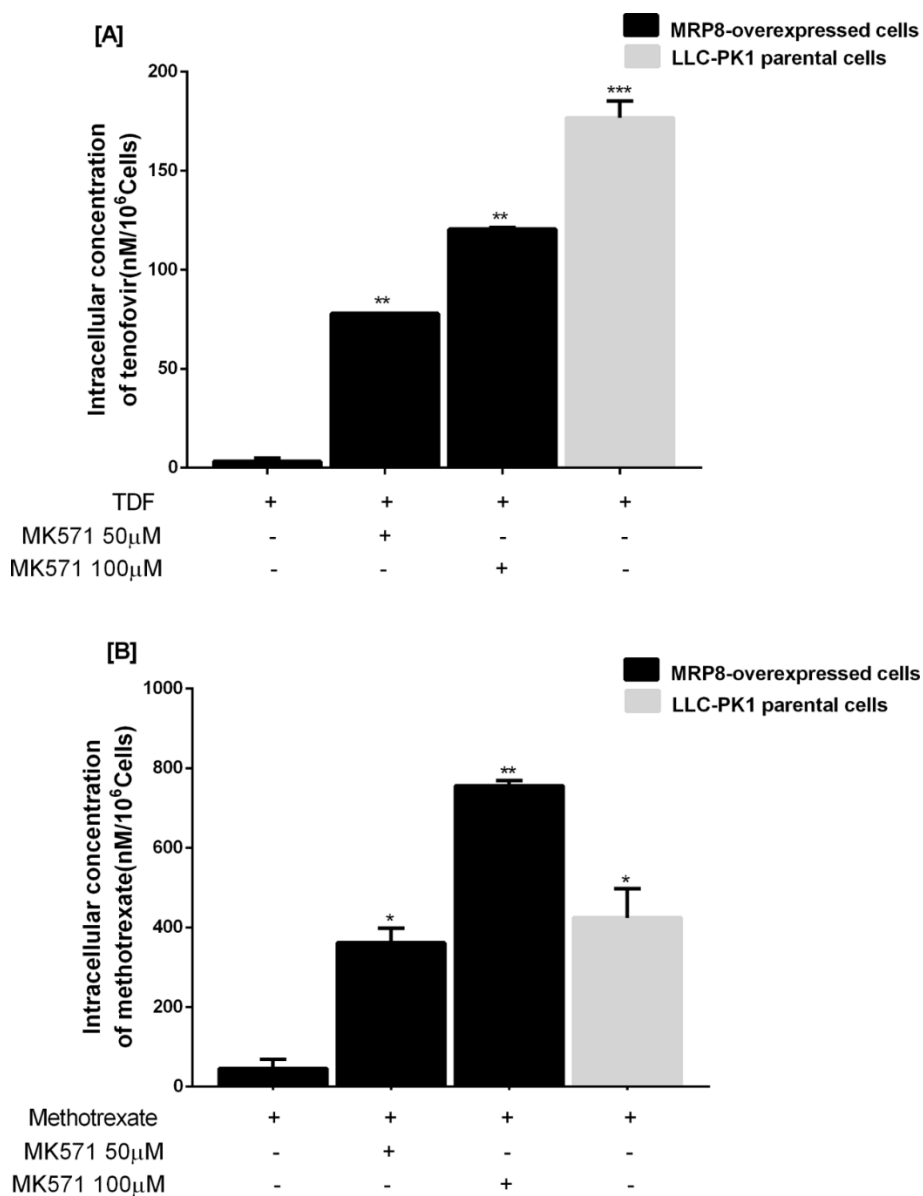
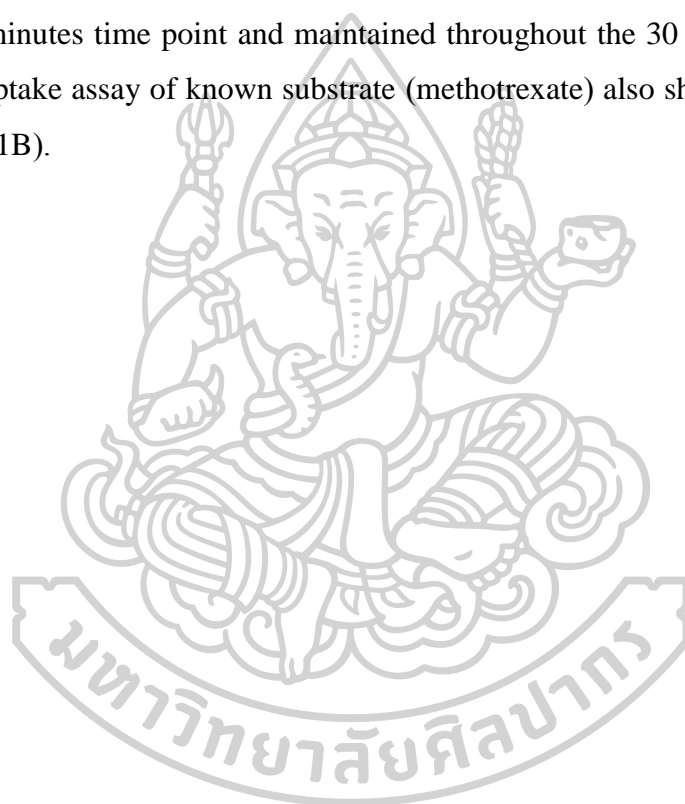


Figure 4.3.1 Intracellular accumulation of tenofovir (A) and methotrexate (B) with and without MRP-specific inhibitor MK-571 in cellular transport assay. Error bars represented standard errors from duplicate independent experiments. Statistical significance was assessed by 2-way ANOVA, multiple comparison assuming equal variance [\* , p-value < 0.01; \*\*, p-value < 0.001 and \*\*\*, p-value < 0.0001]. All values were the means  $\pm$  SD from two independent experiments.



#### 4.4 Vesicular uptake assays.

Vesicular uptake assay was designed by incubation of tenofovir, not TDF, and MTX with ATP or AMP in the presence and absence of MK-571 in MRP8-overexpressed and inside-out Sf9 control membrane vesicles. Addition of ATP, but not AMP, stimulated the uptake of tenofovir (Figure 4.4.1A) and methotrexate (Figure 4.4.1B) into MRP8-overexpressed vesicles. Accordingly, ATP-dependent intravesicular accumulation of tenofovir and MTX in MRP8-overexpressed vesicles was diminished with MRP-specific inhibitor. Significant differences were seen as early as 5 minutes time point and maintained throughout the 30 minutes experiment. Vesicular uptake assay of known substrate (methotrexate) also showed similar results (Figure 4.4.1B).



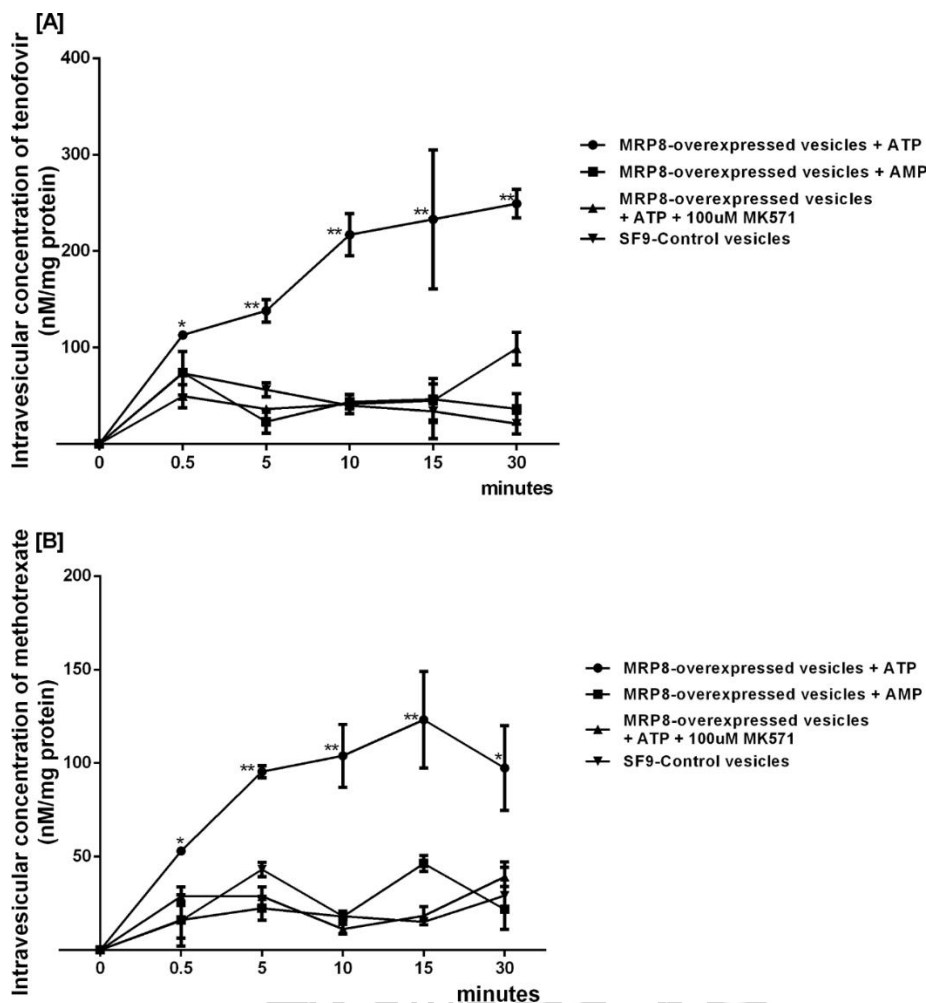


Figure 4.4.1 Time course for uptake of tenofovir and methotrexate by inside-out vesicles from SF9 insect cells. The uptake of tenofovir and methotrexate into MRP8-overexpressed was compared to parental membrane vesicles derived from Sf9 insect cells. [A] Addition of ATP, but not AMP, stimulated the uptake of tenofovir and methotrexate into MRP8-overexpressed vesicles. ATP-dependent intravesicular accumulation of tenofovir in MRP8-overexpressed vesicles was diminished with MRP-specific inhibitor. [B] Intravesicular concentrations of methotrexate also showed the similar result. Error bars represent standard errors from duplicate independent experiments. Statistical significances were assessed by repeated 2-way ANOVA with Turkey's post hoc analysis and unpaired t-test comparisons (\*, p-value < 0.01 and \*\*, p-value < 0.001). All values were the means  $\pm$  SD from two independent experiments.

#### 4.5 Discussion.

In comparison with methotrexate, the known substrate of MRP8, TDF is less cytotoxic to both LLC-PK1-ABCC11-overexpressed and LLC-PK1-parental cells. This may be due to the fact that tenofovir has a very high selectivity index (SI = 324.8) for viral reverse transcriptase enzyme [89] and, therefore, has lower cytotoxicity when compared to methotrexate. However, in the presence of MRP-specific inhibitor MK-571, cytotoxicity of tenofovir in MRP8-overexpressed cells increased almost fifteen fold. Although TDF and MTX were not tested concomitantly in cytotoxicity assay in our study, it may be assumed that intracellular accumulations of tenofovir due to combination of drug known as substrate or inhibitor of MRP8 transporter may contribute to its increased cytotoxicity.

Results of cellular transport assays also indicated that intracellular tenofovir concentration in MRP8-overexpressed cells was evidently and significantly lower (approximately 55 folds) than that of parental cells. As expected, intracellular tenofovir accumulations were increased as the cells were exposed to increasing concentrations of MRP-specific inhibitor. In addition, the data was also in consistence with those from MRP8 and Sf9 inside-out vesicles. Statistically significant increase in intravesicular accumulation of tenofovir in an ATP-dependent manner was observed in all time points (0.5, 5, 10, 15 and 30 minutes) compared to controls (AMP, and parental Sf9 vesicles). MK-571 was able to specifically reverse the intravesicular accumulation of tenofovir. Our study is the first to demonstrate that human MRP8-transporter protein at proximal tubular cells mediates efflux transport of tenofovir. It can be concluded that tenofovir is a new substrate of MRP8-transporter protein. Therefore, alteration on the physiologic functions of this efflux pump may influence the accumulation of drug at proximal renal tubular cells and may contribute to developing nephrotoxicity. Since renal elimination is the major pathway of tenofovir clearance, these findings are very important to expand the basic knowledge of the molecular pharmacology of this drug. The proximal tubular cells are uniquely susceptible to tenofovir toxicity because there exists a various complement of transporters that increase intracellular concentrations of the drug. The inhibition

properties of mtDNA polymerase  $\gamma$  encoded by POLG gene has been proposed to play a central role in tenofovir-induced mitochondrial toxicity which may contribute to its nephropathy [1, 4, 45, 90]. Although tenofovir has not yet been studied, admitted similar theory was raised in supporting that this drug might also induce proximal tubular apoptosis through caspase-9 activation [1, 29, 91] as previously described for other nucleotide-analog reverse transcriptase inhibitors such as adefovir and cidofovir [1]. Whether or not this may have a role in tenofovir-induced renal tubular cells injury will deserve further study.

Genetic variants in a number of transporter proteins involved in tenofovir excretion have not been clearly associated with renal damage. In fact, correlations between genetic variations of genes encoding other ABCC transporters and renal proximal tubulopathy had been shown. Polymorphisms of ABCC4 gene at several positions were identified but their correlation with intracellular accumulation and kidney damage yielded conflicting results [6, 7, 92, 93]. Studies of various SNPs at both intronic and coding regions of ABCC10 [8, 9] and ABCC2 genes also showed discrepancy of their correlations with renal proximal tubulopathy [71]. However, the role of MRP2 as renal efflux transporter of TDF has now been challenged and questionable [1, 4, 5, 9]. Therefore, it remains controversial by which genetic variants may predispose renal cells to TDF toxicity. Since multiple players of efflux transporters existed, it might be difficult to find significant proteins whose polymorphisms could be of significance in tenofovir nephrotoxicity. It was also possible that other compensated efflux mechanisms via other MRPs located on the renal proximal tubular region may play a role. Furthermore, there existed over 48 distinct members of multidrug resistance proteins encoded by *abcc* genes that belong to the ATP-Binding Cassette (ABC) transporter superfamily at the renal proximal tubular region [10-16].

## CHAPTER 5

### CONCLUSIONS

This in vitro study is the first to demonstrate the ability of MRP8 transporter to efflux antiretroviral tenofovir [94]. This transporter protein is highly expressed at proximal renal tubular region (Figure 4.5.1). Genetic polymorphism or concomitant drugs that diminish the physiologic function of MRP8-transporter may contribute to tenofovir intracellular accumulation and, consequently, its nephrotoxicity.

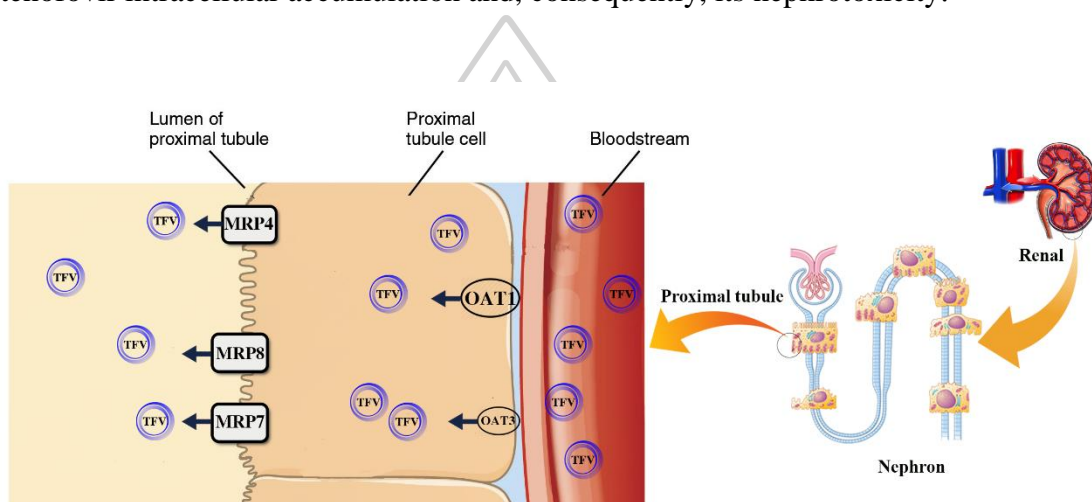


Figure 4.5.1 The handling pathway of tenofovir (TFV) transport at proximal tubular epithelium cells. Approximately, 20 - 30% of tenofovir is actively transported into renal proximal tubular cells by organic anion transporters at the basolateral membrane, hOAT1 and to lesser extent by hOAT3. Subsequently, the drug is secreted by the ABCC4 (MRP-4), ABCC10 (MRP-7) and ABCC11 (MRP-8) (this study).

Source: Tun-Yhong W, et al. (2017). "Tenofovir Disoproxil Fumarate Is a New Substrate of ATP-Binding Cassette Subfamily C Member 11." *Antimicrobial agents and chemotherapy* 61, e01725-16 (reprinted with permission).

## REFERENCES

- [1] Fernandez-Fernandez B, et al. (2011). "Tenofovir nephrotoxicity: 2011 update." **AIDS research and treatment** 2011, 354908.
- [2] Gallant JE, Deresinski S. (2003). "Tenofovir disoproxil fumarate." **Clinical infectious diseases : an official publication of the Infectious Diseases Society of America** 37, 944-50.
- [3] Birkus G, Hitchcock MJ, Cihlar T. (2002). "Assessment of mitochondrial toxicity in human cells treated with tenofovir: comparison with other nucleoside reverse transcriptase inhibitors." **Antimicrobial agents and chemotherapy** 46, 716-23.
- [4] Hall AM. (2013). "Update on tenofovir toxicity in the kidney." **Pediatr Nephrol** 28, 1011-23.
- [5] Jafari A, Khalili H, Dashti-Khavidaki S. (2014). "Tenofovir-induced nephrotoxicity: incidence, mechanism, risk factors, prognosis and proposed agents for prevention." **Eur J Clin Pharmacol** 70, 1029-40.
- [6] Kiser JJ, et al. (2008). "Clinical and genetic determinants of intracellular tenofovir diphosphate concentrations in HIV-infected patients." **J Acquir Immune Defic Syndr** 47, 298- 303.
- [7] Izzedine H, et al. (2006). "Association between ABCC2 gene haplotypes and tenofovir-induced proximal tubulopathy." **J Infect Dis** 194, 1481-91.
- [8] Pushpakom SP, et al. (2011). "Genetic variants of ABCC10, a novel tenofovir transporter, are associated with kidney tubular dysfunction." **The Journal of infectious diseases** 204, 145-53.
- [9] Nishijima T, et al. (2012). "Single nucleotide polymorphisms in ABCC2 associate with tenofovir-induced kidney tubular dysfunction in Japanese patients with HIV-1 infection: a pharmacogenetic study." **Clinical infectious diseases : an official publication of the Infectious Diseases Society of America** 55, 1558-67.
- [10] Toyoda Y, et al. (2008). "MRP class of human ATP binding cassette (ABC) transporters: historical background and new research directions." **Xenobiotica** 38, 833-62.

- [11] Gillet JP, Efferth T, Remacle J. (2007). "Chemotherapy-induced resistance by ATP-binding cassette transporter genes." **Biochim Biophys Acta** 1775, 237-62.
- [12] Han HK. (2011). "Role of transporters in drug interactions." **Arch Pharm Res** 34, 1865-77.
- [13] Russel FG, Masereeuw R, van Aubel RA. (2002). "Molecular aspects of renal anionic drug transport." **Annu Rev Physiol** 64, 563-94.
- [14] Kruh GD, Belinsky MG. (2003). "The MRP family of drug efflux pumps." **Oncogene** 22, 7537-52.
- [15] Kruh GD, et al. (2007). "ABCC10, ABCC11, and ABCC12." **Pflugers Arch** 453, 675-84.
- [16] Kruh GD, et al. (2001). "MRP subfamily transporters and resistance to anticancer agents." **J Bioenerg Biomembr** 33, 493-501.
- [17] Chen ZS, et al. (2005). "Transport of bile acids, sulfated steroids, estradiol 17 beta-D-glucuronide, and leukotriene C4 by human multidrug resistance protein 8 (ABCC11)." **Molecular pharmacology** 67, 545-57.
- [18] Bera TK, et al. (2001). "MRP8, a new member of ABC transporter superfamily, identified by EST database mining and gene prediction program, is highly expressed in breast cancer." **Mol Med** 7, 509-16.
- [19] Tammur J, et al. (2001). "Two new genes from the human ATP-binding cassette transporter superfamily, ABCC11 and ABCC12, tandemly duplicated on chromosome 16q12." **Gene** 273, 89-96.
- [20] Yabuuchi H, et al. (2001). "Multiple splicing variants of two new human ATP-binding cassette transporters, ABCC11 and ABCC12." **Biochem Biophys Res Commun** 288, 933-9.
- [21] Jedlitschky G, Burchell B, Keppler D. (2000). "The multidrug resistance protein 5 functions as an ATP-dependent export pump for cyclic nucleotides." **J Biol Chem** 275, 30069-74.
- [22] Chen ZS, Lee K, Kruh GD. (2001). "Transport of cyclic nucleotides and estradiol 17-beta-D-glucuronide by multidrug resistance protein 4. Resistance to 6-mercaptopurine and 6-thioguanine." **J Biol Chem** 276, 33747-54.

- [23] van Aubel RA, et al. (2002). "The MRP4/ABCC4 gene encodes a novel apical organic anion transporter in human kidney proximal tubules: putative efflux pump for urinary cAMP and cGMP." **Journal of the American Society of Nephrology** 13, 595-603.
- [24] Ray AS, et al. (2006). "Mechanism of active renal tubular efflux of tenofovir." **Antimicrobial agents and chemotherapy** 50, 3297-304.
- [25] Delahunty T, et al. (2009). "The simultaneous assay of tenofovir and emtricitabine in plasma using LC/MS/MS and isotopically labeled internal standards." **Journal of chromatography B, Analytical technologies in the biomedical and life sciences** 877, 1907-14.
- [26] Valluru RK, et al. (2013). "High throughput LC-MS/MS method for simultaneous determination of tenofovir, lamivudine and nevirapine in human plasma." **Journal of chromatography B, Analytical technologies in the biomedical and life sciences** 931, 117-26.
- [27] Guo J, et al. (2011). "Development and validation of an LC/MS/MS method for the determination of tenofovir in monkey plasma." **Biological & pharmaceutical bulletin** 34, 877-82.
- [28] Guo P, et al. (2007). "Determination of methotrexate and its major metabolite 7-hydroxymethotrexate in mouse plasma and brain tissue by liquid chromatography-tandem mass spectrometry." **Journal of pharmaceutical and biomedical analysis** 43, 1789-95.
- [29] Gallant JE, et al. (2005). "Changes in renal function associated with tenofovir disoproxil fumarate treatment, compared with nucleoside reverse-transcriptaseinhibitor treatment." **Clinical infectious diseases : an official publication of the Infectious Diseases Society of America** 40, 1194-8.
- [30] Takakura Y, et al. (1995). "Characterization of LLC-PK1 kidney epithelial cells as an in vitro model for studying renal tubular reabsorption of protein drugs." **Pharmaceutical research** 12, 1968-72.
- [31] Hull RN, Cherry WR, Weaver GW. (1976). "The origin and characteristics of a pig kidney cell strain, LLC-PK." **In vitro** 12, 670-7.
- [32] Mocroft A, Lundgren JD. (2004). "Starting highly active antiretroviral therapy:



- why, when and response to HAART.” **The Journal of antimicrobial chemotherapy** 54, 10-3.
- [33] Delaney WEt, et al. (2006). “Intracellular metabolism and in vitro activity of tenofovir against hepatitis B virus.” **Antimicrobial agents and chemotherapy** 50, 2471-7.
- [34] Cihlar T. (2006). “Nucleotide HIV reverse transcriptase inhibitors: tenofovir and beyond.” **Current opinion in HIV and AIDS** 1, 373-9.
- [35] Ray AS, Fordyce MW, Hitchcock MJ. (2016). “Tenofovir alafenamide: A novel prodrug of tenofovir for the treatment of Human Immunodeficiency Virus.” **Antiviral research** 125, 63-70.
- [36] Chapman T, McGavin J, Noble S. (2003). “Tenofovir disoproxil fumarate.” **Drugs** 63, 1597-608.
- [37] Antoniou T, Park-Wyllie LY, Tseng AL. (2003). “Tenofovir: a nucleotide analog for the management of human immunodeficiency virus infection.” **Pharmacotherapy** 23, 29-43.
- [38] Fauci AS. (2003). “HIV and AIDS: 20 years of science.” **Nature medicine** 9, 839-43.
- [39] Lyseng-Williamson KA, Reynolds NA, Plosker GL. (2005). “Tenofovir disoproxil fumarate: a review of its use in the management of HIV infection.” **Drugs** 65, 413-32.
- [40] Wang H, et al. (2015). “Comparison of the efficacy of tenofovir monotherapy versus tenofovir-based combination therapy in adefovir-experienced chronic hepatitis B patients: a systematic review and meta-analysis.” **International journal of clinical and experimental medicine** 8, 20111-22.
- [41] Yuen MF, et al. (2016). “Chronic Hepatitis B Virus Infection: Disease Revisit and Management Recommendations.” **Journal of clinical gastroenterology** 50, 286-294.
- [42] Idilman R, et al. (2015). “Long-term entecavir or tenofovir disoproxil fumarate therapy in treatment-naive chronic hepatitis B patients in the real-world setting.” **Journal of viral hepatitis** 22, 504-10.
- [43] Heathcote EJ, et al. (2011). “Three-year efficacy and safety of tenofovir disoproxil

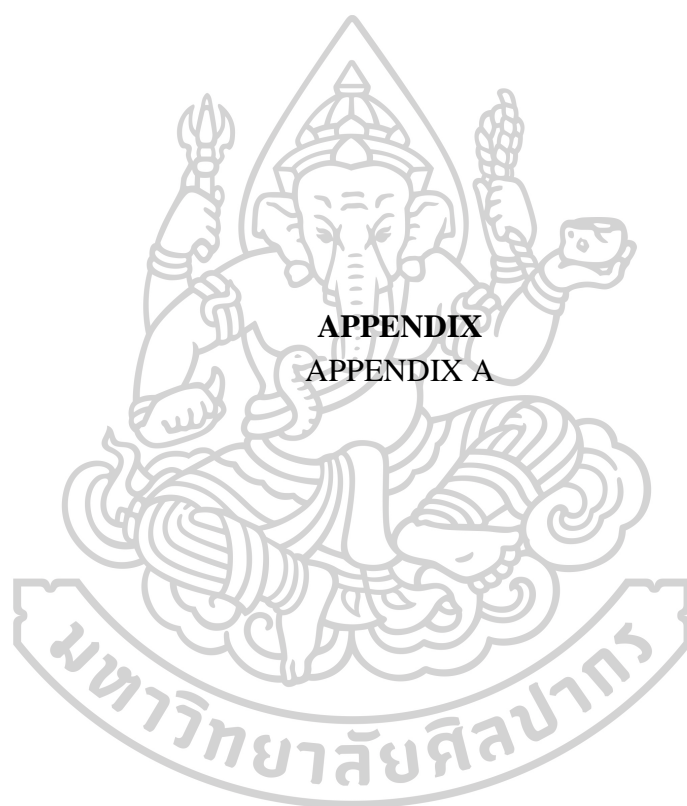
- fumarate treatment for chronic hepatitis B.” **Gastroenterology** 140, 132-43.
- [44] Nekvindova J, et al. (2006). “Inhibition of human liver microsomal cytochrome P450 activities by adefovir and tenofovir.” **Xenobiotica; the fate of foreign compounds in biological systems** 36, 1165-77.
- [45] Gitman MD, et al. (2007). “Tenofovir-induced kidney injury.” **Expert Opin Drug Saf** 6, 155-64.
- [46] Burns RN, Hendrix CW, Chaturvedula A. (2015). “Population pharmacokinetics of tenofovir and tenofovir-diphosphate in healthy women.” **Journal of clinical pharmacology** 55, 629-38.
- [47] Louissaint NA, et al. (2013). “Single dose pharmacokinetics of oral tenofovir in plasma, peripheral blood mononuclear cells, colonic tissue, and vaginal tissue.” **AIDS research and human retroviruses** 29, 1443-50.
- [48] Fung HB, Stone EA, Piacenti FJ. (2002). “Tenofovir disoproxil fumarate: a nucleotide reverse transcriptase inhibitor for the treatment of HIV infection.” **Clinical therapeutics** 24, 1515-48.
- [49] De Clercq E. (2003). “Potential of acyclic nucleoside phosphonates in the treatment of DNA virus and retrovirus infections.” **Expert Rev Anti Infect Ther** 1, 21-43.
- [50] De Clercq E. (2003). “Clinical potential of the acyclic nucleoside phosphonates cidofovir, adefovir, and tenofovir in treatment of DNA virus and retrovirus infections.” **Clinical microbiology reviews** 16, 569-96.
- [51] Johnson AA, et al. (2001). “Toxicity of antiviral nucleoside analogs and the human mitochondrial DNA polymerase.” **J Biol Chem** 276, 40847-57.
- [52] Kohler JJ, et al. (2011). “Tenofovir renal proximal tubular toxicity is regulated by OAT1 and MRP4 transporters.” **Lab Invest** 91, 852-8.
- [53] Moss DM, Neary M, Owen A. (2014). “The role of drug transporters in the kidney: lessons from tenofovir.” **Frontiers in pharmacology** 5, 248.
- [54] Gallant JE, et al. (2004). “Efficacy and safety of tenofovir DF vs stavudine in combination therapy in antiretroviral-naive patients: a 3-year randomized trial.” **Jama** 292, 191-201.
- [55] Krummel T, et al. (2005). “Tenofovir-induced acute renal failure in an HIV patient

- with normal renal function.” **Nephrol Dial Transplant** 20, 473-4.
- [56] Hynes P, et al. (2007). “Acute renal failure after initiation of tenofovir disoproxil fumarate.” **Renal failure** 29, 1063-6.
- [57] Malik A, Abraham P, Malik N. (2005). “Acute renal failure and Fanconi syndrome in an AIDS patient on tenofovir treatment--case report and review of literature.” **J Infect** 51, E61-5.
- [58] Rodriguez-Novoa S, et al. (2010). “Impairment in kidney tubular function in patients receiving tenofovir is associated with higher tenofovir plasma concentrations.” **AIDS (London, England)** 24, 1064-6.
- [59] Monteiro N, et al. (2014). “The impact of tenofovir disoproxil fumarate on kidney function: four-year data from the HIV-infected outpatient cohort.” **Journal of the International AIDS Society** 17, 19565.
- [60] Quesada PR, et al. (2015). “Incidence and risk factors for tenofovir-associated renal toxicity in HIV-infected patients.” **International journal of clinical pharmacy** 37, 865-72.
- [61] Chaisiri K, et al. (2010). “Incidence and risk factors for tenofovir-associated renal function decline among Thai HIV-infected patients with low-body weight.” **Curr HIV Res** 8, 504-9.
- [62] Kiertiburanakul S, et al. (2011). “Monitoring of Renal Function among HIV-Infected Patients Receiving Tenofovir in a Resource-Limited Setting.” **J Int Assoc Physicians AIDS Care (Chic)** 10, 297-302.
- [63] Marcellin P, et al. (2008). “Tenofovir disoproxil fumarate versus adefovir dipivoxil for chronic hepatitis B.” **N Engl J Med** 359, 2442-55.
- [64] Marcellin P, et al. (2013). “Regression of cirrhosis during treatment with tenofovir disoproxil fumarate for chronic hepatitis B: a 5-year open-label follow-up study.” **Lancet (London, England)** 381, 468-75.
- [65] Kohler JJ, et al. (2009). “Tenofovir renal toxicity targets mitochondria of renal proximal tubules.” **Lab Invest** 89, 513-9.
- [66] Brinkman K, Kakuda TN. (2000). “Mitochondrial toxicity of nucleoside analogue reverse transcriptase inhibitors: a looming obstacle for long-term antiretroviral therapy?”. **Current opinion in infectious diseases** 13, 5-11.

- [67] Herlitz LC, et al. (2010). "Tenofovir nephrotoxicity: acute tubular necrosis with distinctive clinical, pathological, and mitochondrial abnormalities." **Kidney international** 78, 1171-7.
- [68] Perazella MA. (2010). "Tenofovir-induced kidney disease: an acquired renal tubular mitochondriopathy." **Kidney international** 78, 1060-3.
- [69] Gupta SK. (2008). "Tenofovir-associated Fanconi syndrome: review of the FDA adverse event reporting system." **AIDS Patient Care STDS** 22, 99-103.
- [70] Zhou SF, et al. (2008). "Substrates and inhibitors of human multidrug resistance associated proteins and the implications in drug development." **Current medicinal chemistry** 15, 1981-2039.
- [71] Rodriguez-Novoa S, et al. (2009). "Predictors of kidney tubular dysfunction in HIV-infected patients treated with tenofovir: a pharmacogenetic study." **Clinical infectious diseases : an official publication of the Infectious Diseases Society of America** 48, e108-16.
- [72] Kelly L, et al. (2010). "Functional hot spots in human ATP-binding cassette transporter nucleotide binding domains." **Protein Sci** 19, 2110-21.
- [73] Keppler D. (2011). "Multidrug resistance proteins (MRPs, ABCs): importance for pathophysiology and drug therapy." **Handbook of experimental pharmacology** 201, 299-323.
- [74] Gottesman MM, Ambudkar SV. (2001). "Overview: ABC transporters and human disease." **J Bioenerg Biomembr** 33, 453-8.
- [75] Dean M, Annilo T. (2005). "Evolution of the ATP-binding cassette (ABC) transporter superfamily in vertebrates." **Annu Rev Genomics Hum Genet** 6, 123-42.
- [76] Stefkova J, Poledne R, Hubacek JA. (2004). "ATP-binding cassette (ABC) transporters in human metabolism and diseases." **Physiol Res** 53, 235-43.
- [77] Dean M, Rzhetsky A, Allikmets R. (2001). "The human ATP-binding cassette (ABC) transporter superfamily." **Genome Res** 11, 1156-66.
- [78] Matsumoto H, et al. (2014). "ABCC11/MRP8 Expression in the Gastrointestinal Tract and a Novel Role for Pepsinogen Secretion." **Acta histochemica et cytochemica** 47, 85-94.

- [79] Uhlen M, et al. ABCC11, KIDNEY - Expression summary 2005. <<http://www.proteinatlas.org/ENSG00000121270-ABCC11/tissue/kidney> (Retrieved 2016-05-10).
- [80] Uhlen M, et al. (2005). "A human protein atlas for normal and cancer tissues based on antibody proteomics." **Molecular & cellular proteomics : MCP** 4, 1920-32.
- [81] Uhlen M, et al. (2015). "Proteomics. Tissue-based map of the human proteome." **Science (New York, NY)** 347, 1260419.
- [82] Gstraunthaler G, Pfaller W, Kotanko P. (1985). "Biochemical characterization of renal epithelial cell cultures (LLC-PK1 and MDCK)." **The American journal of physiology** 248, F536-44.
- [83] Nielsen R, et al. (1998). "Characterization of a kidney proximal tubule cell line, LLC-PK1, expressing endocytotic active megalin." **Journal of the American Society of Nephrology : JASN** 9, 1767-76.
- [84] Robillard KR, Hoque T, Bendayan R. (2012). "Expression of ATP-binding cassette membrane transporters in rodent and human sertoli cells: relevance to the permeability of antiretroviral therapy at the blood-testis barrier." **The Journal of pharmacology and experimental therapeutics** 340, 96-108.
- [85] Cihlar T, et al. (2009). "Novel nucleotide human immunodeficiency virus reverse transcriptase inhibitor GS-9148 with a low nephrotoxic potential: characterization of renal transport and accumulation." **Antimicrobial agents and chemotherapy** 53, 150-6.
- [86] D'Avolio A, et al. (2008). "A new assay based on solid-phase extraction procedure with LC-MS to measure plasmatic concentrations of tenofovir and emtricitabine in HIV infected patients." **Journal of chromatographic science** 46, 524-8.
- [87] Rodin I, et al. (2013). "A validated LC-MS/MS method for rapid determination of methotrexate in human saliva and its application to an excretion evaluation study." **Journal of chromatography B, Analytical technologies in the biomedical and life sciences** 937, 1-6.
- [88] Giraldo J, et al. (2002). "Assessing the (a)symmetry of concentration-effect curves:

- empirical versus mechanistic models.” **Pharmacology & therapeutics** 95, 21-45.
- [89] Balestrieri E, et al. (2005). “Protective effect of the acyclic nucleoside phosphonate tenofovir toward human T-cell leukemia/lymphotropic virus type 1 infection of human peripheral blood mononuclear cells in vitro.” **Antiviral research** 68, 154-62.
- [90] Bendele RA, Richardson FC. (2002). “Adefovir nephrotoxicity and mitochondrial DNA depletion.” **Hum Pathol** 33, 574.
- [91] Hall AM, et al. (2011). “Tenofovir-associated kidney toxicity in HIV-infected patients: a review of the evidence.” **American journal of kidney diseases : the official journal of the National Kidney Foundation** 57, 773-80.
- [92] Likanonsakul S, et al. (2016). “A Single-Nucleotide Polymorphism in ABCC4 Is Associated with Tenofovir-Related Beta2-Microglobulinuria in Thai Patients with HIV-1 Infection.” **PloS one** 11, e0147724.
- [93] Rungtivasuwan K, et al. (2015). “Influence of ABCC2 and ABCC4 polymorphisms on tenofovir plasma concentrations in Thai HIV-infected patients.” **Antimicrobial agents and chemotherapy** 59, 3240-5.
- [94] Tun-Yhong W, et al. (2017). “Tenofovir Disoproxil Fumarate Is a New Substrate of ATP-Binding Cassette Subfamily C Member 11.” **Antimicrobial agents and chemotherapy** 61, e01725-16.



**APPENDIX**  
**APPENDIX A**

## 1. Protein determination by using Bradford assayed.

Table A.1 Protein content detection in vesicular transport assay of tenofovir at different time point by using spectrophotometer at 595 nm.

Tenofovir	0 min		0.5 min		5 min		10 min		15 min		30 min		Average	SD
	1	2	1	2	1	2	1	2	1	2	1	2		
MRP-8 overexpressed + ATP	1.185	1.183	1.181	1.179	1.177	1.189	1.192	1.175	1.185	1.195	1.181	1.183	1.184	0.006
MRP-8 overexpressed + AMP	1.180	1.177	1.185	1.185	1.188	1.185	1.180	1.183	1.177	1.174	1.180	1.176	1.181	0.004
MRP-8 overexpressed + MK-571+ATP	1.172	1.180	1.185	1.185	1.185	1.185	1.185	1.185	1.180	1.185	1.182	1.179	1.182	0.004
LLC-PK1 cells + ATP	1.175	1.181	1.185	1.185	1.176	1.189	1.187	1.184	1.185	1.183	1.183	1.185	1.183	0.004

Table A.2 Protein content detection in vesicular transport assay of methotrexate at different time point by using spectrophotometer at 595 nm.

Methotrexate	0 min		0.5 min		5 min		10 min		15 min		30 min		Average	SD
	1	2	1	2	1	2	1	2	1	2	1	2		
MRP-8 overexpressed + ATP	1.183	1.188	1.182	1.181	1.179	1.180	1.200	1.177	1.181	1.198	1.181	1.180	1.184	0.007
MRP-8 overexpressed + AMP	1.180	1.178	1.184	1.180	1.188	1.182	1.188	1.188	1.167	1.172	1.182	1.188	1.181	0.007
MRP-8 overexpressed + MK-571+ATP	1.175	1.171	1.189	1.191	1.198	1.181	1.168	1.191	1.178	1.180	1.189	1.178	1.183	0.009
LLC-PK1 cells + ATP	1.170	1.165	1.193	1.197	1.209	1.177	1.157	1.199	1.180	1.183	1.178	1.171	1.181	0.015



**The example of calculation:**

$$\begin{aligned}
 \text{Protein content of each sampling} &= \frac{(\text{Absorbance} - 0.826)}{0.004053} \\
 \text{time in uptake assay (mcg)} &= \frac{(1.185 - 0.826)}{0.004053} \\
 &= 87.6 \text{ mcg}
 \end{aligned}$$

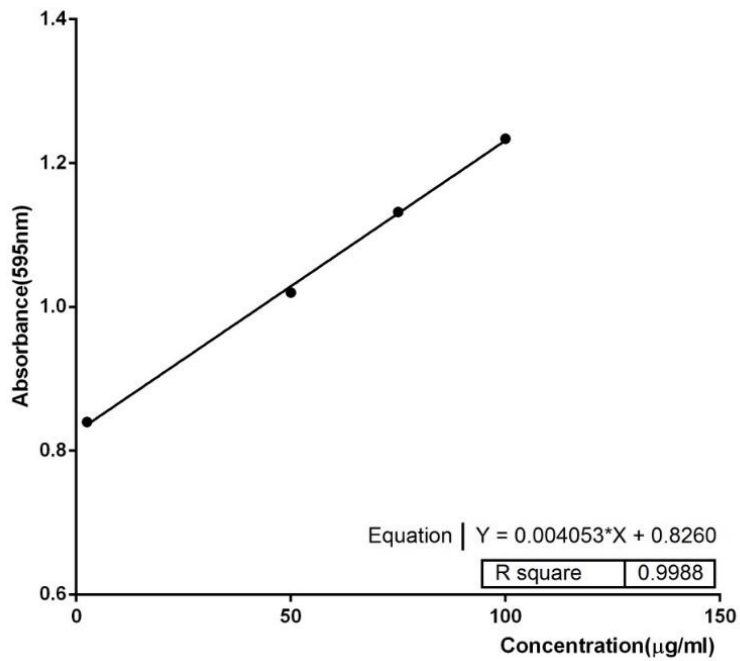


Figure A.1 Standard curve of absorbance at 595 nm vs protein concentration (µg/ml).

Table A.3 Quantification of protein content ( $\mu\text{g}$ ) in vesicular transport assay of tenofovir at different time point by using spectrophotometer at 595 nm.

Tenofovir	0 min		0.5 min		5 min		10 min		15 min		30 min		Average	SD
	1	2	1	2	1	2	1	2	1	2	1	2		
MRP-8 overexpressed + ATP	87.6	87.1	86.6	86.1	85.6	88.5	89.2	85.1	87.6	90.0	86.6	87.1	87.2	1.44
MRP-8 overexpressed + AMP	86.3	85.6	87.6	87.6	88.2	87.6	86.3	87.1	85.5	84.9	86.3	85.3	86.5	1.08
MRP-8 overexpressed + MK-571+ATP	84.4	86.3	87.6	87.6	87.6	87.6	87.6	87.6	86.3	87.6	86.8	86.1	86.9	1.00
LLC-PK1 cells + ATP	85.1	86.6	87.6	87.6	85.4	88.5	88.0	87.3	87.6	87.1	87.1	87.6	87.1	1.00

Table A.4 Quantification of protein content ( $\mu\text{g}$ ) in vesicular transport assay of methotrexate at different time point by using spectrophotometer at 595 nm.

Methotrexate	0 min		0.5 min		5 min		10 min		15 min		30 min		Average	SD
	1	2	1	2	1	2	1	2	1	2	1	2		
MRP-8 overexpressed + ATP	87.1	88.3	86.8	86.6	86.1	86.3	91.1	85.6	86.6	90.7	86.6	86.3	87.4	1.71
MRP-8 overexpressed + AMP	86.3	85.9	87.3	86.3	88.3	86.8	88.3	88.3	83.1	84.3	86.8	88.4	86.7	1.60
MRP-8 overexpressed + MK-571+ATP	85.1	84.1	88.5	89.0	90.7	86.6	83.5	89.0	85.9	86.4	88.5	85.9	87.0	2.11
LLC-PK1 cells + ATP	83.9	82.7	89.5	90.5	93.3	85.6	80.7	91.0	86.3	87.0	85.9	84.1	86.7	3.57

### 1. Cytotoxicity evaluation using MTT assay

Table A.5 The percentage of cells viability of MK-571 on MRP8-overexpressed cells after incubation for 96 h.

N	Concentration ( $\mu\text{M}$ )				
	M199*	Vinblastine*	50	100	150
1	100	1.60	98.70	104.10	104.30
2	100	-1.80	99.10	104.30	104.40
3	100	1.00	98.90	104.10	104.40
4	100	-1.40	98.00	103.00	104.00
5	100	0.30	94.40	103.00	103.30
6	100	-0.30	94.60	103.30	103.30
7	100	-2.50	94.10	103.40	103.40
8	100	0.10	94.00	103.10	103.40
9	100	1.70	103.10	103.00	103.30
10	100	-0.20	93.80	103.40	103.40
Avg	100	1.026	96.87	103.47	103.72
SD	1.54	0.70	3.15	0.51	0.49

\*M199 as control and 100  $\mu\text{M}$  of vinblastine as a positive control

Table A.6 The percentage of cells viability of MK-571 on LLC-PK1 cells after incubation for 96 h.

N	Concentration ( $\mu\text{M}$ )				
	M199*	Vinblastine*	50	100	150
1	100	0.60	98.4	98.7	102.80
2	100	-0.80	96.3	96	101.00
3	100	2.00	99.5	99.3	103.20
4	100	-0.40	98	97.7	103.40
5	100	-0.70	99	96.7	102.70
6	100	0.70	96.8	99.1	102.40
7	100	-1.50	96.8	98.4	101.50
8	100	-0.90	97	96.5	102.90
9	100	2.70	99.4	96.3	104.20
10	100	-1.20	99.1	96.2	102.20
Avg	100	1.45	98.03	97.49	102.63
SD	1.96	1.43	1.22	1.30	0.92

\*M199 as control and 100  $\mu\text{M}$  of vinblastine as a positive control

Table A.7 The percentage of cells viability of tenofovir without MK-571 on MRP8-overexpressed cells after incubation for 96 h.

N	M199* media	Vinblastine*	Concentration ( $\mu\text{M}$ )											
			$1.75 \times 10^{-4}$	$1.75 \times 10^{-3}$	$1.75 \times 10^{-2}$	0.175	1.75	17.5	175	$1.75 \times 10^3$	$1.75 \times 10^4$	$1.75 \times 10^5$		
1	100	1.12	102.09	101.84	101.84	100.44	99.74	97.64	94.40	96.06	90.72	4.82		
2	100	0.02	101.80	102.09	101.75	100.70	99.48	97.56	95.38	96.34	91.36	4.54		
3	100	3.72	102.01	101.82	101.65	100.69	99.22	97.40	95.32	96.53	91.50	4.51		
4	100	0.32	100.52	101.90	101.55	100.34	98.88	97.41	95.26	96.29	91.38	4.31		
5	100	0.01	101.77	101.70	101.44	100.25	98.56	97.29	95.17	96.10	91.35	3.99		
Average	100.00	1.04	101.64	101.87	101.64	100.48	99.17	97.46	95.10	96.26	91.26	4.43		
SD	2.11	1.57	0.64	0.14	0.16	0.20	0.47	0.14	0.40	0.19	0.31	0.31		

\*M199 as control and 100  $\mu\text{M}$  of vinblastine as a positive controlTable A.8 The percentage of cells viability of tenofovir with 50  $\mu\text{M}$  MK-571 on MRP8-overexpressed cells after incubation for 96 h.

N	M199 media*	Vinblastine*	Concentration ( $\mu\text{M}$ )											
			$1.75 \times 10^{-4}$	$1.75 \times 10^{-3}$	$1.75 \times 10^{-2}$	0.175	1.75	17.5	175	$1.75 \times 10^3$	$1.75 \times 10^4$	$1.75 \times 10^5$		
1	100	1.08	101.71	107.00	105.02	106.11	86.11	100.59	103.65	97.54	114.19	8.28		
2	100	1.01	101.00	106.46	105.00	105.58	85.90	100.49	103.82	97.65	113.81	8.13		
3	100	2.22	101.46	106.43	105.07	105.36	86.16	100.68	103.51	97.66	113.65	8.09		
4	100	-0.01	101.43	106.08	104.92	105.12	85.62	100.48	103.38	97.39	112.93	7.82		
5	100	1.05	101.08	106.13	104.89	104.98	85.92	100.48	102.97	97.13	112.93	7.57		
Average	100.00	1.07	101.34	106.42	104.98	105.43	85.94	100.54	103.46	97.47	113.50	7.97		
SD	1.03	0.79	0.29	0.37	0.07	0.44	0.21	0.09	0.32	0.22	0.56	0.28		

\*M199 as control and 100  $\mu\text{M}$  of vinblastine as a positive control

Table A.9 The percentage of cells viability of tenofovir with 100  $\mu\text{M}$  MK-571 on MRP8-overexpressed cells after incubation for 96 h.

N	M199 media*	Vinblastine*	Concentration ( $\mu\text{M}$ )									
			$1.75 \times 10^{-4}$	$1.75 \times 10^{-3}$	$1.75 \times 10^{-2}$	0.175	1.75	17.5	175	$1.75 \times 10^3$	$1.75 \times 10^4$	$1.75 \times 10^5$
1	100	-0.23	100.62	100.79	121.89	122.59	100.09	100.18	122.85	121.72	25.74	4.29
2	100	1.79	100.79	100.09	121.67	121.93	99.39	100.09	122.98	121.76	25.76	4.00
3	100	1.03	100.19	100.17	121.37	121.28	99.65	100.09	122.66	121.28	26.04	3.98
4	100	-0.01	100.96	100.17	121.48	121.05	99.48	100.09	122.85	121.39	25.95	3.69
5	100	1.02	101.81	100.26	121.33	121.08	99.49	99.91	122.27	120.99	26.62	3.50
Average	100.00	0.72	100.67	100.29	121.54	121.58	99.62	100.07	122.72	121.42	26.02	3.89
SD	0.96	0.83	0.30	0.28	0.23	0.66	0.28	0.10	0.28	0.32	0.36	0.31

\*M199 as control and 100  $\mu\text{M}$  of vinblastine as a positive control

Table A.10 The percentage of cells viability of tenofovir without MK-571 on LLC-PK1 cells after incubation for 96 h.

N	M199 media*	Vinblastine*	Concentration ( $\mu\text{M}$ )									
			$1.75 \times 10^{-4}$	$1.75 \times 10^{-3}$	$1.75 \times 10^{-2}$	0.175	1.75	17.5	175	$1.75 \times 10^3$	$1.75 \times 10^4$	$1.75 \times 10^5$
1	100	-0.01	97.95	97.76	98.23	99.53	95.52	97.85	99.44	100.09	85.90	9.34
2	100	-0.02	97.23	97.32	97.77	98.66	94.55	96.96	99.20	99.37	86.34	8.21
3	100	-0.01	98.67	99.20	99.56	100.71	97.06	98.84	100.53	100.98	88.08	7.65
4	100	0.00	98.78	99.04	99.65	100.96	96.94	98.86	100.87	101.40	88.47	7.34
5	100	-1.03	98.15	97.91	98.23	99.04	95.35	97.83	99.92	100.88	87.88	2.89
Average	100.00	-0.21	98.16	98.25	98.69	99.78	95.88	98.07	99.99	100.54	87.33	7.09
SD	1.01	0.46	0.62	0.93	0.95	1.07	1.20	0.91	0.81	0.91	1.27	0.88

\*M199 as control and 100  $\mu\text{M}$  of vinblastine as a positive control

Table A.11 The percentage of cells viability of tenofovir with 50  $\mu\text{M}$  MK-571 on LLC-PK1 cells after incubation for 96 h.

N	M199 media*	Vinblastine*	Concentration ( $\mu\text{M}$ )											
			$1.75 \times 10^{-4}$	$1.75 \times 10^{-3}$	$1.75 \times 10^{-2}$	0.175	1.75	17.5	175	$1.75 \times 10^3$	$1.75 \times 10^4$	$1.75 \times 10^5$		
1	100	0.11	98.21	99.25	97.36	96.80	92.94	96.61	101.41	101.51	87.19	9.51		
2	100	1.31	98.09	99.91	97.81	96.26	92.62	96.26	101.37	101.37	87.60	8.39		
3	100	-0.03	97.86	99.82	97.77	96.79	93.40	96.07	100.71	101.25	86.89	7.49		
4	100	-0.13	97.64	99.47	97.20	96.50	93.17	95.53	100.44	100.70	88.62	7.27		
5	100	-0.15	97.71	98.53	96.49	96.16	93.22	95.83	100.16	100.82	87.83	4.82		
Average	100.00	0.22	97.90	99.40	97.33	96.50	93.07	96.06	100.82	101.13	87.63	7.50		
SD	2.01	0.62	0.24	0.31	0.30	0.26	0.33	0.45	0.48	0.35	0.76	1.02		

\*M199 as control and 100  $\mu\text{M}$  of vinblastine as a positive controlTable A.12 The percentage of cells viability of tenofovir with 100  $\mu\text{M}$  MK-571 on LLC-PK1 cells after incubation for 96 h.

N	M199 media*	Vinblastine*	Concentration ( $\mu\text{M}$ )											
			$1.75 \times 10^{-4}$	$1.75 \times 10^{-3}$	$1.75 \times 10^{-2}$	0.175	1.75	17.5	175	$1.75 \times 10^3$	$1.75 \times 10^4$	$1.75 \times 10^5$		
1	100	1.06	100.19	99.72	98.41	99.44	99.63	99.35	98.88	100.19	87.00	6.74		
2	100	-0.02	100.54	100.63	101.54	99.10	99.28	98.19	99.19	100.54	86.54	5.24		
3	100	0.00	100.09	100.44	101.42	99.47	100.00	98.49	98.49	100.71	87.16	4.43		
4	100	1.03	99.57	99.74	98.00	98.87	97.48	97.48	98.87	99.57	85.66	4.34		
5	100	1.13	99.35	99.19	98.87	98.30	97.09	97.57	97.90	98.87	86.50	5.25		
Average	100.00	0.64	99.95	99.94	99.65	99.04	98.70	98.22	98.67	99.98	86.57	5.20		
SD	1.30	0.59	0.48	0.47	1.90	0.29	1.12	0.77	0.29	0.50	0.67	1.11		

\*M199 as control and 100  $\mu\text{M}$  of vinblastine as a positive control

Table A.13 The percentage of cells viability of methotrexate without MK-571 on MRP8-overexpressed cells after incubation for 96 h.

N	M199 media *	Vinblastine*	Concentration ( $\mu\text{M}$ )									
			$1.6 \times 10^{-4}$	$1.6 \times 10^{-3}$	$1.6 \times 10^{-2}$	0.16	1.6	16	$1.6 \times 10^2$	$1.6 \times 10^3$	$1.6 \times 10^4$	$5 \times 10^4$
1	100	0.06	95.17	96.36	95.65	95.08	95.18	96.36	95.55	95.31	79.42	17.56
2	100	0.03	96.28	96.28	96.46	96.00	97.77	96.28	95.07	96.18	79.23	19.37
3	100	0.01	96.32	96.69	96.14	95.77	97.33	95.86	94.67	96.05	78.79	19.76
4	100	-0.01	96.19	96.37	96.09	95.73	97.28	95.55	94.64	96.09	80.73	17.80
5	100	-0.04	97.12	96.42	96.86	96.16	97.82	95.72	95.20	96.16	77.82	22.45
Avg	100	0.01	96.22	96.42	96.24	95.75	97.08	95.95	95.03	95.96	79.20	19.39
SD	0.77	0.04	0.69	0.16	0.45	0.41	1.09	0.35	0.38	0.37	1.06	1.96

\*M199 as control and 100  $\mu\text{M}$  of vinblastine as a positive controlTable A.14 The percentage of cells viability of methotrexate with 50  $\mu\text{M}$  MK-571 on MRP8-overexpressed cells after incubation for 96 h.

N	M199 media *	Vinblastine*	Concentration ( $\mu\text{M}$ )									
			$1.6 \times 10^{-4}$	$1.6 \times 10^{-3}$	$1.6 \times 10^{-2}$	0.16	1.6	16	$1.6 \times 10^2$	$1.6 \times 10^3$	$1.6 \times 10^4$	$5 \times 10^4$
1	100	0.00	92.01	92.48	90.68	92.01	90.29	90.29	90.77	91.63	20.28	7.52
2	100	0.03	92.52	92.80	91.51	92.06	90.86	90.67	90.77	91.78	21.82	9.88
3	100	0.01	92.15	92.42	91.06	91.79	90.34	90.43	90.79	91.79	24.53	10.92
4	100	0.04	92.31	92.49	91.06	92.05	90.53	90.88	91.60	92.85	26.09	12.96
5	100	0.01	92.65	92.83	91.33	92.21	90.62	90.62	91.59	92.65	26.28	13.63
Avg	100	0.02	92.33	92.60	91.13	92.02	90.53	90.58	91.10	92.14	23.80	10.98
SD	0.76	0.02	0.22	0.17	0.34	0.13	0.26	0.26	0.41	0.56	2.62	2.26

\*M199 as control and 100  $\mu\text{M}$  of vinblastine as a positive control

Table A.15 The percentage of cells viability of methotrexate with 100  $\mu\text{M}$  MK-571 on MRP8-overexpressed cells after incubation for 96

h.

N	M199 media*	Vinblastine*	Concentration ( $\mu\text{M}$ )									
			$1.6 \times 10^{-4}$	$1.6 \times 10^{-3}$	$1.6 \times 10^{-2}$	0.16	1.6	16	$1.6 \times 10^2$	$1.6 \times 10^3$	$1.6 \times 10^4$	$5 \times 10^4$
1	100	0.01	93.63	92.15	92.52	92.06	91.6	90.58	91.69	91.78	25.24	4.62
2	100	0.02	93.32	91.79	92.24	91.61	90.97	90.61	91.79	91.88	27.06	5.87
3	100	0.03	93.54	92.12	92.57	91.95	91.15	91.06	92.65	92.65	21.29	8.32
4	100	0.01	92.06	90.81	91.65	90.39	89.89	89.56	90.73	91.4	21.05	10.19
5	100	0.00	92.86	91.96	92.78	91.88	91.39	90.73	92.21	92.95	23.22	13.29
Avg	100	0.01	93.08	91.77	92.35	91.58	91.00	90.51	91.81	92.13	23.57	8.46
SD	0.31	0.01	0.64	0.55	0.44	0.68	0.66	0.56	0.72	0.64	2.58	3.46

\*M199 as control and 100  $\mu\text{M}$  of vinblastine as a positive control

Table A.16 The percentage of cells viability of methotrexate with 150  $\mu\text{M}$  MK-571 on MRP8-overexpressed cells after incubation for 96

h.

N	M199 media*	Vinblastine*	Concentration ( $\mu\text{M}$ )									
			$1.6 \times 10^{-4}$	$1.6 \times 10^{-3}$	$1.6 \times 10^{-2}$	0.16	1.6	16	$1.6 \times 10^2$	$1.6 \times 10^3$	$1.6 \times 10^4$	$5 \times 10^4$
1	100	0.00	95.43	95.72	95.43	94.77	93.53	93.72	93.34	94.77	21.61	2.38
2	100	-0.01	95.94	95.75	95.38	95.11	93.44	93.91	93.26	94.92	23.39	4.34
3	100	0.02	94.15	93.65	93.07	92.23	91.73	92.40	91.98	93.65	28.46	10.61
4	100	0.00	94.62	94.54	94.04	93.54	93.29	92.80	92.63	94.29	29.45	12.09
5	100	0.00	95.00	95.08	94.83	94.34	93.68	93.52	93.52	95.49	23.84	5.78
Avg	100	0.00	95.03	94.95	94.55	94.00	93.13	93.27	92.95	94.62	25.35	7.04
SD	0.98	0.01	0.69	0.88	1.00	1.15	0.80	0.64	0.64	0.69	3.41	4.15

\*M199 as control and 100  $\mu\text{M}$  of vinblastine as a positive control



Table A.17 The percentage of cells viability of methotrexate without MK-571 on LLCPK1 cells after incubation for 96 h.

N	M199 media*	Vinblastine*	Concentration ( $\mu\text{M}$ )									
			$1.6 \times 10^{-4}$	$1.6 \times 10^{-3}$	$1.6 \times 10^{-2}$	0.16	1.6	16	$1.6 \times 10^2$	$1.6 \times 10^3$	$1.6 \times 10^4$	$5 \times 10^4$
1	100	0.46	87.97	87.97	86.18	83.44	81.65	80.17	78.27	74.38	25.48	1.27
2	100	0.27	88.43	88.33	86.23	83.49	82.02	80.34	78.13	74.65	25.58	1.68
3	100	0.08	88.56	88.46	86.57	83.63	82.27	80.90	78.38	76.33	25.99	1.99
4	100	-0.11	89.20	88.99	87.00	83.96	82.81	81.55	78.83	74.87	26.94	2.41
5	100	-0.31	89.25	88.83	87.06	84.13	83.09	81.73	79.02	77.06	25.44	2.92
Avg	100	0.08	88.68	88.52	86.61	83.73	82.37	80.94	78.53	75.46	25.89	2.05
SD	1.06	0.30	0.54	0.41	0.41	0.30	0.58	0.70	0.38	1.17	0.63	0.64

\*M199 as control and 100  $\mu\text{M}$  of vinblastine as a positive controlTable A.18 The percentage of cells viability of methotrexate with 50  $\mu\text{M}$  MK-571 on LLCPK1 cells after incubation for 96 h.

N	M199 media*	Vinblastine*	Concentration ( $\mu\text{M}$ )									
			$1.6 \times 10^{-4}$	$1.6 \times 10^{-3}$	$1.6 \times 10^{-2}$	0.16	1.6	16	$1.6 \times 10^2$	$1.6 \times 10^3$	$1.6 \times 10^4$	$5 \times 10^4$
1	100	0.33	89.45	89.15	87.22	84.08	83.16	81.64	79.11	77.92	25.58	5.17
2	100	0.23	93.35	94.95	93.69	91.08	91.25	89.65	87.46	84.05	22.86	2.02
3	100	0.12	93.39	94.90	93.72	90.96	91.30	89.71	87.53	85.20	23.51	2.76
4	100	-0.2	92.94	94.85	93.60	90.86	91.20	89.62	87.29	85.04	23.99	3.32
5	100	-0.21	93.30	94.97	93.70	90.82	90.98	89.15	87.47	87.31	27.74	7.42
Avg	100	0.05	92.49	93.76	92.39	89.56	89.58	87.95	85.77	83.90	24.74	4.14
SD	1.33	0.30	1.71	2.58	2.89	3.07	3.59	3.54	3.73	3.55	1.96	2.17

\*M199 as control and 100  $\mu\text{M}$  of vinblastine as a positive control

Table A.19 The percentage of cells viability of methotrexate with 100  $\mu\text{M}$  MK-571 on LLCPK1 cells after incubation for 96 h.

N	M199 media*	Vinblastine*	Concentration ( $\mu\text{M}$ )										
			$1.6 \times 10^{-4}$	$1.6 \times 10^{-3}$	$1.6 \times 10^{-2}$	0.16	1.6	16	$1.6 \times 10^2$	$1.6 \times 10^3$	$1.6 \times 10^4$	$5 \times 10^4$	
1	100	-0.12	85.21	79.94	80.34	81.26	79.33	80.65	74.77	68.29	1.6x10 <sup>3</sup>	1.6x10 <sup>4</sup>	5x10 <sup>4</sup>
2	100	0.31	87.40	82.68	83.81	82.79	81.76	82.38	77.36	71.21	24.53	24.54	1.02
3	100	0.02	88.50	83.88	84.91	83.16	82.85	82.85	77.93	72.18	24.03	24.03	1.64
4	100	0.01	88.51	84.21	85.33	83.38	83.18	83.49	78.46	73.03	24.51	24.51	1.64
5	100	0.00	88.46	84.47	85.29	83.55	83.35	83.07	78.75	73.34	22.41	22.41	0.25
Avg	100	0.04	87.62	83.04	83.94	82.83	82.09	82.49	77.45	71.61	24.00	24.00	1.05
SD	1.21	0.16	1.43	1.86	2.10	0.92	1.66	1.10	1.59	2.03	0.92	0.92	0.60

\*M199 as control and 100  $\mu\text{M}$  of vinblastine as a positive control

Table A.20 The percentage of cells viability of methotrexate with 150  $\mu\text{M}$  MK-571 on LLCPK1 cells after incubation for 96 h.

N	M199 media*	Vinblastine*	Concentration ( $\mu\text{M}$ )										
			$1.6 \times 10^{-4}$	$1.6 \times 10^{-3}$	$1.6 \times 10^{-2}$	0.16	1.6	16	$1.6 \times 10^2$	$1.6 \times 10^3$	$1.6 \times 10^4$	$5 \times 10^4$	
1	100	1.08	94.98	96.03	90.49	92.89	88.61	87.88	88.19	82.06	25.87	25.87	0.84
2	100	0.24	96.96	99.69	94.12	94.65	92.03	89.51	90.98	81.74	25.47	25.47	0.62
3	100	0.00	97.07	99.79	94.35	94.87	92.25	90.26	91.73	82.62	27.05	27.05	0.83
4	100	0.03	97.18	99.69	94.26	94.68	92.28	90.51	91.87	83.00	23.04	23.04	0.23
5	100	1.21	96.89	99.69	93.89	94.51	92.02	90.47	91.92	83.21	22.24	22.24	0.83
Avg	100	0.51	96.62	98.98	93.42	94.32	91.44	89.73	90.94	82.53	24.73	24.73	0.67
SD	1.73	0.59	0.92	1.65	1.65	0.81	1.59	1.11	1.58	0.62	2.02	2.02	0.26

\*M199 as control and 100  $\mu\text{M}$  of vinblastine as a positive control

**2. Calculation of 50% cytotoxic concentration value (CC<sub>50s</sub>,  $\mu$ M) of tenofovir and methotrexate by using GraphPad™ 6.0 with nonlinear regression model.**

Table A.21 The CC<sub>50s</sub> ( $\mu$ M) value of methotrexate without MK-571 on LLC-PK1 cells after incubation for 96 h. (Calculation by GraphPad™ 6.0 with nonlinear regression model)

Asymmetric Sigmoidal, 5PL, X is log(concentration)	1	2	3	4	5
Best-fit values					
LogCC <sub>50s</sub>	3.69	3.688	3.71	3.687	3.703
HillSlope	18.86	34.13	37.19	31.85	37.72
S	0.03732	0.02065	0.02105	0.02138	0.02134
Top	98.73	98.32	98.01	97.59	97.08
Bottom	15.69	15.51	15.4	14.74	14.83
CC <sub>50s</sub>	4,896	4,872	5,129	4,863	5,042
Goodness of Fit					
Robust Sum of Squares	1.149	1.188	1.358	1.409	1.46
RSDR	7.322	7.443	6.995	6.528	6.553
Number of points					
Analyzed	10	10	10	10	10

Table A.22 The CC<sub>50s</sub> ( $\mu$ M) value of methotrexate with 50  $\mu$ M of MK-571 on LLC-PK1 cells after incubation for 96 h. (Calculation by GraphPad™ 6.0 with nonlinear regression model)

Asymmetric Sigmoidal, 5PL, X is log(concentration)	1	2	3	4	5
Best-fit values					
LogCC50s	3.7	3.699	3.713	3.713	3.743
HillSlope	37.82	60.03	40.57	40.38	31.88
S	0.02245	0.01522	0.02414	0.02415	0.03555
Top	94.83	97.98	97.24	96.68	92.58
Bottom	14.8	8.048	8.078	8.246	8.328
CC50s	5,010	5,001	5,168	5,165	5,537
Goodness of Fit					
Robust Sum of Squares	1.429	1.955	1.935	1.865	1.823
RSDR	6.948	3.602	3.692	3.752	4.192
Number of points					
Analyzed	10	10	10	10	10

Table A.23 The  $CC_{50S}$  ( $\mu\text{M}$ ) value of methotrexate with 100  $\mu\text{M}$  of MK-571 on LLC-PK1 cells after incubation for 96 h. (Calculation by GraphPad™ 6.0 with nonlinear regression model)

Asymmetric Sigmoidal, 5PL, X is log(concentration)	1	2	3	4	5
Best-fit values					
Log $CC_{50S}$	3.678	3.679	3.674	3.683	3.682
HillSlope	21.92	24.34	33	32.95	24.97
S	0.02977	0.02814	0.02148	0.02201	0.03025
Top	99.29	98.98	98.36	98.36	99.75
Bottom	19.53	17.15	16.45	16.05	16.08
$CC_{50S}$	4,767	4,774	4,724	4,821	4,804
Goodness of Fit	3.678	3.679	3.674	3.683	3.682
Robust Sum of Squares	21.92	24.34	33	32.95	24.97
RSDR	0.02977	0.02814	0.02148	0.02201	0.03025
Number of points					
Analyzed	10	10	10	10	10

Table A.24 The  $CC_{50S}$  ( $\mu\text{M}$ ) value of methotrexate with 150  $\mu\text{M}$  of MK-571 on LLC-PK1 cells after incubation for 96 h. (Calculation by GraphPad™ 6.0 with nonlinear regression model)

Asymmetric Sigmoidal, 5PL, X is log(concentration)	1	2	3	4	5
Best-fit values					
Log $CC_{50S}$	3.705	3.67	3.687	3.671	3.669
HillSlope	37.72	35.44	33.75	33.84	35.77
S	0.02149	0.02022	0.02173	0.02299	0.0224
Top	99.16	99.38	99.17	99.77	99.17
Bottom	8.515	5.66	5.396	5.519	5.772
$CC_{50S}$	5,074	4,680	4,867	4,690	4,664
Goodness of Fit					
Robust Sum of Squares	1.468	2.073	1.867	1.93	1.929
RSDR	5.827	4.549	4.606	4.451	4.471
Number of points					
Analyzed	10	10	10	10	10

Table A.25 The  $CC_{50S}$  ( $\mu\text{M}$ ) value of methotrexate without MK-571 on MRP8-overexpressed cells after incubation for 96 h. (Calculation by GraphPad™ 6.0 with nonlinear regression model)

Asymmetric Sigmoidal, 5PL, X is log(concentration)	1	2	3	4	5
Best-fit values					
Log $CC_{50S}$	4.489	4.467	4.459	4.463	4.432
HillSlope	6.187	4.530	4.560	4.525	8.245
S	0.2533	0.3676	0.3615	0.4219	0.1681
Top	94.03	92.92	91.69	93.02	81.71
Bottom	4.256	3.476	3.582	3.736	3.134
$CC_{50S}$	30,838	29,279	28,805	29,064	27,035
Goodness of Fit					
Robust Sum of Squares	5.728	3.874	4.435	3.944	3.508
RSDR	1.056	1.442	1.341	1.488	1.802
Number of points					
Analyzed	10	10	10	10	10

Table A.26 The  $CC_{50S}$  ( $\mu\text{M}$ ) value of methotrexate with 50  $\mu\text{M}$  MK-571 on MRP8-overexpressed cells after incubation for 96 h. (Calculation by GraphPad™ 6.0 with nonlinear regression model)

Asymmetric Sigmoidal, 5PL, X is log(concentration)	1	2	3	4	5
Best-fit values					
Log $CC_{50S}$	3.791	3.824	3.787	3.778	3.762
HillSlope	6.463	10.36	5.600	4.844	4.351
S	1.222	0.7164	1.488	4.039	5.008
Top	92.49	90.12	89.11	87.10	86.47
Bottom	8.668	8.331	8.582	8.189	8.060
$CC_{50S}$	6,186	6,666	6,124	5,996	5,779
Goodness of Fit					
Robust Sum of Squares	4.626	4.802	4.565	4.796	5.231
RSDR	1.795	1.632	1.730	1.650	1.575
Number of points	3.791	3.824	3.787	3.778	3.762
Analyzed	10	10	10	10	10

Table A.27 The  $CC_{50S}$  ( $\mu\text{M}$ ) value of methotrexate with 100  $\mu\text{M}$  MK-571 on MRP8-overexpressed cells after incubation for 96 h. (Calculation by GraphPad™ 6.0 with nonlinear regression model)

Asymmetric Sigmoidal, 5PL, X is log(concentration)	1	2	3	4	5
Best-fit values					
Log $CC_{50S}$	3.819	3.829	3.727	3.815	3.735
HillSlope	12.5	6.394	3.677	9.726	4.539
S	0.1975	1.103	3.085	0.7455	2.356
Top	95.38	94.15	91.9	89.81	86.77
Bottom	7.982	8.222	7.697	9.122	7.794
$CC_{50S}$	6,596	6,742	5,335	6,533	5,434
Goodness of Fit					
Robust Sum of Squares	7.74	5.396	4.092	4.804	5.422
RSDR	0.8936	1.372	1.86	1.743	1.335
Number of points					
Analyzed	10	10	10	10	10

Table A.28 The  $CC_{50S}$  ( $\mu\text{M}$ ) value of methotrexate with 150  $\mu\text{M}$  MK-571 on MRP8-overexpressed cells after incubation for 96 h. (Calculation by GraphPad™ 6.0 with nonlinear regression model)

Asymmetric Sigmoidal, 5PL, X is log(concentration)	1	2	3	4	5
Best-fit values					
Log $CC_{50S}$	3.804	3.798	3.806	3.754	3.768
HillSlope	5.548	6.234	4.996	3.084	3.679
S	1.355	0.5982	2.764	9.623	4.778
Top	97.66	95.68	89.46	88.52	94.54
Bottom	5.239	5.054	7.087	6.175	5.455
$CC_{50S}$	6,368	6,282	6,391	5,676	5,856
Goodness of Fit					
Robust Sum of Squares	3.71	3.918	4.733	4.701	3.734
RSDR	1.883	1.886	1.649	1.432	1.707
Number of points					
Analyzed	10	10	10	10	10

Table A.29 The  $CC_{50s}$  ( $\mu M$ ) value of tenofovir without MK-571 on LLC-PK1 cells after incubation for 96 h. (Calculation by GraphPad™ 6.0 with nonlinear regression model)

Asymmetric Sigmoidal, 5PL, X is log(concentration)	1	2	3	4	5
Best-fit values					
Log $CC_{50s}$	4.510	4.525	4.530	4.532	4.540
HillSlope	1.935	1.927	1.929	1.950	1.977
S	4.689	4.604	4.535	4.414	4.247
Top	93.24	94.60	95.29	95.54	100.1
Bottom	1.366	1.946	0.3674	0.3037	1.323
$CC_{50s}$	32,389	33,481	33,900	34,061	34,639
Goodness of Fit					
Robust Sum of Squares	3.803	3.174	2.740	2.580	2.936
RSDR	1.635	2.084	1.744	2.070	2.153
Number of points					
Analyzed	10	10	10	10	10

Table A.30 The  $CC_{50s}$  ( $\mu M$ ) value of tenofovir with 50  $\mu M$  MK-571 on LLC-PK1 cells after incubation for 96 h. (Calculation by GraphPad™ 6.0 with nonlinear regression model)

Asymmetric Sigmoidal, 5PL, X is log(concentration)	1	2	3	4	5
Best-fit values					
Log $CC_{50s}$	4.535	4.542	4.537	4.543	4.559
HillSlope	1.932	1.926	1.928	2.017	1.951
S	3.921	3.945	3.766	4.317	3.618
Top	93.41	94.70	95.56	95.40	98.51
Bottom	1.573	1.503	1.591	1.938	2.238
$CC_{50s}$	34,275	34,830	34,459	34,892	36,238
Goodness of Fit					
Robust Sum of Squares	3.444	2.712	2.389	2.241	2.354
RSDR	3.271	4.101	4.002	4.220	4.006
Number of points					
Analyzed	10	10	10	10	10

Table A.31 The  $CC_{50S}$  ( $\mu\text{M}$ ) value of tenofovir with 100  $\mu\text{M}$  MK-571 on LLC-PK1 cells after incubation for 96 h. (Calculation by GraphPad™ 6.0 with nonlinear regression model)

Asymmetric Sigmoidal, 5PL, X is log(concentration)	1	2	3	4	5
Best-fit values					
Log $CC_{50S}$	4.526	4.520	4.525	4.521	4.535
HillSlope	1.881	1.875	1.884	1.877	1.877
S	4.675	4.771	4.946	4.755	4.398
Top	96.41	97.92	98.76	98.81	98.09
Bottom	0.3995	0.08393	0.009430	1.061	1.374
$CC_{50S}$	33,562	33,131	33,478	33,183	34,297
Goodness of Fit					
Robust Sum of Squares	2.079	3.352	3.174	2.208	2.871
RSDR	1.021	1.327	1.256	1.678	1.330
Number of points					
Analyzed	10	10	10	10	10

Table A.32 The  $CC_{50S}$  ( $\mu\text{M}$ ) value of tenofovir without MK-571 on MRP8-overexpressed cells after incubation for 96 h. (Calculation by GraphPad™ 6.0 with nonlinear regression model)

Asymmetric Sigmoidal, 5PL, X is log(concentration)	1	2	3	4	5
Best-fit values					
Log $CC_{50S}$	5.190	5.217	5.191	5.219	5.217
HillSlope	15.95	25.32	16.14	29.57	25.55
S	0.08456	0.05342	0.08455	0.04650	0.05372
Top	161.5	175.6	162.0	176.5	176.0
Bottom	0.5665	0.6701	0.8502	1.085	1.006
$CC_{50S}$	154,866	164,881	155,303	165,494	164,839
Goodness of Fit					
Robust Sum of Squares	2.403	2.327	2.214	2.099	2.174
RSDR	4.731	4.689	4.901	5.085	4.966
Number of points					
Analyzed	10	10	10	10	10



Table A.33 The  $CC_{50S}$  ( $\mu\text{M}$ ) value of tenofovir with 50  $\mu\text{M}$  MK-571 on MRP8-overexpressed cells after incubation for 96 h. (Calculation by GraphPad™ 6.0 with nonlinear regression model)

Asymmetric Sigmoidal, 5PL, X is log(concentration)	1	2	3	4	5
Best-fit values					
Log $CC_{50S}$	5.145	5.139	5.139	5.137	5.141
HillSlope	5.486	5.242	5.269	5.203	5.384
S	3.844	3.741	3.823	4.045	4.372
Top	114.3	114.1	114.1	114.0	114.3
Bottom	-3.119	-3.053	-2.983	-2.848	-2.695
$CC_{50S}$	139,622	137,706	137,837	137,013	138,400
Goodness of Fit					
Robust Sum of Squares	3.666	4.072	3.957	4.122	3.860
RSDR	8.252	7.390	7.435	7.106	7.485
Number of points					
Analyzed	10	10	10	10	10

Table A.34 The  $CC_{50S}$  ( $\mu\text{M}$ ) value of tenofovir with 100  $\mu\text{M}$  MK-571 on MRP8-overexpressed cells after incubation for 96 h. (Calculation by GraphPad™ 6.0 with nonlinear regression model)

Asymmetric Sigmoidal, 5PL, X is log(concentration)	1	2	3	4	5
Best-fit values					
Log $CC_{50S}$	4.024	4.028	4.028	4.029	4.039
HillSlope	2.234	2.244	2.208	2.203	2.216
S	2.342	1.174	5.599	7.281	1.373
Top	95.85	96.14	96.17	96.47	96.66
Bottom	-11.26	-10.98	-10.80	-10.80	-10.66
$CC_{50S}$	10,579	10,677	10,676	10,700	10,936
Goodness of Fit					
Robust Sum of Squares	1.734	1.829	1.820	1.834	1.807
RSDR	22.37	21.91	21.45	21.45	21.36
Number of points					
Analyzed	10	10	10	10	10

Table A.35 The  $CC_{50s}$  ( $\mu M$ ) value of tenofovir on MRP8-overexpressed cells and LLC-PK1 cells after incubation for 96 h.(Calculation by GraphPad™ 6.0 with nonlinear regression model)

N	MRP-8 overexpressed cells( $CC_{50s}$ , $\mu M$ )			LLCPK1 cells( $CC_{50s}$ , $\mu M$ )		
	No MK-571	+ 50 $\mu M$ of MK-571	+ 100 $\mu M$ of MK-571	No MK-571	+ 50 $\mu M$ of MK-571	+ 100 $\mu M$ of MK-571
1	164,839	138,400	10,936	32,389	34,275	33,562
2	154,866	139,622	10,579	33,481	34,830	33,131
3	164,881	137,706	10,677	33,900	34,459	33,478
4	155,303	137,837	10,676	34,061	34,892	33,183
5	165,494	137,013	10,700	34,639	36,238	34,297
Average	161,076.60	138,115.60	10,713.60	33,694.00	34,938.80	33,530.20
SD	5,478.33	976.12	132.78	839.43	770.19	466.80

Table A.36 The  $CC_{50s}$  ( $\mu M$ ) value of methotrexate on MRP8-overexpressed cells and LLC-PK1 cells after incubation for 96.(Calculation by GraphPad™ 6.0 with nonlinear regression model)

N	MRP-8 overexpressed cells( $CC_{50s}$ , $\mu M$ )			LLCPK1 cells( $CC_{50s}$ , $\mu M$ )		
	No MK-571	+50 $\mu M$ of MK-571	+100 $\mu M$ of MK-571	No MK-571	+50 $\mu M$ of MK-571	+100 $\mu M$ of MK-571
1	30,838	6,186	6,596	4,896	5,010	4,767
2	29,279	6,666	6,742	4,872	5,001	4,774
3	28,805	6,124	5,335	5,129	5,168	4,724
4	29,064	5,996	6,533	4,863	5,165	4,821
5	27,035	5,779	5,434	5,042	5,537	4,804
Average	29,004.20	6,150.20	6,128.00	4,960.40	5,176.20	4,778.00
SD	1,260.80	849.77	639.31	113.64	44.51	56.83
			592.13			91.46

Table A. 37 The percentage of cells viability of tenofovir on MRP8-overexpressed cells after incubation for 96 h. at six different concentrations.

N	M199* media	Vinblastine*	Concentration ( $\mu\text{M}$ )					
			1.75	17.5	175	$1.75 \times 10^3$	$1.75 \times 10^4$	$1.75 \times 10^5$
1	100	2.22	101.42	99.80	102.98	99.02	97.77	7.01
2	100	1.02	102.37	103.37	99.45	99.07	96.71	6.93
3	100	2.01	103.74	97.64	99.06	99.72	95.40	5.82
4	100	0.34	99.48	101.56	101.34	101.36	94.38	4.54
5	100	0.71	99.22	97.40	99.53	101.50	95.32	3.51
6	100	-0.23	98.88	97.41	98.29	102.38	96.26	2.31
7	100	2.56	99.46	103.09	102.33	99.28	97.13	3.19
8	100	3.01	99.56	97.29	100.10	102.35	95.17	4.99
9	100	1.32	98.82	97.38	100.37	101.55	94.36	5.80
10	100	1.39	102.66	97.24	100.15	102.37	94.23	3.35
Average	100.00	1.44	100.56	99.22	100.36	100.86	95.67	4.74
SD	2.11	1.02	1.81	2.54	1.46	1.43	1.24	1.64

\*M199 as control and 100  $\mu\text{M}$  of vinblastine as a positive control

Table A.38 The percentage of cells viability of tenofovir on LLC-PK1 cells after incubation for 96 h. at six different concentrations.

N	M199* media	Vinblastine*	Concentration ( $\mu\text{M}$ )					
			1.75	17.5	175	$1.75 \times 10^3$	$1.75 \times 10^4$	$1.75 \times 10^5$
1	100	1.63	101.39	103.87	105.55	106.24	91.18	9.91
2	100	0.02	97.97	102.46	103.78	102.96	89.45	8.51
3	100	2.03	98.82	101.63	102.36	102.81	89.67	7.79
4	100	-0.31	99.58	100.53	101.58	105.11	89.96	7.46
5	100	0.01	100.00	101.87	103.87	103.74	89.92	6.60
6	100	-0.01	101.11	100.86	102.84	103.95	90.38	6.36
7	100	2.40	102.46	99.97	105.17	104.20	90.75	7.17
8	100	2.07	99.04	100.68	102.90	104.17	90.55	3.15
9	100	1.37	98.74	101.25	103.68	102.60	90.21	5.01
10	100	1.00	98.02	100.58	102.72	103.71	90.35	3.97
Average	100.00	1.02	99.71	101.37	103.44	103.95	90.24	6.59
SD	1.83	1.02	1.51	1.14	1.23	1.10	0.51	2.07

\*M199 as control and 100  $\mu\text{M}$  of vinblastine as a positive control

Table A.39 The percentage of cells viability of methotrexate on MRP8-overexpressed cells after incubation for 96 h. at six different concentrations.

N	M199* media	Vinblastine*	Concentration ( $\mu\text{M}$ )					
			1.6	16	$1.6 \times 10^2$	$1.6 \times 10^3$	$1.6 \times 10^4$	$5 \times 10^4$
1	100	3.03	96.46	94.70	92.93	93.42	75.87	14.64
2	100	1.00	98.18	96.36	94.55	95.31	77.42	16.56
3	100	1.32	97.74	96.05	94.27	95.49	77.27	17.29
4	100	1.20	97.77	96.28	95.07	96.18	78.23	19.37
5	100	0.53	97.34	95.86	94.67	96.05	77.79	19.76
6	100	0.61	97.28	95.55	94.64	96.09	77.73	20.80
7	100	3.52	97.82	95.72	95.20	96.16	77.82	22.45
8	100	5.11	98.19	95.94	95.68	96.81	78.36	23.66
9	100	-0.01	98.28	96.13	96.05	97.25	78.62	24.25
10	100	-0.08	98.38	96.16	95.99	97.27	78.80	24.77
Average	100.00	1.62	97.74	95.88	94.90	96.00	77.79	20.35
SD	2.35	1.71	0.59	0.48	0.93	1.12	0.84	3.46

\*M199 as control and 100  $\mu\text{M}$  of vinblastine as a positive control

Table A.40 The percentage of cells viability of methotrexate on LLC-PK1 cells after incubation for 96 h. at six different concentrations.

N	M199* media	Vinblastine*	Concentration ( $\mu\text{M}$ )					
			1.6	16	$1.6 \times 10^2$	$1.6 \times 10^3$	$1.6 \times 10^4$	$5 \times 10^4$
1	100	2.59	94.10	90.01	88.08	85.24	25.09	7.72
2	100	1.32	94.12	91.18	89.14	86.31	26.13	7.92
3	100	0.03	94.93	91.43	89.40	86.70	26.49	8.34
4	100	0.01	95.06	92.02	89.44	87.30	26.97	8.99
5	100	0.09	95.31	92.51	89.72	87.60	27.37	9.39
6	100	1.11	95.77	92.76	90.09	87.86	27.73	9.80
7	100	0.02	95.59	92.61	89.85	87.86	28.15	10.49
8	100	2.53	95.83	92.54	89.91	88.05	28.73	11.18
9	100	1.79	95.77	92.40	89.79	88.06	28.99	11.73
10	100	-0.07	95.90	92.34	89.64	88.03	29.45	12.41
Average	100.00	0.94	95.24	91.98	89.51	87.30	27.51	9.80
SD	2.86	1.08	0.68	0.87	0.57	0.94	1.38	1.62

\*M199 as control and 100  $\mu\text{M}$  of vinblastine as a positive control

### 3. Determination of intracellular tenofovir accumulation in transport assay

#### The example of calculation:

$$\begin{aligned} \text{Intracellular concentration of} &= \frac{(\text{Area under the curve} - 90.08)}{31.96} \\ \text{tenofovir (nM/400,000 cells)} &= \frac{(130.50 - 90.08)}{31.96} \\ &= 1.26 \text{ nM} \\ \text{Intracellular concentration of} &= \frac{1.26 \times 10^6 \text{ nM}}{0.4 \times 10^6} \\ \text{tenofovir (nM/10}^6 \text{ cells)} &= 3.16 \text{ nM} \end{aligned}$$

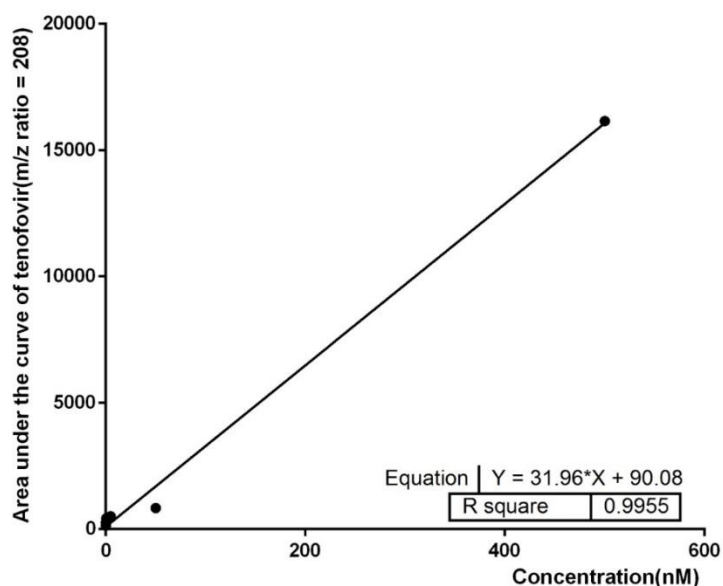


Figure A.2 Standard curve of tenofovir (areas under the curve (m/z ratio = 208)) in cellular transport assay.

Table A.41 The intracellular tenofovir accumulation of transport assay.

Conditions	Area under the curve (m/z = 208)		Average	SD	Concentration	
	1	2			nM	(nM/10 <sup>6</sup> cells)
MRP8	151	110	130.50	28.99	1.26	3.16
MRP8+ 50uM MK-571	1,089	1,086	1,087.50	2.12	31.21	78.02
MRP8+ 100uM MK-571	1,643	1,618	1,630.50	17.68	48.20	120.50
Parental cells	2,242	2,459	2,350.50	153.44	70.73	176.82

#### 4. Determination of intracellular methotrexate accumulation in transport assay

The example of calculation:

$$\begin{aligned} \text{Intracellular concentration of methotrexate (nM/400,000 cells)} &= \frac{(\text{Area under the curve} - 46.01)}{8.699} \\ &= \frac{(205.0 - 46.01)}{8.699} \\ &= 18.28 \text{ nM} \\ \text{Intracellular concentration of tenofovir (nM/10}^6 \text{ cells)} &= \frac{18.28 \times 10^6 \text{ nM}}{0.4 \times 10^6} \\ &= 45.69 \text{ nM} \end{aligned}$$

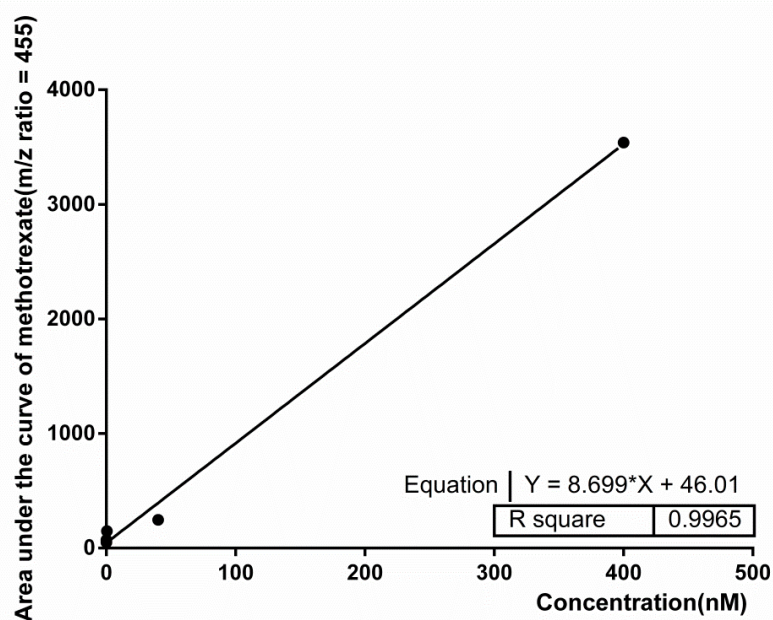


Figure A.3 Standard curve of methotrexate (areas under the curve (m/z ratio = 455)) in cellular transport assay.

Table A.42 The intracellular methotrexate accumulation of transport assay.

Conditions	Area under the curve (m/z = 455)		Average	SD	Concentration	
	1	2			nM	(nM/10 <sup>6</sup> cells)
MRP8	124	286	205.0	114.55	18.28	45.69
MRP8+ 50uM MK-571	1,431	1,175	1303.0	181.02	144.50	361.25
MRP8+ 100uM MK-571	2,723	2,632	2677.5	64.35	302.50	756.26
Parental cells	1,777	1,268	1522.5	359.92	169.73	424.33



## 5. Determination of intravesicular tenofovir accumulation in uptake assay

### The example of calculation:

$$\begin{aligned}
 \text{Intravesicular concentration of} & & & = \frac{(\text{Area under the curve} - 90.08)}{31.96} \\
 \text{tenofovir(nM/mg*protein)} & & & = \frac{(404.1 - 90.08)}{31.96} \\
 & & & = 9.83 \text{ nM} \\
 & & & = \frac{9.83 \times 10^3 \text{ nM}}{87 \text{ mcg*protein}} \\
 & & & = 112.95 \text{ nM/mg*protein}
 \end{aligned}$$

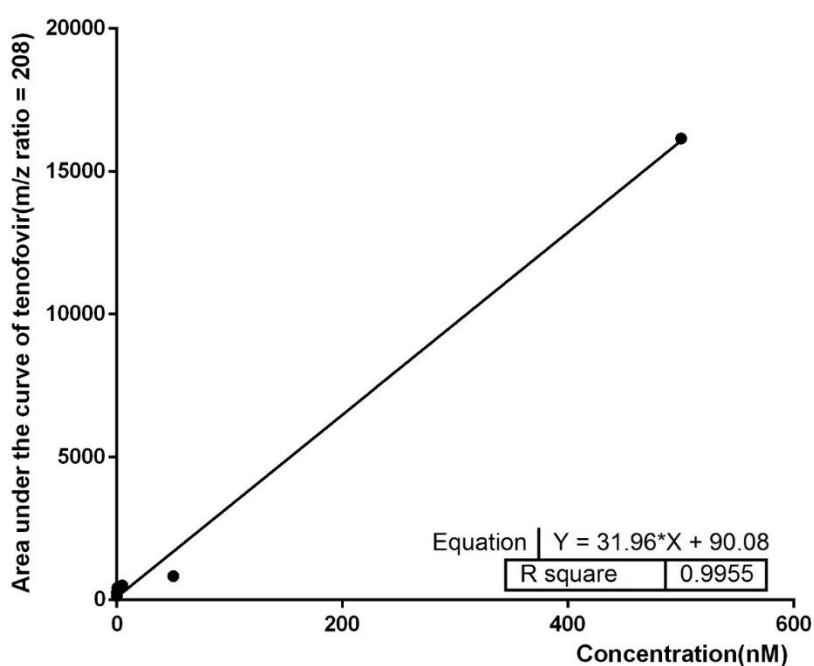


Figure A.4 Standard curve of tenofovir (areas under the curve (m/z ratio = 208)) in vesicular uptake assay.

Table A.43 The intravesicular tenofovir accumulation of uptake assay.

Times	Conditions	Area under the curve (m/z = 208)		Average	SD	Concentration	
		1	2			(nM)	(nM/mg*Protein)
0.5 min	MRP8+ ATP	402	407	404.1	1.3	9.83	112.95
	MRP8+ AMP	286	304	295.4	4.6	6.42	73.83
	MRP8+ MK-571	194	261	227.7	17.1	4.31	49.49
	Parental vesicles	231	357	293.8	31.9	6.38	73.28
5 min	MRP8+ ATP	441	507	473.8	16.8	12.01	138.01
	MRP8+ AMP	187	121	154.0	16.8	2.00	22.98
	MRP8+ MK-571	187	194	190.6	1.8	3.14	36.14
	Parental vesicles	226	266	246.2	10.2	4.89	56.16
10 min	MRP8+ ATP	632	755	693.4	31.1	18.88	216.98
	MRP8+ AMP	191	231	211.1	10.2	3.79	43.54
	MRP8+ MK-571	177	232	204.6	14.0	3.58	41.19
	Parental vesicles	210	192	200.9	4.5	3.47	39.84
15 min	MRP8+ ATP	938	537	737.5	63.7	20.26	232.84
	MRP8+ AMP	159	278	218.7	30.3	4.02	46.24
	MRP8+ MK-571	278	151	214.6	32.4	3.90	44.80
	Parental vesicles	105	263	184.1	40.3	2.94	33.80
30 min	MRP8+ ATP	824	742	782.8	20.8	21.68	249.14
	MRP8+ AMP	235	147	191.1	22.4	3.16	36.32
	MRP8+ MK-571	318	412	365.0	23.7	8.60	98.89
	Parental vesicles	119	178	148.5	15.0	1.83	21.00

## 6. Determination of intravesicular methotrexate accumulation in uptake assay

### The example of calculation:

$$\begin{aligned} \text{Intravesicular concentration of} &= \frac{(\text{Area under the curve} - 140.3)}{43.64} \\ \text{tenofovir(nM/mg*protein)} &= \frac{(341.5 - 140.3)}{43.64} \\ &= 4.61 \text{ nM} \\ &= \frac{4.61 \times 1000 \text{ nM}}{87} \\ &= 52.99 \text{ nM/mg*protein} \end{aligned}$$

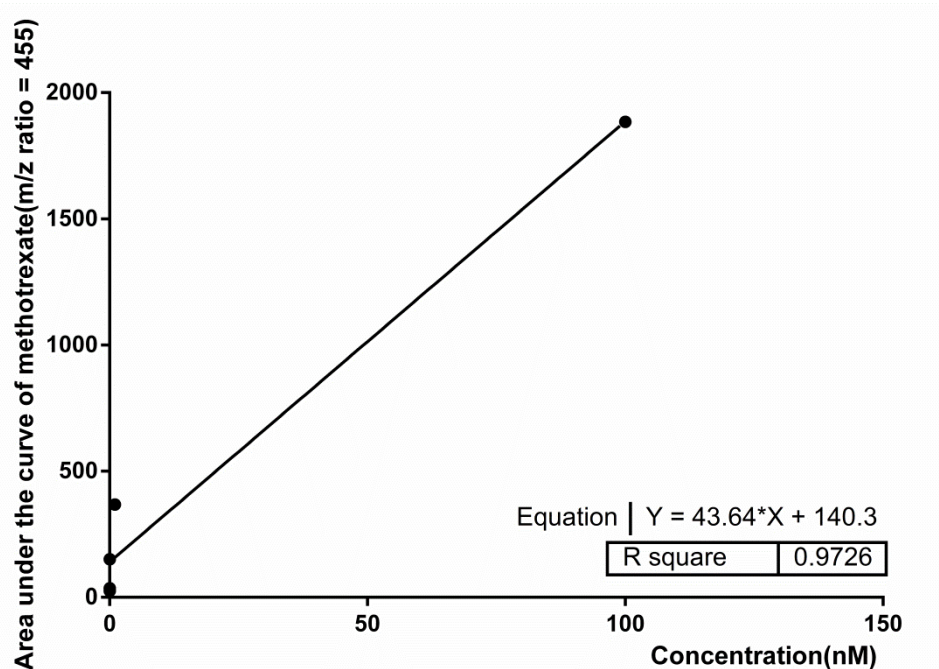


Figure A.5 Standard curve of methotrexate (areas under the curve (m/z ratio = 455)) in vesicular uptake assay.

Table A.44 The intravesicular methotrexate accumulation of uptake assay.

Times	Conditions	Area under the curve (m/z = 455)		Average	SD	Concentration	
		1	2			(nM)	(nM/mg*Protein)
0.5 min	MRP8+ ATP	337	346	341.5	1.8	4.61	52.99
	MRP8+ AMP	164	238	201.1	13.7	1.39	16.02
	MRP8+ MK-571	231	268	249.5	7.0	2.50	28.77
	Parental vesicles	148	252	200.2	19.4	1.37	15.79
5 min	MRP8+ ATP	490	515	502.4	4.6	8.30	95.38
	MRP8+ AMP	201	250	225.3	9.0	1.95	22.39
	MRP8+ MK-571	231	268	249.5	7.0	2.50	28.77
	Parental vesicles	289	319	303.9	5.5	3.75	43.08
10 min	MRP8+ ATP	471	598	534.6	23.7	9.04	103.87
	MRP8+ AMP	198	219	208.3	4.0	1.56	17.92
	MRP8+ MK-571	173	192	182.7	3.5	0.97	11.18
	Parental vesicles	217	200	208.8	3.2	1.57	18.04
15 min	MRP8+ ATP	706	510	607.9	36.5	10.72	123.17
	MRP8+ AMP	332	300	315.9	6.0	4.02	46.25
	MRP8+ MK-571	191	228	209.6	6.9	1.59	18.25
	Parental vesicles	198	198	197.6	0.0	1.31	15.09
30 min	MRP8+ ATP	596	424	509.8	32.1	8.47	97.33
	MRP8+ AMP	218	227	222.6	1.7	1.89	21.69
	MRP8+ MK-571	269	309	289.1	7.3	3.41	39.18
	Parental vesicles	320	182	250.9	25.6	2.53	29.13

### 7. Calculation of relative gene expression

The relative *mrp8* gene expressions values were calculated follow this equation;

$$\begin{aligned} \text{Relative } mrp8 \text{ gene expression} &= \frac{2^{(\text{Ct GOI of untreated cells} - \text{Ct GOI of treated cells})}}{2^{(\text{Ct Rf of untreated cells} - \text{Ct Rf of treated cells})}} \\ &= 2^{(12.20-6.86)/2^{(10.17-11.7)}} \\ &= 2^{(6.77)} \\ &= 109.13 \end{aligned}$$

Table A.45 The relative gene expression of *mrp8* to  $\beta$ -actin.

	No	Ct(GOI)	Ct actin	Fold change (Ratio to Ref-gene)	Average	SD
<b>MRP8-overexpressed</b>	1	6.86	11.70	109.13	100.82	7.20
	2	7.17	11.53	96.33		
	3	7.39	12.24	97.00		
<b>Parental cells</b>	1	12.20	10.17	0.009	0.013	0.009
	2	12.83	10.60	0.010		
	3	10.86	9.11	0.010		



## 8. Chromatogram of tenofovir and methotrexate in transport assay and uptake assay.

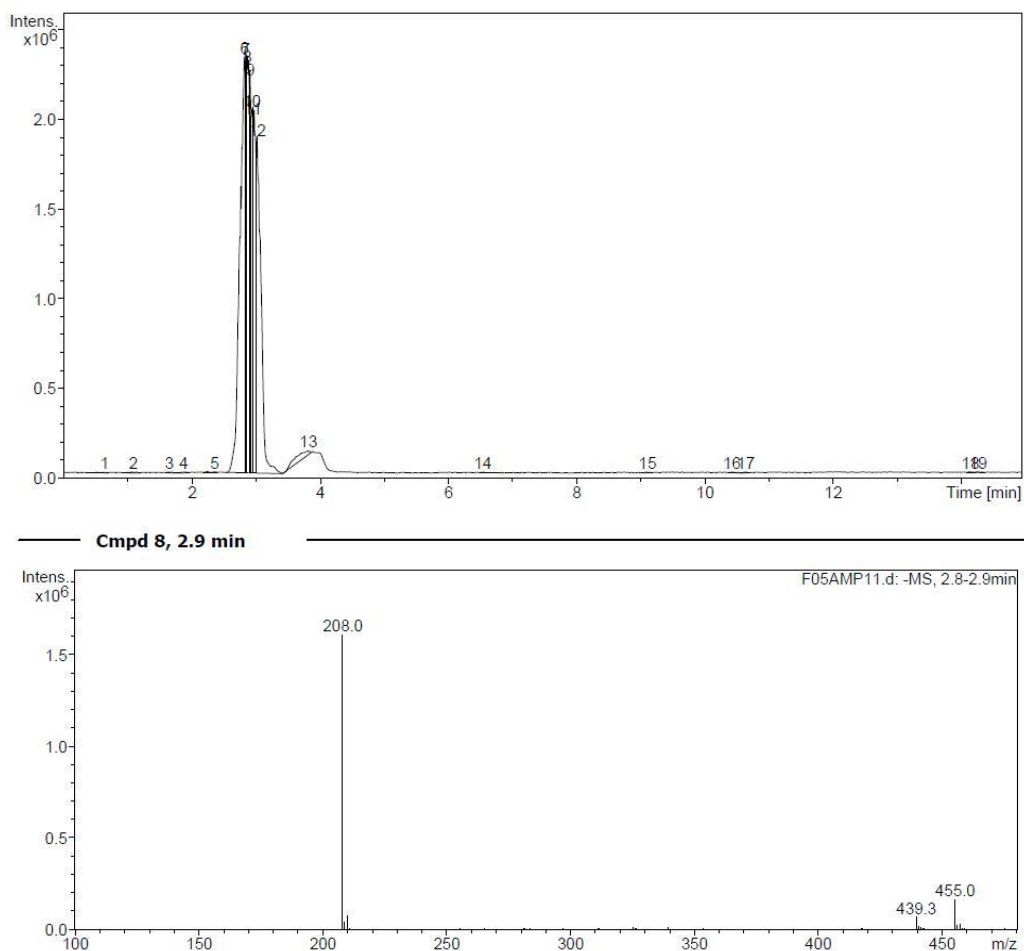


Figure A.6 The example of tenofovir LC-MS chromatogram ( $m/z = 208$ ) in standard solution.

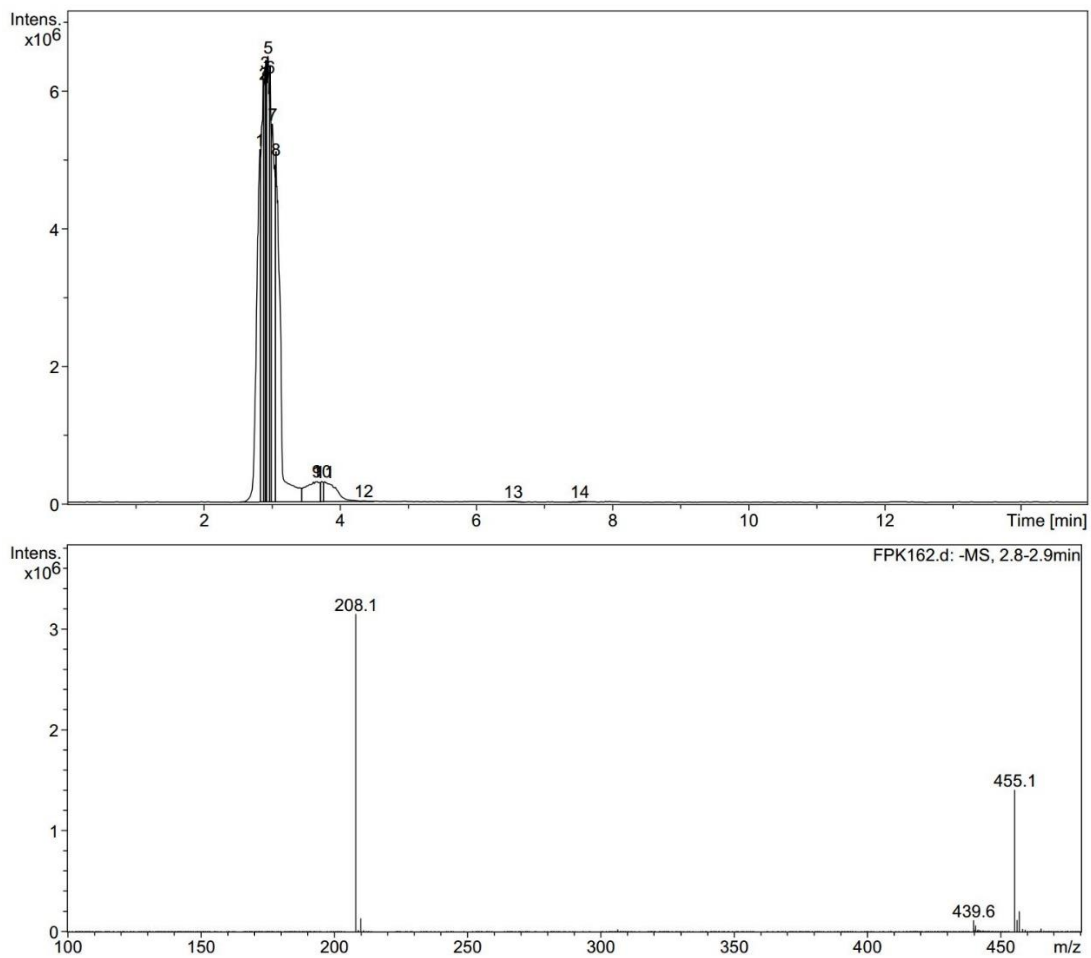


Figure A.7 The example of tenofovir LC-MS chromatogram ( $m/z = 208$ ) in transport assay.

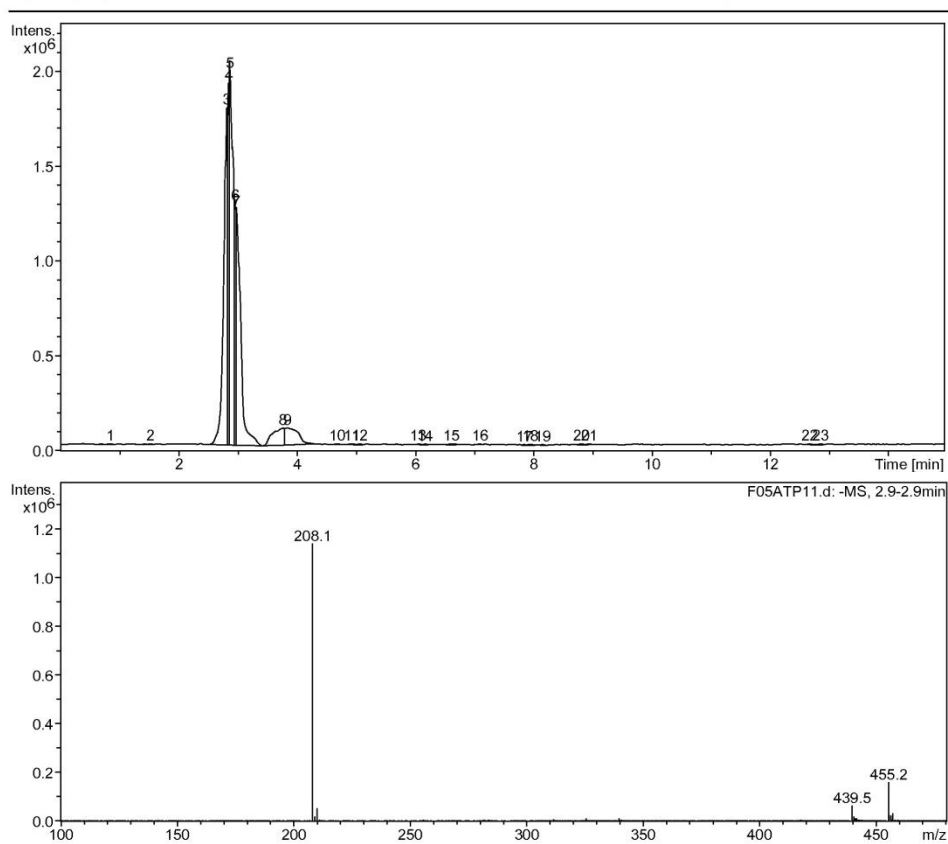
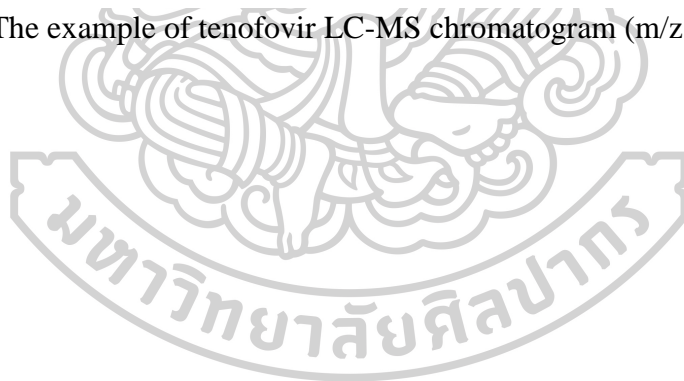


Figure A.8 The example of tenofovir LC-MS chromatogram ( $m/z = 208$ ) in uptake assay.





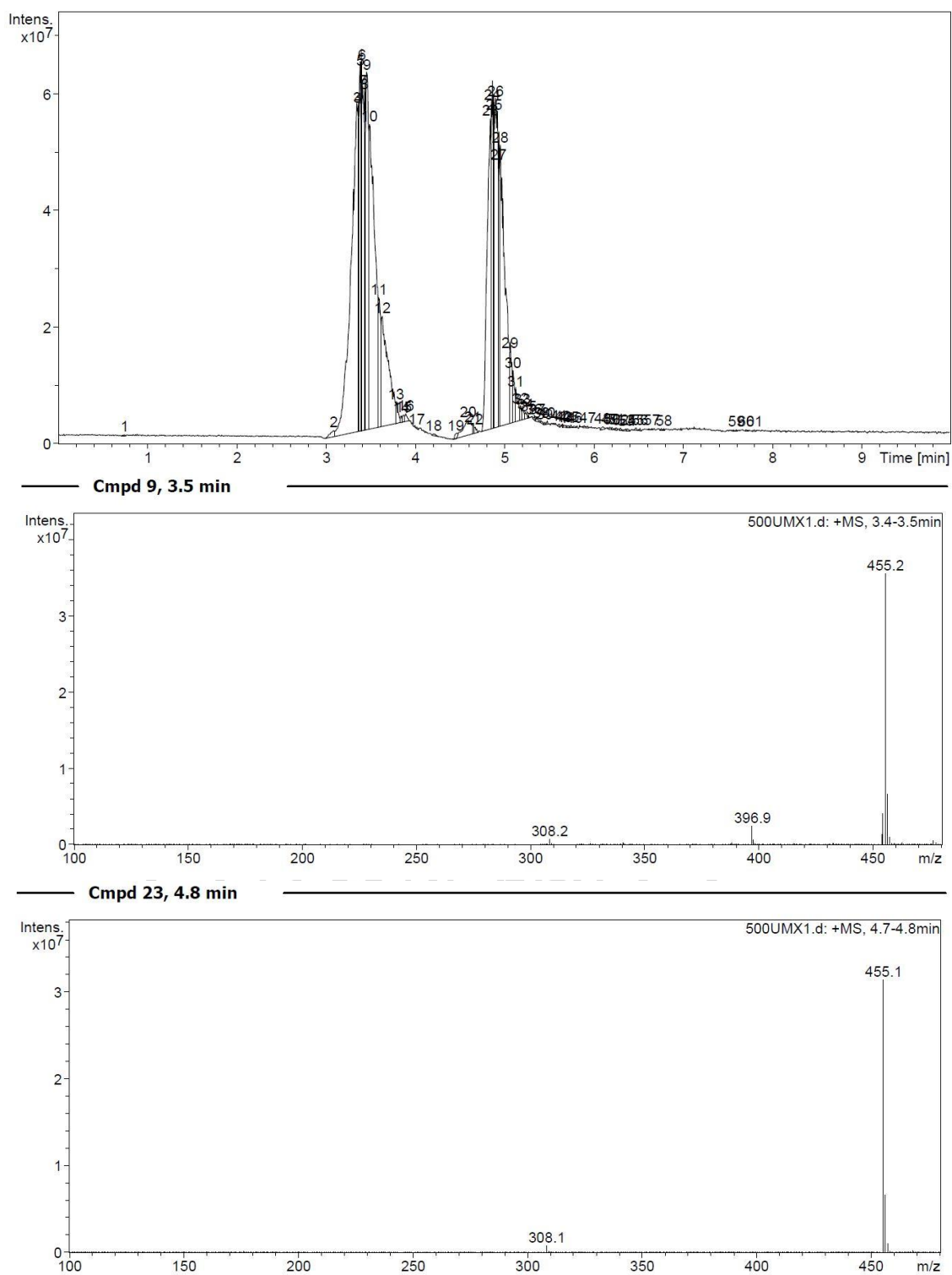


Figure A.9 The example of methotrexate LC-MS chromatogram ( $m/z = 455$ ) in standard solution.

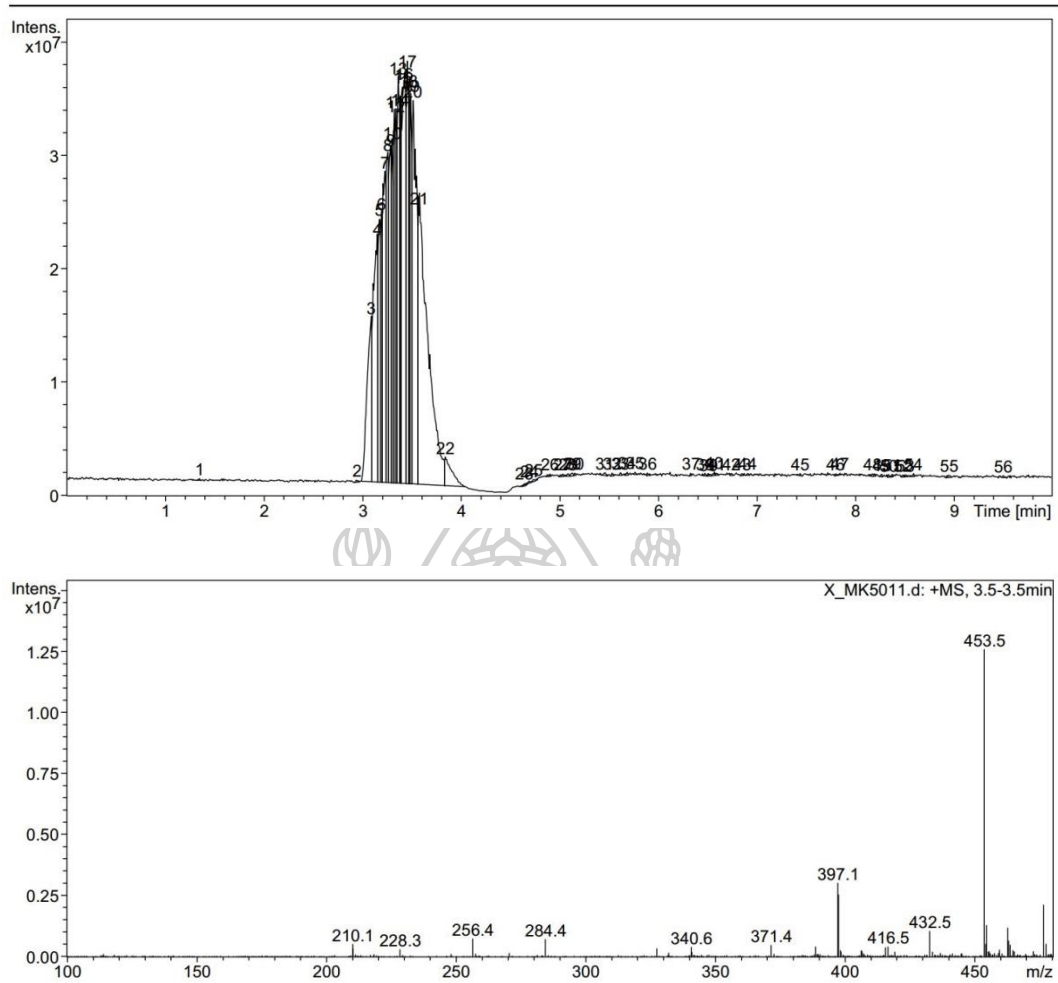


Figure A.10 The example of methotrexate LC-MS chromatogram ( $m/z = 455$ ) in transport assay.

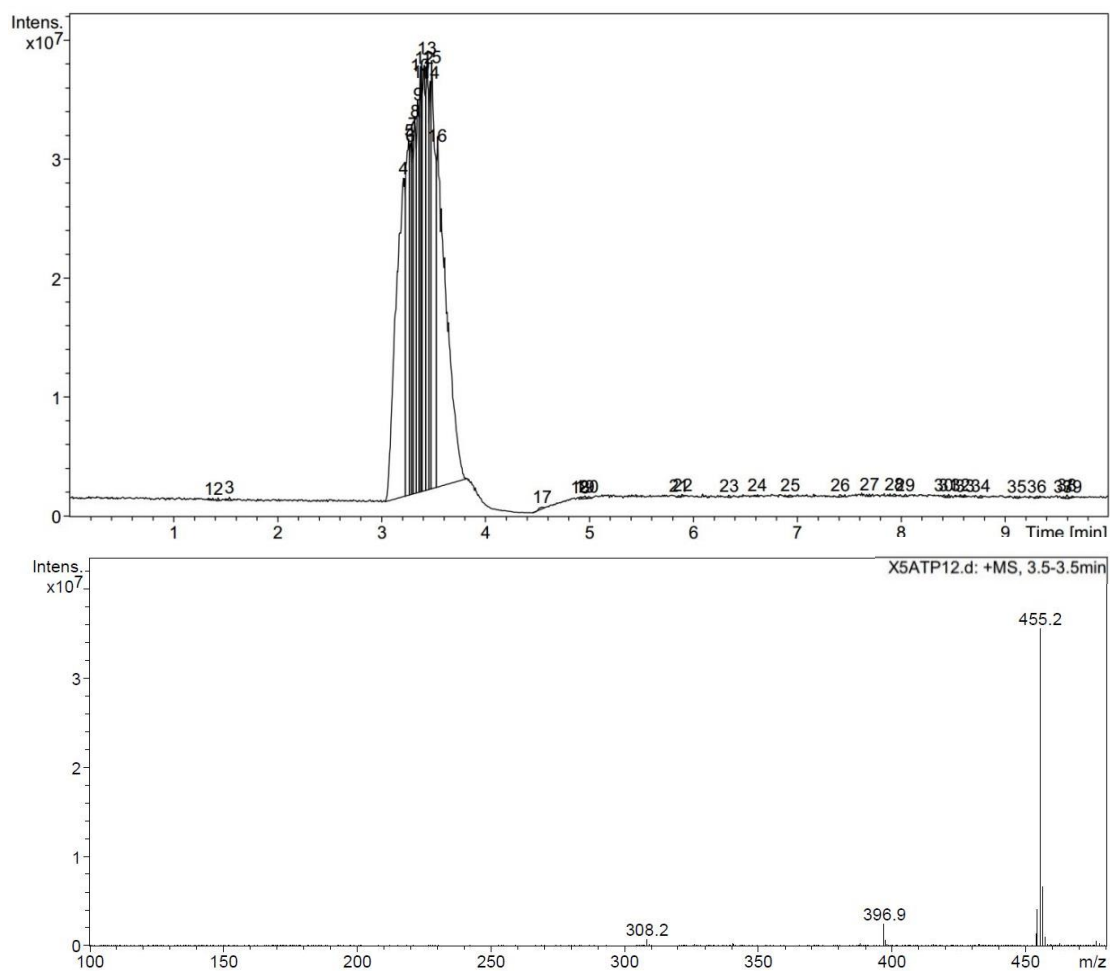


Figure A.11 The example of methotrexate LC-MS chromatogram ( $m/z = 455$ ) in uptake assay.

## VITA

**NAME** WISITH TUN-YHONG

**DATE OF BIRTH** 5 APRIL 1975

**PLACE OF BIRTH** CHONBURI, THAILAND

**INSTITUTIONS ATTENDED** FACULTY OF PHARMACY, SILPAKORN UNIVERSITY, THAILAND.

**HOME ADDRESS** 46/208 Grand Manerin Sammook Bangsaen, Bangsane sai 4, Sansook, Meoung, Chonburi, Thailand.

**PUBLICATION**

1. T. Wisith. A dangerous interaction between meropenem and valproic acid in Thai children; a case report and literature reviewed. Chonburi Hospital Journal. 2010;35(1), p.27-32.
2. C. Chulathida, T. Wilaslak, T. Wisith. Theophylline overdose in premature neonate : a case report and reviewed of pharmacokinetics. Siriraj Medical Journal. 2006;58(9).
3. T. Wisith. Role of sodium-glucose transporter (SGLT) in treatment of type II diabetes mellitus, a reviewed article. Chonburi Hospital Journal. 2009;34(3), p.177-184.
4. T. Wisith. Direct rennin inhibitore (DRIs), a novel mechanism of antihypertensive drugs, a reviewed article. Chonburi Hospital Journal. 2007;32(2), p.147-150.
5. T. Wisith. Drugs resistance of Mettalo  $\beta$ -lactamases producing organism, a reviewed article. Chonburi Hospital Journal. 2006;31(1), p.37-46. 6. T. Wisith. Proton pump inhibitors, a reviewed article. Chonburi Hospital Journal. 2002;27(3), p.159-167.

